Facoltà di Farmacia e Medicina – Dipartimento di Medicina Molecolare

Tesi di Dottorato di ricerca – XXXII Ciclo

p38α, the β-catenin chromatin associated kinase, as promising target in colorectal cancer stem cells for personalized therapy

Dottorando:

Dott.sa Martina Lepore Signorile

Relatore:

Chiar.mo Prof. Gianluca Canettieri

Supervisore:

Chiar.mo Prof. Cristiano Simone

Anno Accademico: 2019-2020

Summary

List of abbreviations

3MA, 3-methyladenine;

5-FU, 5-fluorouracil;

AKT, Rac-alpha serine/threonine-protein kinase;òl

AOM, azoxy-methan;

AP-1, activator protein1;

APC, adenomatous polyposis coli;

ATCC, american type culture collection;

ATF2, activating transcription factor 2;

ATP, adenosine triphosphate;

BAF60c, Brg1-brd associated factor subunit 60c;

BAX, Bcl-2-associated X protein;

BER, base-excision DNA repair mechanism;

BHLH, basic helix-loop-helix;

BMP, bone morphogenetic protein;

BRAF, serine/threonin-protein kinase B-raf;

BRR, Bannayan-Riley-Ruvalcaba;

c-MET, c-mesenchymal epithelial transition factor;

CD44, cluster of differentiation 44;

CD133, cluster of differentiation;

Cdc25, cell division control protein 25;

CDDP, cisplatin;

CHX, cycloheximide;

CIMP, CpG island methylator phenotype;

CIMP1, CpG island methylator phenotype 1;

CIMP2, CpG island methylator phenotype 2;

CIN, chromosomal instability;

Cis, cisplatin;

CKI, casein kinase I;

c-Myc; myelocitomatosis virus;

COX-2, cyclooxygenase-2;

CRC, Colorectal Cancer;

CRC-SC, colorectal cancer stem cell;

CR-SC, colorectal stem cell;

CSC, Cancer Stem Cell;

DCC, deleted in colorectal;

DFG, Asp-Phe-Gly motif;

DMEM, Dulbecco's modified eagle medium;

DMSO, dimethyl sulfoxide;

EDTA, ethylene diamine tetracetic acid;

EGF, epidermal growth factor;

EGFR, epidermal growth factor receptor;

ENU, ethylnitrosourea;

ERK1/2, extracellular-signal-regulated kinases 1/2;

FAP, familial adenomatous polyposis;

FBS, fetal bovine serum;

FOLFIRI, folinic acid-fluorouracil-irinotecan;

FOLFOX, folinic acid-fluorouracil-oxaliplatin;

FoxO3A, forkhead transcription factor FKHR-L1;

GADD45α, growth arrest and DNA-damage inducible 45 alpha;

GSK3β, glycogen synthase kinase 3 beta;

HDAC, histone deacetylase;

HER3, receptor tyrosine protein kinase erB3;

HIF1α, hypoxia-inducible factor 1 alpha;

HNPCC, hereditary non-polyposis colorectal cancer;

HSP27, heat shock protein 27;

JNK, c-Jun N-terminal kinase;

JNK1-3, c-Jun N-terminal kinase 1-3;

JNKIP2, JNK-interacting protein 2;

JP, Juvenile Polyposis;

KLF4, kruppel-like factor4;

KRAS, V-Ki ras2 Kirsten rat sarcoma viral oncogene homolog;

LC3I-II, light chain 3 I/II;

LEF/TCF lymphoid enhancer factor/T cell factor;

LGR5, leucin-rich repeat-containing G-protein coupled receptor 5;

LKB1/STK11, liver kinase B1/serine-threonine kinase 11;

LOH, loss of heterozygosity;

LZ, leucin zipper;

MAP1LC3, Microtubule-associated proteins 1A/1B light chain 3B;

MAP2K, mitogen-activated protein kinase kinase;

MAPK, mitogen-activated protein kinase;

MAPK14-11-12-13 , mitogen-activated protein kinase 14-11-12-13;

MAPK5, mitogen-activated protein kinase 5;

MAPKAP-2/3, mitogen-activated protein kinase-activated protein kinase 2;

MAPKK, mitogen-activated protein kinase kinase;

MAPKKK, mitogen-activated protein kinase kinase kinase;

MDM2, mouse double minute 2 homolog;

MEF-2, myocyte enhancer factor 2;

MEK1/2, mitogen/extracellular signal-regulated kinase 1/2;

MEKK1-4, mitogen-activated protein kinase kinase kinase 1-4;

MIN, microsatellite instability;

Min, multiple intestinal neoplasia;

MK2, MAP kinase-activated protein kinase 2;

MKK3/6, mitogen-activated protein kinase kinase 3/6;

MKK3Be, mitogen-activated protein kinase kinase 3Be;

MKK4/7, mitogen-activated protein kinase kinase 4/7;

MMP1, matrix metalloproteinase 1;

MMP13, matrix metalloproteinase 13;

MMP3, matrix metalloproteinase 3;

MMR, mismatch repair system;

MNK1/2, MAP kinase-interacting serine/thereonine protein;

MSC, mesenchimal stem cell;

MSH2, MutS protein homolog 2;

MSH6, MutS protein homolog 6;

MSI, microsatellite instability;

MSK1/2, mitogen-and stress-activated protein kinase 1/2;

MYOD, myogenin D;

Notch, neurogenic locus of notch homolog;

$p21^{Cip1}$, cycline -dependent kinase inhibitor 1;

PBS, phosphate buffered saline;

PDI, protein disulfide-isomerase;

P-gp, P-glycoprotein;

PI3K, phosphoinositide 3-kinase;

PI3K class I, phosphoinositide 3-kinase class I;

PI3K class III, phosphoinositide 3-kinase class III;

PI3KCA, phosphatidylinositol-4,5-bisphosphate-3 kinase, catalytic subunit alpha;

PJ, Peutz-Jeghers;

PP2A, protein phosphatase 2A;

PRAK, p38-regulated/activated protein kinase;

PTEN, phosphatase and tensin homologue;

RAF, Rapidly Accelerated Fibrosarcoma;

RAF-1, Raf proto-oncogene serine/thereonine- protein kinase;

RAS, Rat Sarcoma;

ROS, reactive oxygen species;

RTK, receptor tyrosine kinase;

S62, serine 62;

SIRT1, NAD-dependent deacetylase sirtuin 1;

SMAD4, SMAD family member 4;

SOX9, sex determining region Y

T58, threonine 58;

TBP, TATA binding protein;

TCF4, transcription factor 4;

TCF7, transcription factor 7;

TGF-β, transforming growth factor beta;

TP53, tumor protein p53;

Ub, ubiquitination;

VEGF, vascular endothelial growth factor;

Wnt, Wingless intergrate;

WRE, wnt responsive element;

WST-1, water soluble tetrazolium salt.

Abstract

Colorectal cancer (CRC) is the third most frequent malignancy, but the second cause of death for tumor in the western population. Only 14% of patients with advanced and metastatic disease survive five years from diagnosis. Recently, it has been shown that tumor relapse and chemoresistance depend on a small population of cells, called cancer stem cells (CSCs). Current evidence indicates that the Wnt cascade is the main driver in controlling CSC fate; the key player in this pathway is β-catenin, a cytoplasmic protein whose stability is regulated by the so-called "destruction complex". During carcinogenesis, the increasing amount of β-catenin resulting from APC inactivation translocates into the nucleus, causing the transcriptional activation of several mitogenic genes, including c-Myc. c-Myc is one of the most important factors involved in CRC initiation and progression; indeed, it functions as a link connecting malignancy with stemness. During colorectal carcinogenesis, c-Myc is maintained upregulated through β-catenin-mediated transcriptional activation and ERK-mediated post-translational stabilization. Our data showed that p38α, a kinase involved in CRC metabolism and survival, contributes to both mechanisms. Previous reports in other tissues provided evidence that Wnt3a can activate p38, and the p38 pathway feeds into the canonical Wnt/β-catenin pathway at least at the level of GSK3β. Our findings also highlighted that CRC cells and colorectal cancer stem cells (CRC-SCs) have higher levels of activated p38 than their normal counterparts, and experiments using kinase-specific inhibitors revealed that these cells are "addicted" to p38 activity. Importantly, we found that p38α co-immunoprecipitates with β-catenin in both normal and cancer cells; however, these proteins are confined to the cytoplasm in colonocytes, while they significantly occupy discrete nuclear regions in CRC cells, CRC-SCs, and *in vivo* models. These data were further corroborated by the inhibitory effect of p38α blockade on several β-catenin-responsive genes (i.e. c-Myc, cyclin D1/2, survivin, and others). This functional interaction was further characterized by chromatin immunoprecipitation experiments, which demonstrated that p38α is a chromatin-associated β-catenin kinase required for the transcriptional induction of several Wnt target genes, including c-Myc. Additionally, we demonstrated that p38α, like ERK, stabilizes c-Myc protein levels by preventing its ubiquitination. The finding that the phenotypes arising after APC loss in the intestine are fully dependent on c-Myc target gene expression suggests that c-Myc inhibition may

be a good target for chemoprevention in CRC. These considerations underline the relevance of molecular profiling and preclinical investigation in order to achieve more efficient and accurate therapies. Indeed, our study identifies p38α as a promising therapeutic target acting directly on c-Myc and CRC-SCs, which are thought to be responsible for tumor proliferation, metastatic dissemination, and chemoresistance.

Introduction

1.1 The genetic-epigenetic interplay in Cancer

Cancer is a set of more than 100 different diseases in which abnormal cells divide in an uncontrolled way and can invade other tissues (metastasize). Carcinogenesis is driven by the accumulation of different types of alterations, which affect the structure and the function of the genome. Primarily, it has been described as a consequence of the accumulation of genetic mutations. This view has now been expanded to include epigenetic changes. Genetic and epigenetic alterations allow cells to lose all physiological processes and mechanisms of control which regulate the homeostatic balance between cell proliferation and cell death (Hanahan D and Weinberg RA, 2011). Studying the complexity of cancer, ten biological capabilities were identified as "Hallmarks of cancer", as common principles acquired during the multistep development of human tumors. These characteristics, that distinguish cancer cells from normal cells, include: self-sufficient cell division, insensitivity to signals to stop cell division, resisting cell death, limitless reproductive potential, creating their own blood supply, ability to invade other organs, ability to survive with little oxygen, evading the immune system, genome instability and inflammation. Epigenetic mechanisms contribute to each hallmark by modulating chromatin structure and factors involved in this regulation through tumor suppressor silencing, oncogene activation by repurposed enhancers, or cell fate transitions **(Figure 1)**.

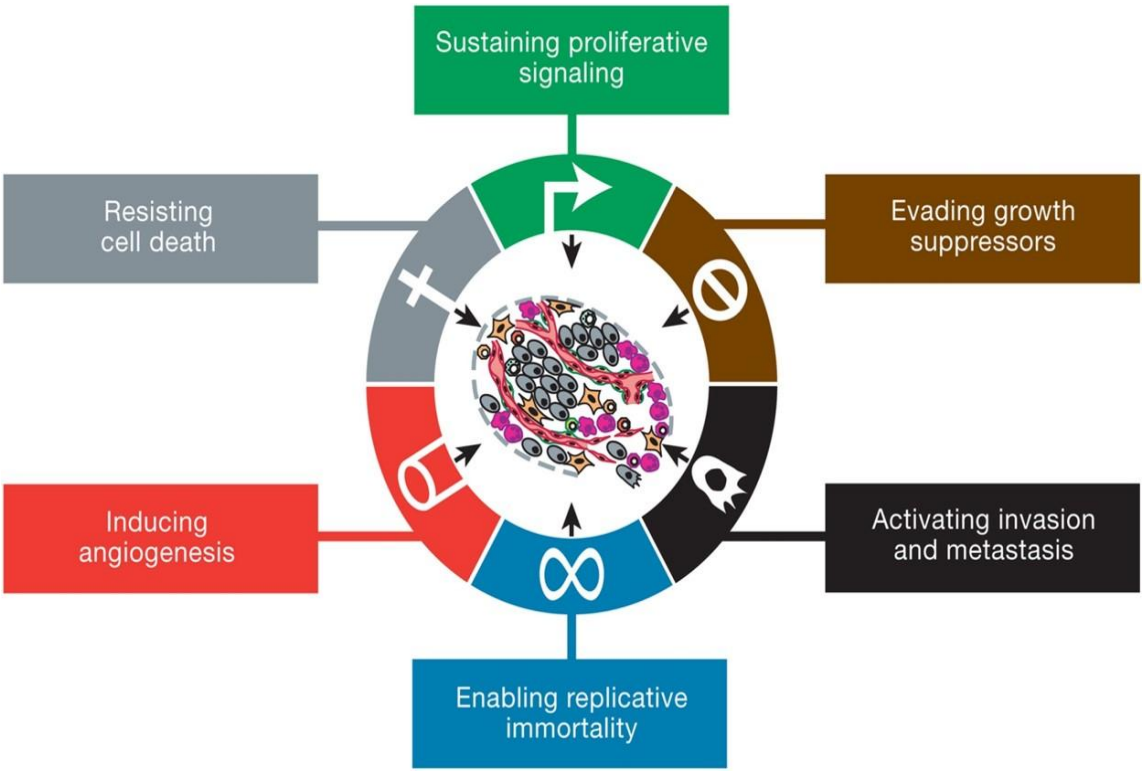

Figure 1. The hallmarks of cancer. Ten functional capabilities are acquired in the multistep carcinogenesis that leads to human cancer. The order in which they are acquired and the importance of their contributions appears to vary across the spectrum of human cancers. (Adapted from Hanahan D and Weinberg RA, 2011).

1.2 Colorectal cancer

Colorectal cancer (CRC) is the main malignant tumor affecting the gastrointestinal tract and it is the third most common cancer in both men and women (Haggar FA and Boushey RP, 2009; Bhandari A, Woodhouse M, and Gupta S, 2017). Worldwide, about 2 million people each year will develop CRC (WORLD HEALTH ORGANIZATION -2018- https://www.who.int/news-room/fact-sheets/detail/cancer) with a substantial variation in the five-year relative survival rate in relation to the stage of disease at diagnosis. 93% of patients diagnosed with the earliest stage of disease survived five-years from diagnosis compared to only 14% of those with advanced disease which had spread to other parts of the body at diagnosis **(Figure 2)**.

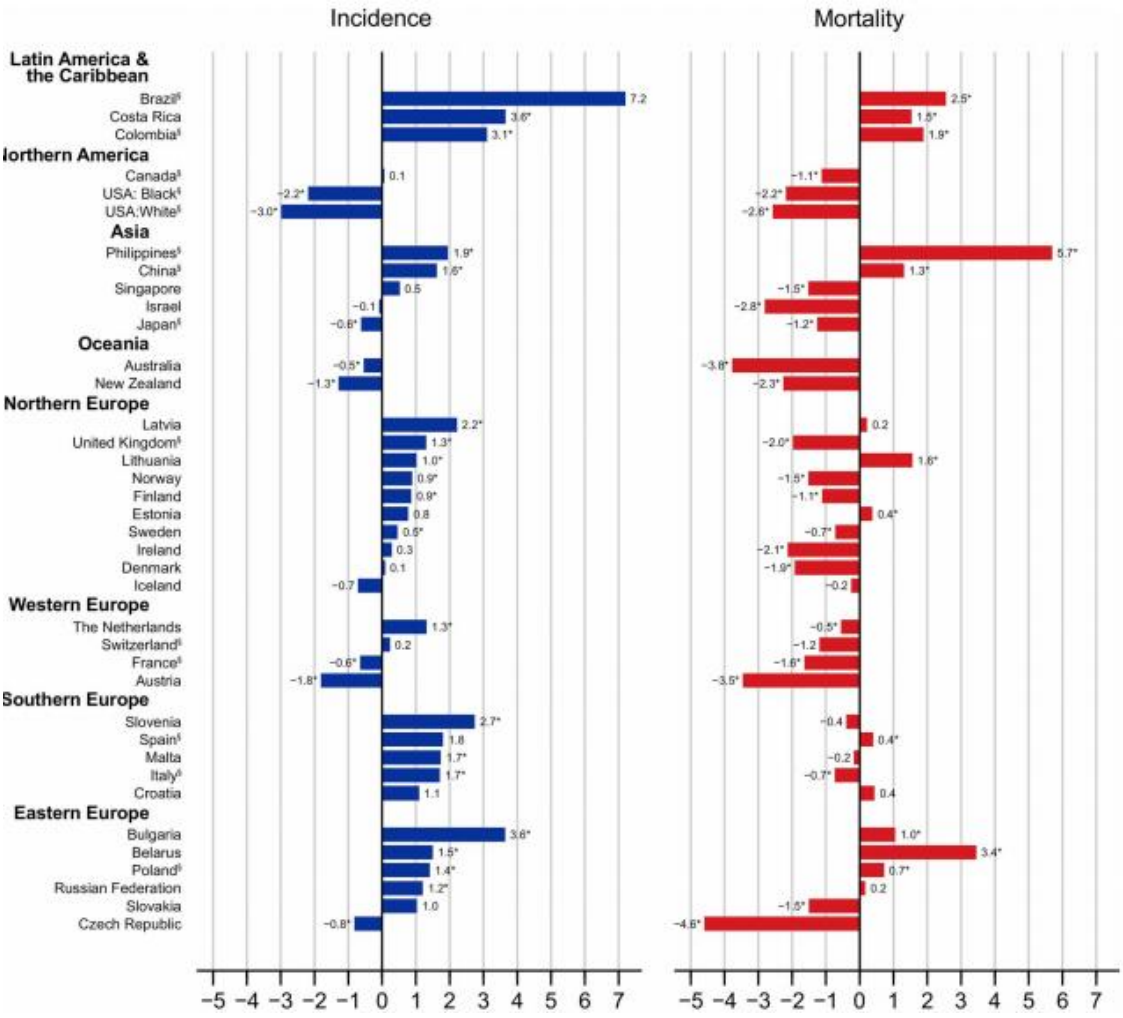

Figure 2. Average annual percentage change of colorectal cancer incidence and mortality in the most recent period (10 years). (Adapted from Arnold M et al, 2016).

Every year in our country, about 27,000 people suffer from CRC, and over half of them die due to illness (data from AIRTUM -Associazione Italiana Registro Tumori 2017-). The risk of CRC increases with age, indeed the median age at diagnosis is 68 in men and 72 in women. Furthermore males are affected slightly more often than females **(Figure 3)**.

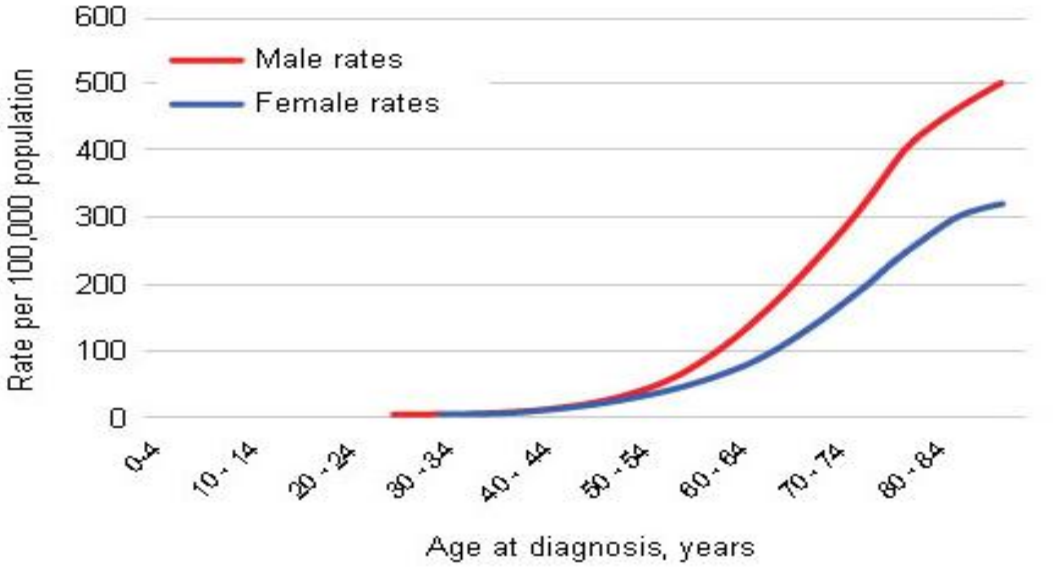

Figure 3. Age-specific incidence of CRC in men and women. (Adapted from Cancer Research: bowel cancer incidence statistics, 2017).

Approximately 5% of men and women will be diagnosed with CRC in their lifetime. People with a first-degree relative (parent, sibling or child) who has been diagnosed with CRC have 2 to 3 times the risk of developing the disease compared to people without this family history, depending on the age at diagnosis and the number of affected relatives. Risk is also increased among people with a first or second-degree relative diagnosed with adenomas. Also, hereditary factors, such as Lynch syndrome (HNPCC), familial adenomatous polyposis (FAP) and rare hamartomatous polyposis such as the Peutz-Jeghers (PJ) syndrome, the juvenile polyposis (JP) syndrome, the Cowden syndrome and the Bannayan-Riley-Ruvalcaba (BRR) syndrome increase CRC risk **(Figure 4)**.

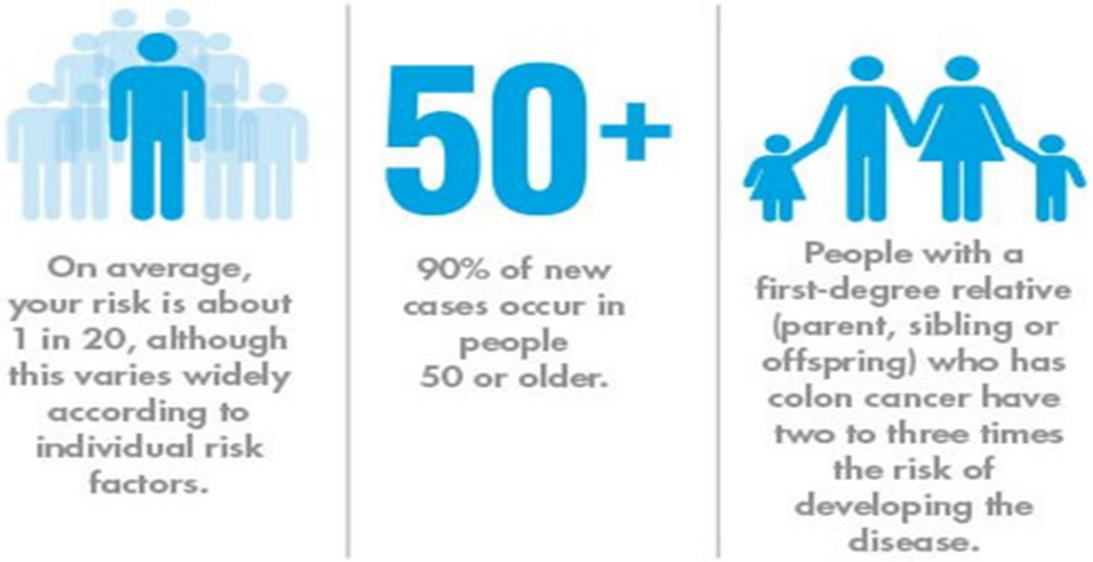

Figure 4. CRC at a glance. The risk of CRC during lifetime is approximately 5%. People older than 50 years old are at the highest risk for CRC (90% of cases occur in people aged 50+) and therefore should receive regular screenings. This is particularly important if a first degree family's medical record shows history of polyps and colon cancer which could double or even triple the risk of developing the disease. (From Gastrointestinal Specialists, 2018).

Aside from age and family history, many of the known risk factors for CRC are behaviors traditionally associated with high-income countries, such as a sedentary lifestyle, western diet, and smoking. The prevalence of these factors is reflected in the substantial variation in CRC incidence worldwide, which is highest in developed countries and lowest in sub-Saharan Africa (Arnold M et al, 2016).

The slow course of growth from precancerous polyp to invasive cancer provides a unique opportunity for the prevention and early detection of CRC. Screening can prevent cancer through the detection and removal of precancerous growths and can detect cancer at an early stage, when treatment is usually more successful. As a result, screening such as fecal occult blood test and colonoscopy, reduce CRC mortality both by the decreasing incidence of disease and by increasing the likelihood of survival.

Surgery is the most common treatment for CRC which has not spread. Chemotherapy, alone for colon cancer or in combination with radiation for rectal cancer, is given before (neoadjuvant) or after (adjuvant) surgery to most patients whose cancer has penetrated the bowel wall deeply or spread to lymph nodes. For metastatic CRC treatment typically include chemotherapy with FOLFIRI (5-Fluorouracil or capecitabine and irinotecan) or

FOLFOX (oxaliplatin and irinotecan) and/or targeted therapy. Indeed, the core of the chemotherapy regimens is 5-FU, a fluorinated pyrimidine which inhibits DNA synthesis, with the addition of calcium leucovorin increasing the response rate (Zhang ZG et al, 1992; Petrelli N et al, 1989). Other compounds used in systemic chemotherapy are Capecitabine, an orally administered form of 5-FU, Oxaliplatin, a DNA replication inhibitor, and Irinotecan, a topoisomerase inhibitor. All these compounds were developed to preferentially target cancer cells due to their higher growth rate compared to normal cells. However, as several normal cell types in the human body display high proliferation levels, and because these chemical compounds target every cell in the organism, the side effects associated with the therapies are of great relevance. Among these the most common are: stomatitis, hand-foot syndrome, diarrhea, neutropenia, nausea, alopecia, and sensory neuropathy. Moreover, the chemotherapy affects apoptosis by inducing DNA damage response, but gene mutations at apoptotic and/or anti-apoptotic loci cause the acquisition of chemoresistance.

Due to the requirement for more selective pharmaceutical compounds, a class of humanized antibodies targeting growth and angiogenic factors were developed and are now available for clinical trials. According to ClinicalTrials.gov (https://clinicaltrials.gov/ct2/results?cond=colorectal+cancer&term=&cntry=&state=&city=&dist=) 1850 studies on CRC are currently ongoing. Recently, Bevacizumab, a monoclonal antibodies targeting vascular endothelial growth factor (VEGF), and Cetuximab or Panitumumab, two chimeric monoclonal antibody targeting epidermal growth factor receptor (EGFR) used in KRAS wild type tumors, have entered routine clinical practice in metastatic CRC (Goldberg R M, Montagut C, Wainberg R A, Ronga P, Audhuy F, Taieb J, Stintzing S, Siena S, Santini D, 2018). In combination with chemotherapy, they offer higher survival advantages compared to chemotherapy alone. The major limitation is the limited presence of the targeted antigen on the cancer cell's surface or in the cancer microenvironment. For instance, VEGF is over-expressed in 50% of CRC and the addition of Bevacizumab to normal chemotherapy led to a 10% improvement in the response rate (44,8% versus 34,8%). Nonetheless, rare but serious side effects have been observed using Bevacizumab. Clinical trials are now directed at evaluating new drug combinations, treatment schedules, and new ways of diagnostic imaging to enhance tumor regression, increasing overall survival, and improving the quality of life for patients. Indeed, today, there is a new trial ongoing, which combined MEK and

MDM2 inhibition in order to induce apoptosis in RAS/BRAF-mutant and TP53 wild-type CRC models. Clinicians are using new inhibitors, such as Trametinib, an orally bioavailable inhibitor of MEK/ERK kinases with potential antineoplastic activity. Trametinib specifically binds to and inhibits MEK 1 and 2, resulting in an inhibition of growth factor-mediated cell signaling and cellular proliferation in various cancers (Flaherty KT et al, 2012). Finally, the main purpose of another in-progress clinical trial is to evaluate the safety of the drug Prexasertib (cell cycle checkpoint kinase 1 and 2 inhibitor) in combination with Ralimetinib, p38α inhibitor, in participants with advanced or metastatic CRC (Bence A L, McNeely S C, and Beckmann R P, 2017). However, other therapeutic targets are being awaited to develop new strategies, which are expected to prove more effective, more specific and possibly associated with fewer side effects.

1.2.1 Genetic alteration and progression of CRC

CRC arises from adenomas, which gradually progress through an increase in size, dysplasia and the acquisition of villous morphology. At the beginning, the proliferation is induced by the loss or inactivation of the familial adenomatous polyposis (APC) gene on chromosome 5 or by activating a mutation of β-catenin on chromosome 3. One of these hyperproliferating cells may then give rise, by clonal expansion, to a small adenoma. Subsequently, mutation in the RAS pathway (KRAS 50% or BRAF 11%) appears to occur and through clonal expansion produces a larger and more dysplastic adenoma. After which, usually happens allelic deletions of chromosome 18q and 17q with the loss of SMAD4 and p53 genes. Tumors continue to progress once carcinomas have formed, and the accumulated loss of suppressor genes on additional chromosomes correlates with the ability of carcinomas to metastasize and cause death (Fearon ER and Vogelstein B, 1990; Kinzler KW and Vogelstein B, 1996; Kinzler KW and Vogelstein B, 1996). The evolution from benign growth to invasive stages often occurs over 10 to 20 years. This gives rise to dynamic processes whose genetic contributions interconnect with each other and with the environment. The adenoma-carcinoma sequence is characterized by the lack of allelic balance at several chromosomal loci (APC 5q, DCC/SMAD4 18q and p53 17q), and chromosomal amplification and translocation which together contribute to tumor aneuploidy and chromosomal instability (CIN). This canonical pathway happens in 85% of sporadic CRCs.

The remaining sporadic cases, about 15%, are microsatellite instability (MSI) phenotypes, mostly due to mismatch (MMR) and base-excision (BER) DNA repair mechanism impairments, giving rise to frameshift or base-pair substitutions in short tandem-repeat sequences. This is the case for mutations in various genes (MLH1, MSH2, MSH6) often associated with CpG methylation-silenced promoter regions (MLH1) and in genes (MINT1, MINT2, MINT3) involved in NOTCH signaling. Interestingly, together with methylation most of the defects in MMR or BER genes specifically induce cancer initiation. The HNPCC syndrome is linked to mutations in MMR genes, which are inherited in a dominant pattern and cause multiple primary CRCs, acceleration of tumor progression in the case of somatic mutations, as well as other tumors (Markowitz SD and Bertagnolli MM, 2009).

As well as CIN- or MSI-associated CRCs, several low-penetrant mutations have been observed, inducing rare syndromes. Germline mutations of the LKB1/STK11 tumor suppressor gene on chromosome 19p, driven by LOH or by missense mutations and frameshifts, have been shown to cause the rare PJ syndrome (Howe JR et al, 1998). Additionally, mutations in the tumor suppressor PTEN, which are frequently observed in tumors, are linked to the Cowden syndrome and the BRR syndrome, a spectrum of conditions collectively known as PTEN hamartoma tumor syndromes.

Epigenetic alterations in CRCs are widely reported, mainly the gene promoter DNA methylation. Classification of CRCs according to DNA methylation status has identified a subset of tumors with extensive epigenetic instability, characterized by the concordant promoter hypermethylation (Toyota M et al, 2000). The existence of a CpG island methylator phenotype (CIMP) and its correlation with clinicopathologic features has been confirmed extensively by the use of high-throughput techniques (Estecio MR et al, 2007; Weisenberger DJ et al, 2006). Typical high-level CIMP (CIMP high, CIMP1) CRCs are associated with microsatellite instability through epigenetic silencing of mismatch repair gene MLH1. They often have a BRAF mutation, and they occur predominantly in the proximal colon. Low-level CIMP (CIMP low, CIMP2) has been characterized by DNA methylation of a limited group of genes and mutation of KRAS (Shen L et al, 2007) **(Figure 5)**.

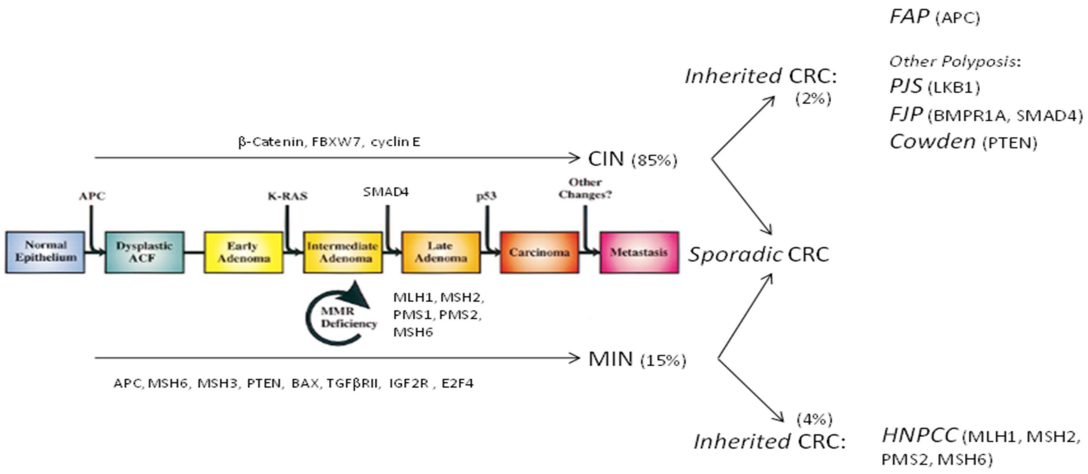

Figure 5. Colorectal tumorigenesis. Schematic representation of hereditary and sporadic predisposition. (Adapted from Kinzler W and Vogelstein B. Cell, 87: 159-170; 1996).

Activation of the Wnt pathway has been linked to CRC since the recognition that abnormalities of chromosome 5q were early events in the carcinogenic process for sporadic and hereditary (FAP) tumors. Encoded at 5q is the APC gene, the protein product of which is a key component of the β-catenin destruction complex, together with GSK3β, Axin and CK1. About 90% of sporadic CRC show high levels of nuclear β-catenin resulting from mutations in the APC gene (90%) or β-catenin itself (5%) (Jeong W-J, Ro E J and Choi K-Y, 2018). Stabilized β-catenin exerts its oncogenic role by activating the transcription of many regulatory genes, such as c-Myc **(Figure 6)**.

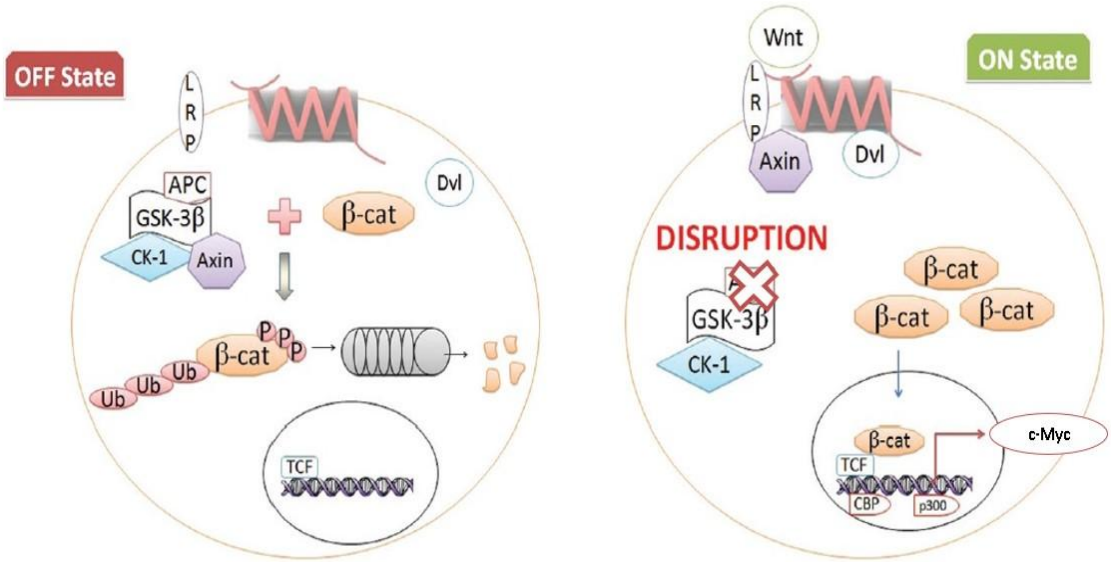

Figure 6. The Wnt canonical pathway. Wnt ligand binds to G-protein coupled receptors called Frizzled and initiates intracellular signaling cascade leading to nuclear accumulation of β-catenin and activation of target genes, which are mainly involved in proliferation. In the absence of Wnt, cellular β-catenin is phosphorylated by GSK3β and with the destruction complex catalyzed its degradation. High level of nuclear β-catenin results from mutation in the APC protein or β-catenin itself, leading to costitutive activation of the Wnt pathway, loss of normal cellular architecture and neoplastic conversion. (Adapted From Kazi M, Trivedi T, Kobawala T, Ghosh N, 2016).

1.3 c-Myc oncogene: regulation and function

The *c-Myc* proto-oncogene was identified for the first time as the cellular homolog to the viral oncogene (v-*myc*) of the avian myelocytomatosis retrovirus (Pelengaris S and Khan M, 2013).

c-Myc protein belongs to the Myc family of transcription factors, which also includes *n-Myc* and *l-Myc* genes. c-Myc as transcription factor contains a basic helix-loop-helix (bHLH) and leucine zipper (LZ) motives. Through its bHLH DNA-binding motif, c-Myc interacts with the E-box sequence, a specific DNA sequence (CACGTG), while the leucine zipper TF-binding motif allows the dimerization with another bHLH transcription factor called Max **(Figure 7)**.

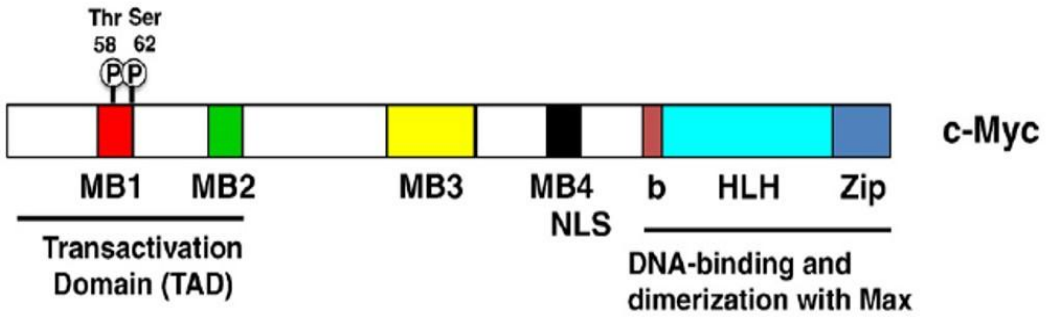

Figure 7. Structure of the c-Myc protein. TAD, transcriptional activation domain; Thr-58 and Ser-62, regulatory phosphorylation sites; MB1-4, the evolutionary conserved Myc boxes 1–4; NLS, nuclear localization signal; bHLHZip, basic region/helix–loop–helix/leucine zipper. (Adapted from Larsson LG and Henriksson MA, 2010)

Surprisingly, Samson et al, in 2008 found that after APC loss, nuclear β-catenin was not sufficient to induce any phenotypes in the absence of c-Myc, indeed over half of Wnt target significantly induced after APC loss were no longer up-regulated in the absence of c-Myc. These data indicate that the phenotypes acquired after APC loss in the intestine are fully dependent on c-Myc target gene expression (Wilkins JA and Sansom OJ, 2008).

c-Myc is one of the most important factors implied at the beginning and during the progression of CRC, indeed it is found overexpressed in up to 70-80% of CRCs. Considering its role in intestinal tumorigenesis, it is important to underline that it is maintained upregulated in CRC by two different mechanisms. On the one hand there is the transcriptional activation by β-catenin due to APC inactivation, on the other hand there is the post-translational stabilization due to serine 62 (S62) phosphorylation mediated by ERK, a downstream kinase at KRAS, which represents the second mutation in the classic adenoma-carcinoma sequence.

Indeed the stability of c-Myc protein is controlled by phosphorylation at two specific sites: S62 and threonine 58 (T58). Phosphorylation at T58 but not at S62 making c-Myc prone to the subsequent proteasome degradation (Sears R, 2004) **(Figure 8)**.

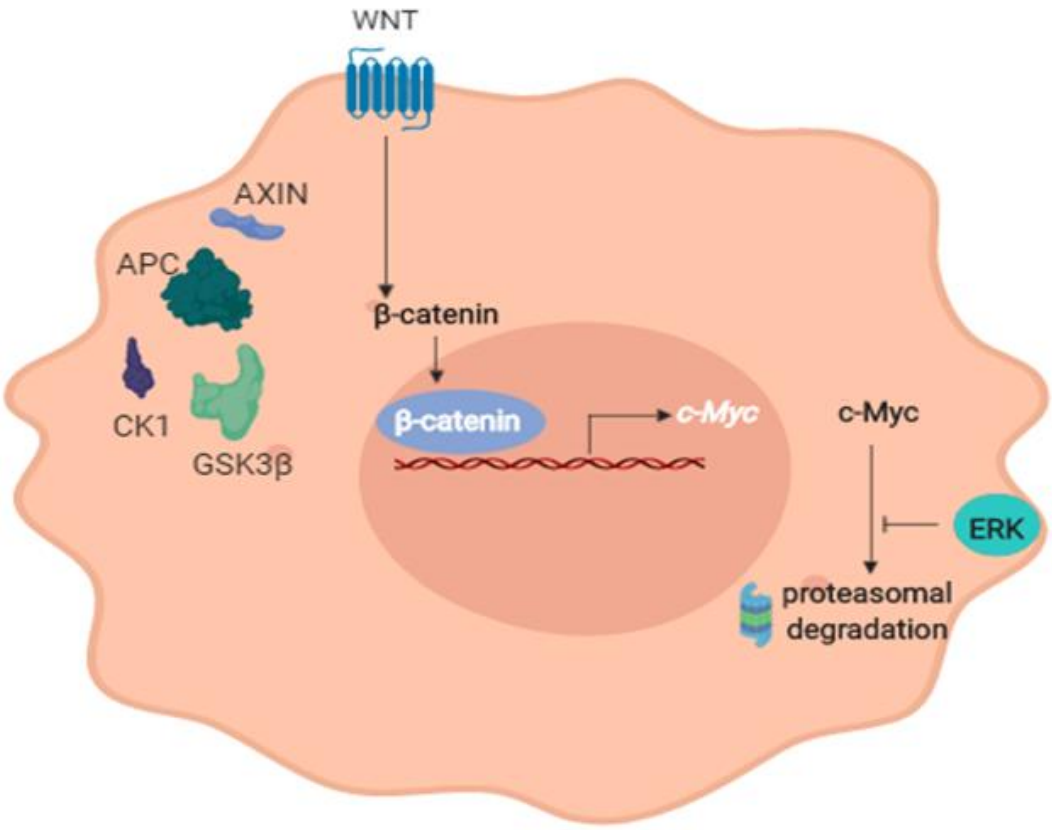

Figure 8. The upregulation of c-Myc in CRC. c-Myc is maintened upregulated in CRC by two different mechanism. On the one hand there is the transcriptional activation by β-catenin due to APC inactivation, on the other hand there is the post-translational stabilization due to serine 62 phosphorylation mediated by ERK.

c-Myc deregulation is implicated in many pathological conditions, including genomic instability, uncontrolled cell proliferation, immortalization, escape from immune cells, angiogenesis and metastasis (Dang C V et al, 2006). Moreover, c-Myc can act on control points of gene expression programs that determine the cancer stem cells (CSCs) features. Indeed, c-Myc is highly expressed in these cells and required for maintaining their phenotypes, so its functions as a link connecting malignancy and 'stemness' (Zhang H et al, 2019). It has been shown that c-Myc is indispensable for the self-renewal properties of colorectal cancer stem cells (CRC-SCs), since its ablation reduces the formation of tumorspheres (Sanchita R and Adhip P N M, 2012). Invasive and migratory abilities are critical features of CRC-SCs, which promote the establishment of a functional phenotype associated with tumor aggressiveness. It has been demonstrated that c-Myc plays a fundamental role in invasion and migration of CRC-SCs since its knockdown inhibits these two features. Moreover, c-Myc is considered the core of CRC-SCs chemoresistance mechanism. Indeed it was reported that c-Myc expression in surviving tumor cells (CRC-SCs), increases after treatment with platinum-based chemotherapy (Walker T L et al, 1996). Furthermore, it has been shown that c-Myc induces a high expression of the ATP-binding cassette and multidrug resistance protein, since its silencing decreases the expression of ABCG2 and ABCB5 and sensitizes CRC-SCs to chemotherapy-induced cytotoxicity (Zhang HL et al, 2019). Once tumor cells become resistant to conventional therapy such as cisplatin, they naturally develops cross-resistance to many other chemotherapeutic agents leading to multi-drug cross-resistance. Since c-Myc protects tumor genomes from therapeutic DNA damaging drugs, it could be a promising target to overcome chemoresistance in various types of cancers, including CRC (Elbadawy M, Usui T, Yamawaki H and Sasaki K, 2019) **(Figure 9)**.

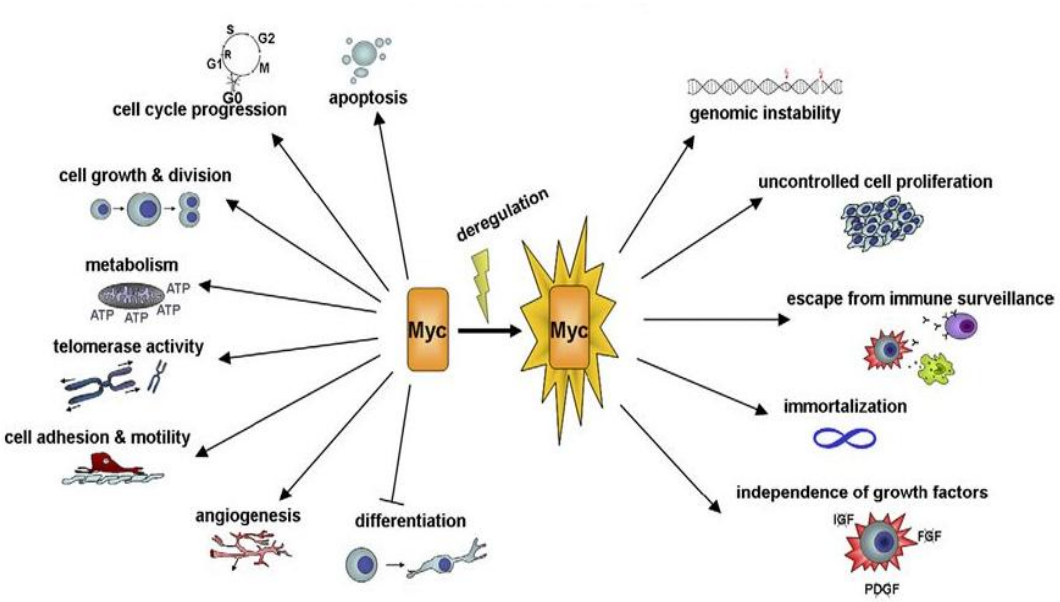

Figure 9. Cellular processes controlled by c-Myc during normal conditions and during tumorigenesis. c-Myc is a key regulator of many biological activities including cell growth and division (regulation of chromatin modification and components of the biosynthetic machinery); cell-cycle progression (modulation of cyclins, cyclin-dependent kinases, cyclin-dependent kinase inhibitors and phosphatases); apoptosis (p53 dependent or independent mechanisms); cell differentiation (downregulation of growth arrest genes); cell metabolism (glycolysis, amino acid biosynthesis and transport, synthesis of macromolecules and DNA metabolism); angiogenesis (upregulation of VEGF); cell adhesion and motility (control of expression of integrins). Deregulation of Myc may result in apoptosis, genomic instability, uncontrolled cell proliferation, escape from immune surveillance, growth factor independence, and immortalization. (From Vita M and Henriksson M, 2006).

1.4 Cancer stem cell in CRC initiation and progression

It is assumed that the tumor is a heterogeneous entity produced by the proliferation of tumor-initiating cells. So many similarities have been widely assessed between these undifferentiated cells and normal stem cells that the name of "cancer stem cells" (CSC) has been given to the tumor-initiating cells (Saulnier N et al, 2009).

Self-renewal and multi-lineage differentiation are the main features of stem cells and these two peculiarities in addition to the tumorigenic potential typical of cancer cells, produced the three main parameters that outline the profile of CSC. Specifically, stem cells can undergo asymmetric division by which a cell can self-renew producing one daughter cell that preserves stemness and another cell that has the potential to differentiate during cell division. Multi-lineage differentiation is defined as the ability of a stem cell to give rise to many specialized cell types. It happens in the intestinal crypt where a colorectal stem cell (CR-SC) should be able to produce several cell types, which include enterocytes, goblet cells, paneth cells, and enteroendocrine cells (Abetov D et al, 2015). The tumorigenic potential expresses itself through tumor initiation and recurrence. Indeed, following the growth of the primary tumor, CSCs are implicated in the metastasis program through dormancy, re-initiation, and escape of immune surveillance. This can be achieved by Wnt signaling that can re-initiate cell cycle progression in dormant CSCs by upregulating *c-Myc* expression. Accordingly, stable c-Myc knockdown decreases colony formation on primary and secondary organs (Wolfer A et al, 2010). Moreover, CSCs are generally resistant to chemotherapy because of the enhancement of active ABC transporters that rapidly efflux chemotherapeutic agents. Indeed, indiscriminate use of chemotherapeutic agents may select the growth of CSCs that can survive this treatment, with the result that they then encounter less competition for resources. In support of this concept, CD133+ cells (a marker for CSC) were enriched when xenografts derived from CRC-SCs were exposed to oxaliplatin (Dallas NA et al, 2009). Additionally, CSC can tolerate radiotherapy upregulating multiple pathways of DNA damage response (Vila PM et al, 2017). Thus, CSCs are thought to be responsible for cancer relapse and to contribute to tumor chemo and radioresistance **(Figure 10)**.

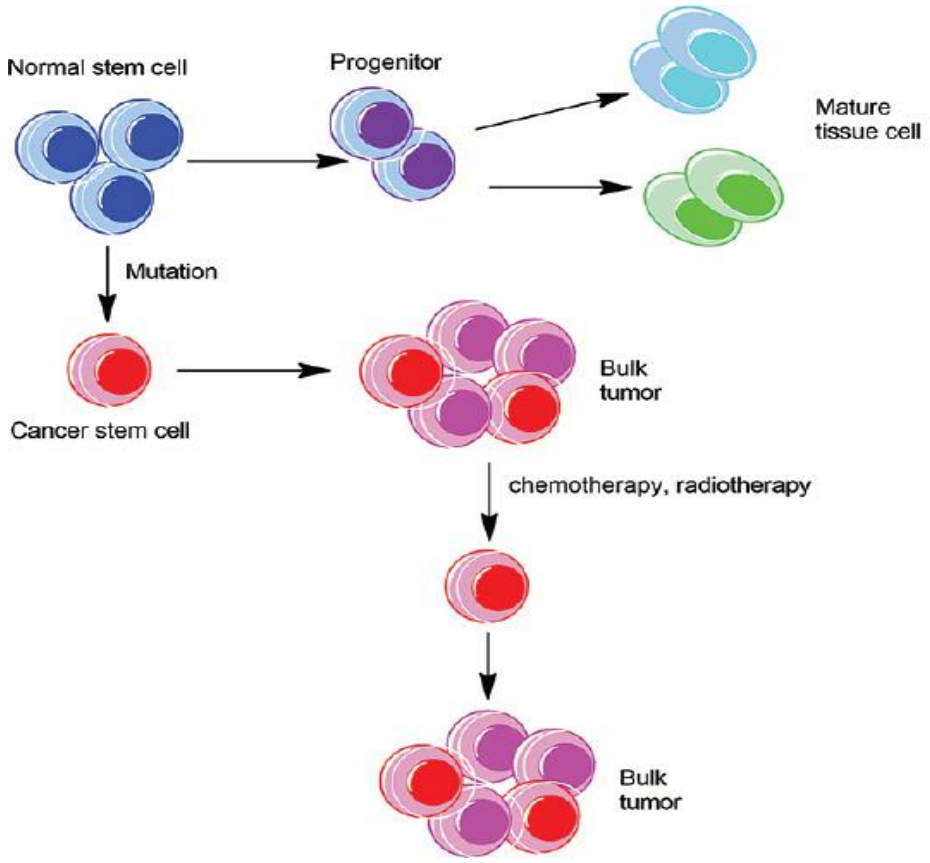

Figure 10. The role of cancer stem cells. Normal tissues arise from a central stem cell that grows and differentiates to create progenitor and mature cell populations. Cancer stem cells arise by means of a mutation in normal stem cells or progenitor cells and subsequently grow and differentiate to create primary tumors. Like normal stem cells, cancer stem cells can self-renew, give rise to heterogeneous populations of daughter cells, and proliferate extensively to form tumor at the end. During chemotherapy and radiotherapy, the majority of cells in a primary tumor may be destroyed; however, if the cancer stem cells are not eradicated, the tumor may regrow and cause a relapses.(Adapted from Wang Z, Yang H, Wang, X, Wang L, Cheng Y, Zhang Y and Tu Y, 2016).

Usually, CRC-SCs have the same molecular signaling profile as normal stem cells (Abetov D et al, 2015). Indeed, it is important to underline how the microenvironment of the intestinal crypt plays a key role in the initiation and maintenance of CRC. CRC-SCs in the crypt receive Wnt factors that stimulate the undifferentiated state, obtain NOTCH ligands from neighboring cells required to block differentiation, and receive many mitogenic stimuli that activate the epidermal growth factor receptor (EGFR). Also, the niche defend CRC-SCs from cytostatic signals derived from bone-morphogenetic protein (BMP) and the transforming growth factor β (TGFβ) pathways (Batlle E and Clevers H, 2017). In this signal network, the Wnt pathway plays the most

important role in maintaining the CRC-SC crypt population at a proliferative state. When the pathway is over-activated, crypts enlarge; when the pathway is blocked they disappear. c-Myc, as the main Wnt target, plays a major role in this switch by direct repression of the p21 promoter. Indeed declined expression of c-Myc results in the transcription of p21, which in turn triggers G1 arrest (Elbadawy M, Usui T, Yamawaki H and Sasaki K, 2019). Finally, Muncan et al. have found that genetic ablation of c-Myc resulted in rapid loss of crypts and decreased cell numbers in crypts that remained (Muncan V et al, 2006) **(Figure 11)**.

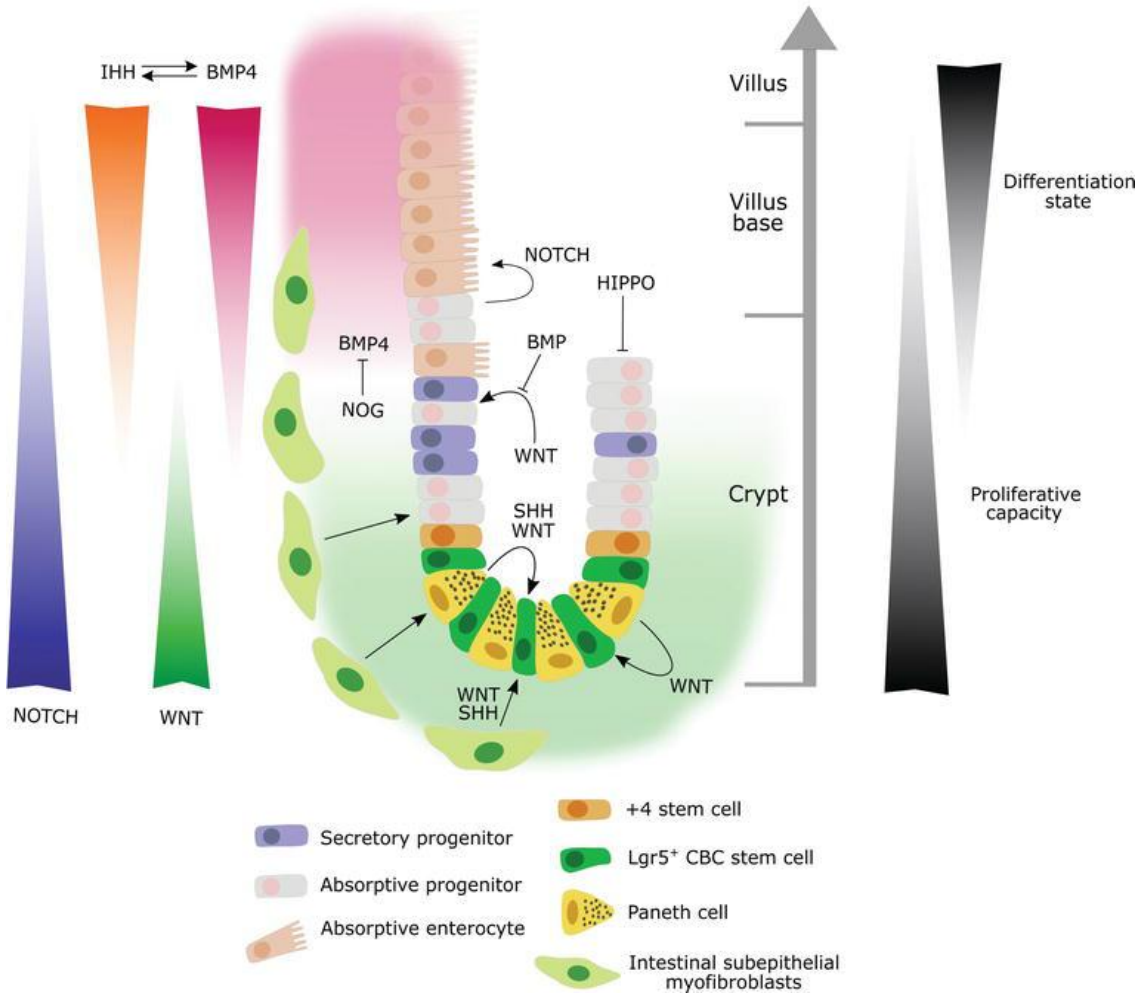

Figure 11. Schematic representation of the major signaling pathways involved in CSC biology. A gradient of BMP and Hh signaling, with relatively high activity in the villus and less activity within the crypt, regulates cell renewal and lineage specification. Wnt and Notch signaling gradients in the opposite direction (highest expression at the crypt base) play an important role in maintaining the stem cell compartment. (From Gleizes A, Cavailles V and Lapierre M, 2018).

1.5 The MAPK signaling: mechanism and functions in CRC

As mentioned above c-Myc is upregulated in intestinal tumorigenesis by transcriptional activation of β-catenin and the post-translational stabilization mediated by ERK.

The importance of ERK activation in the intestinal tumorigenesis was highlighted in a work carried out by Sung Hee Lee and colleagues, by the use of the $APC^{Min/+}$ model. The $APC^{Min/+}$ mouse was identified in 1990 from an ethylnitrosourea (ENU) mutagenesis screen in C57Bl/6J mice, which represents an animal model of FAP. The genetic basis for the intestinal phenotype is a T-to-A transversion at nucleotide 2,549 of the mouse *APC* gene that truncates the APC protein at amino acid 850. These mice develop multiple intestinal neoplasia (Min) after they spontaneously lose the heterozygous wild-type *APC* allele in intestinal epithelial cells, and consequently die by the time they reach 6 months of age (Moser AR et al, 1990). Sung Hee Lee and colleagues revealed that the activation of ERK in these cells is essential for tumor growth in $APC^{Min/+}$ mice via the stabilization of c-Myc protein (Lee SH et al, 2010).

In CRC, the MEK/ERK signaling pathway has been frequently found to be overactive due to activating mutations in the upstream kinases RAS (50%) and BRAF (11%). This pathway is activated by a variety of different stimuli, many of which promote cell proliferation and inhibit anti-proliferative and pro-apoptotic responses. This pathway is being widely studied as a promising pharmacological target.

ERK belongs to MAPKs family, which is composed of protein kinases whose function and regulation have been conserved during evolution from unicellular organism such as brewers' yeast to complex organisms including humans (Widmann C et al, 1999). MAPKs are expressed in all cell types and regulate a variety of physiological processes such as cell growth, metabolism, differentiation, and cell death. MAPK signaling is over-activated in cancer, especially in CRC.

To date, six distinct groups of MAPKs have been characterized in mammals: the ERK 1/2, ERK 3/4, ERK5, ERK 7/8 family, the Jun N-terminal kinases JNK 1/2/3 and the p38 MAPKs p38α/β/γ/δ (Kyriakis JM and Avruch J, 2001-2012).

It is becoming increasingly clear that the pathways rather than the individual genes appear to govern the course of tumorigenesis. A paradigm of this view is represented by the p38 pathway, which is involved in proliferation, differentiation, metabolism and cell death (Hui L et al, 2004; Simone C et al, 2004; Grossi et al, 2014).

In mammals, four genes have been identified that encode p38 MAPKs: MAPK14 (p38α), MAPK11 (p38β), MAPK12 (p38γ) and MAPK13 (p38δ). p38α and p38β are closely related proteins that might have overlapping functions. While p38α and p38β expression is ubiquitous, the expression of p38γ and δ is only related to some specific tissue, e.g. muscle expresses p38γ and p38δ is identified in skin, small intestine and kidney (Cuadrado A and Nebreda AR, 2010; Cuenda A and Rousseau S, 2007). In addition, the differentiation status of the cell controls the expression profile of p38 isoforms. For example, undifferentiated intestinal epithelial cells show the α, β and γ isoforms, while differentiated cells express the α, γ and δ isoforms (Vachon PH et al, 2002; Comes F et al, 2007) **(Figure 12)**.

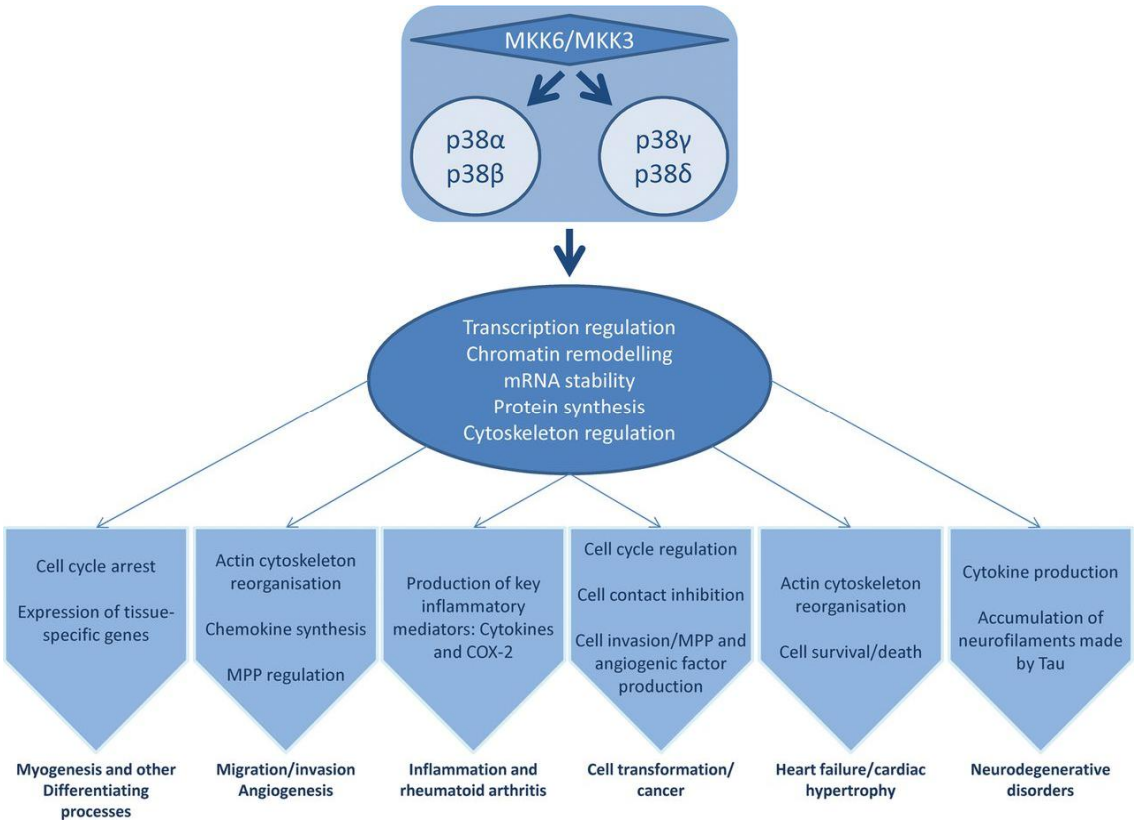

Figure 12. p38 MAPK family regulate multiple cellular processes and physiological functions. Deregulation of p38 MAPKs pathway lead to the development of several pathological conditions. (Adapted from Oeztuerk-Winder F and Ventura JJ, Biochemical Journal, 2012).

The strict regulation of life/death signals by p38 MAPKs can result in opposite molecular functions during tumor growth. Currently, it is assumed that p38 acts as

tumor suppressor in normal cells at the onset of cellular transformation, subsequently after the acquisition of the malignant phenotype p38 acts as an oncogene (Dolado I et al, 2007; Hui L et al, 2007). Several studies, taking advantage of mouse models deficient in p38 or its upstream activators (such as MAPKKs, GADD45α, MAPK5), demonstrated higher susceptibility to tumor development (Ventura JJ et al, 2007; Brancho D et al, 2003; Bulavin DV et al, 2004; Tront JS et al, 2006).

However, after the acquisition of the malignant phenotype, p38 is involved in sustaining tumor growth in many types of cancer including follicular lymphoma, lung, thyroid, colorectal, ovarian (Matrone A et al, 2010; Grossi V and Simone C, 2012) and breast carcinomas, as well as gliomas and head and neck squamous cell carcinomas (Junttila MR et al, 2007; Bakin AV et al, 2002; Hsieh YH et al, 2007; Kim MS et al, 2003). In these cases, depending on the type and stage of the tumor, cancer cells with pro-tumorigenic activation of the p38 MAPK pathway may have a selective advantage.

The different p38 MAPK isoforms have been shown to have redundant, specific or even opposite functions depending on the cell type involved and the nature of the stimulus. The p38α signaling pathway shows the typical kinase cascade of the MAPK family, which result in the regulation of several cellular functions (Oeztuerk-Winder F and Ventura J-J, 2012). The potential pro-tumorigenic role of p38α signaling is based on correlations with bad prognosis in cancer, and there is evidence that this pathway may contribute to the survival or proliferation of cancer cell lines from different origins, including breast (Chen L et al, 2009), colorectal (Chiacchiera F and Simone C, 2009), prostate (Ricote M et al, 2006) or skin (Schindler EM et al, 2009). In addition, p38α is involved in cancer cell metabolism by driving HIF1α stabilization (Emerling BM et al, 2005), in chondrosarcoma cell proliferation (Halawani D et al, 2004) and tumor dormancy (Adam AP et al, 2009). Typical features of cancer aggressiveness, such as migration and invasion, are also positively regulated by p38 MAPK activation in breast, head and neck squamous and hepatocellular carcinomas (Junttila MR et al, 2007; Bakin AV et al, 2002; Hsieh YH et al, 2007; Kim MS et al, 2003). Importantly, in our lab, we also detected aberrant activation of p38α in high-grade CRC biopsies (Chiacchiera F et al, 2012) and inflammatory bowel disease-associated human CRC specimens (Simone C, unpublished results). Our lab has previously reported that p38α is required for CRC cell proliferation and survival and that its genetic depletion or the pharmacological blockade of its kinase activity induces growth arrest, autophagy and cell death in a cell-

type-specific manner (Comes F et al, 2007; Simone C, 2007; Madia F et al, 2012). Studies indicate that the autophagy response to p38α blockade initially represents a survival pathway, while prolonged inactivation of the kinase leads to cell death (Comes F et al, 2007; Chiacchiera F et al, 2009). *In vivo*, pharmacological blockade of p38α has both a cytostatic and cytotoxic effect on colorectal neoplasms, and is associated with nuclear enrichment of FoxO3A and expression of its target genes p21 and PTEN (Chiacchiera F et al, 2009) **(Figure 13)**.

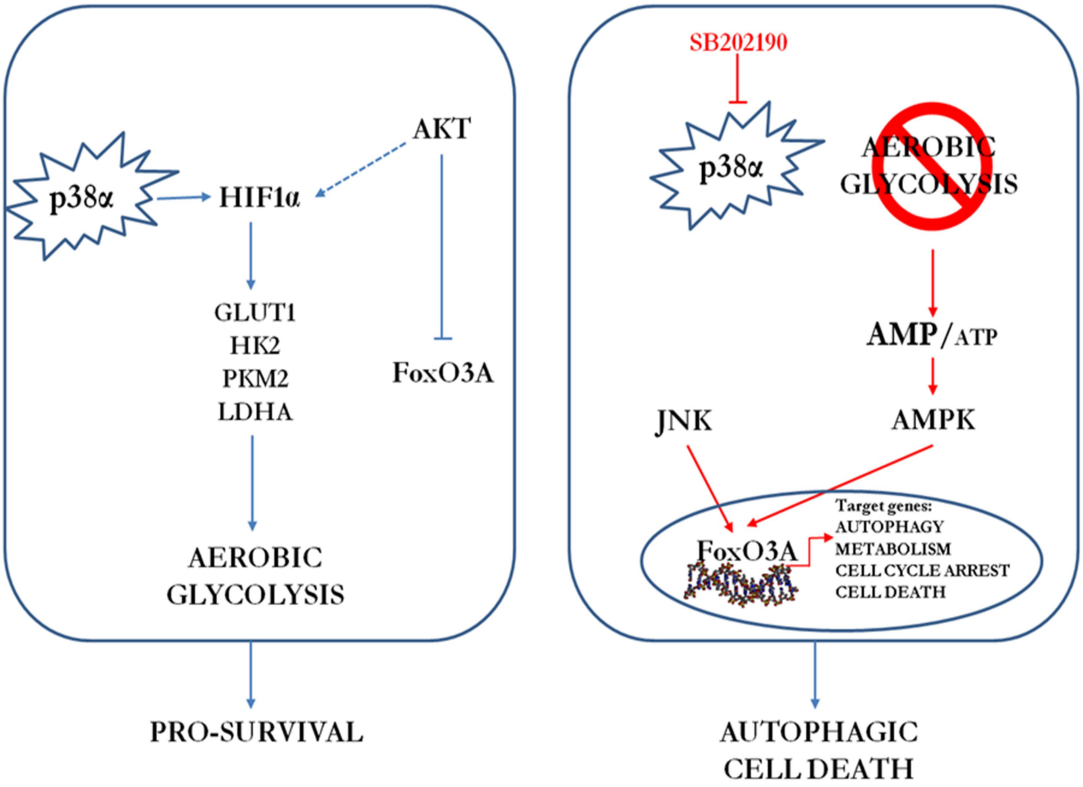

Figure 13. Schematic representation of the p38α involvement in CRC. (**a**) p38α is involved in the regulation of key metabolic cascades in CRC, sustaining HIF1α protein expression and the transcription of HIF1α target genes, such as GLUT1, HK2, PKM2 and LDHA. (**b**) p38α blockade causes a significant decrease in the intracellular levels of ATP, which correlates with a time-dependent reduction of HIF1α protein levels and the consequent decrease in HIF1α target gene expression and phospho-activation of AMPK. AMPK activity is required for the nuclear accumulation of FoxO3A and the subsequent activation of FoxO3A target genes involved in autophagy, metabolism, cell cycle arrest and cell death, leading to autophagic cell death in CRC in vitro and in vivo. PI3K/Akt and JNK kinases regulate the nuclear/cytoplasmic shuttling of FoxO3A proteins by phosphorylation. (Adapted from Grossi et al, 2014).

Recently, we demonstrated the existence of p38α and ERK crosstalk which is crucial for CRC therapy response. Indeed, p38α inhibition by SB202190 upregulates HER3, one of the receptor tyrosine kinases (RTK) of the EGF pathway and this effect is dependent upon the activity of FoxO3A and its cofactor Sirt1 (Brunet A et al, 2004). Concomitant MEK inhibition triggers Bax dependent apoptosis, and in fact the combined inhibition of p38α and MEK1 efficiently reduces the volume of xenografted orthotopic tumors and colitis-associated (mice treated with AOM/DSS) tumors *in vivo* (Chiacchiera F, et al 2012). Sorafenib is reported to potently inhibit nine protein kinases, including BRAF, the kinase upstream of MEK/ERK. It has also been shown to target the DFG-out conformational state, which is the inactive state of p38α kinase *in vitro*. In our lab was tested the association of Sorafenib, a type II kinase inhibitor, with SB202190, a type I inhibitor, which acts on p38α in DFG-in conformational state. The results indicated that simultaneous inhibition of p38α DFG-in and -out conformations and BRAF leads to a synergistic increase of the apoptotic response in CRC cells (Grossi V et al, 2012).

It is quite evident that p38 MAPK plays a critical role in several aspects of cancer biology including cell survival, cell death, cell differentiation/dedifferentiation, apoptosis, checkpoint control, overcoming dependence on addictive oncogenic pathways, drug resistance, cell migration, invasion and metastasis (Koul H et al, 2013).

p38 MAPK is relatively inactive in its non-phosphorylated form and becomes rapidly activated by phosphorylation of two residues Thr-Gly-Tyr motifs (Zhang F et al, 1994; Wilson KP et al, 1996). Phosphorylated p38 proteins can activate a variety of kinases, including MNK1, MNK2, MSK1, PRAK, MAPKAPK2 and MAPKAPK3, which are involved in controlling cytoplasmic and/or nuclear signaling networks and response to cytokines, growth factors, toxins and pharmacological drugs. Intriguingly, p38α can be considered a prototype of chromatin-associated kinase. Indeed, it is able to associate with and phosphorylate many transcription factors and it can recruit subunits of the SWI/SNF ATP-dependent remodeling complexes directly on DNA, thereby modulating chromatin structure and transcription. For instance, p38α phosphorylates MEF2 and stimulates the heterodimerization between MyoD/E47, inducing MyoD-dependent transcription (Simone C et al, 2004). Moreover, it has been proved that p38α phosphorylates BAF60c on threonine 229 promoting chromatin remodeling and assembly of the transcriptome for initiation of the transcription of MyoD target genes (Forcales S et al, 2012). Also, p38α phosphorylates MSK1, which in turn can

phosphorylates serine 10 on histone 3, inducing a chromatin modification permissive for transcriptional activation (Soloaga A et al, 2003). Additionally, p38α can physically interact with RNA Polymerase II and promote the elongation step of the transcription process (Alepuz P M et al, 2003). Finally, p38 can phosphorylate the TATA-binding protein (TBP) component of the TFIID transcription factor complex and enhance its binding to the TATA box (Biggs J R et al, 1998). In recent years, an emerging role has also been established for the p38-hsp27 pathway. Indeed, it seems that p38 promotes survival in hypoxic and serum-starved CRC-SCs (Lin SP et al, 2012), and mediates CSC drug resistance to oxaliplatin and anti-angiogenic agents (Chen SF et al, 2012). Moreover, p38 inhibited cells showed significantly reduced expression of CSC markers and sphere-forming ability in head and neck squamous cell carcinoma (Shomereeta R et al, 2018). In addition, the activation of p38 stabilizes Nanog and Klf4 mRNA through increased inactivating phosphorylation of RNA binding protein ZFP36L1, and promotes specification of the breast cancer stem cells phenotype (Haiquan L et al, 2018). Furthermore, breast cancer stem cells are resistant to pulsed proton beams by the upregulation of p38 and ERK pathway, indeed MAPK inhibitors could overcome this type of radio-resistance (Myung-Hwan J and Jeong Chan P, 2015). Moreover, it has been shown that p38 modulated tobacco smoke-stimulated hepatic CSC-like properties, as evidenced by the findings that long term tobacco smoke exposure activated p38, and that tobacco smoke-induced stemness was abolished by p38 inhibition (Chunfeng X et al, 2019). Additionally, it has been demonstrated that p38 activates AP-1 and upregulates MMP-2/9 and VEGF expression in melanoma cancer stem cells (CD133+ cells), promoting cell proliferation and angiogenesis (Kumar D et al, 2016). It would also seem that the activation of p38 mediated by Wnt4 is a critical step in the enhancement of the osteogenic differentiation in mesenchymal stem cells (MSCs) (Chang J et al, 2007). Indeed, Wnts have been reported to be capable of activating p38. Recently, it was shown that p38 MAPK is transiently activated upon Wnt3a stimulation and this activation is dependent on both G-protein and Dishevelleds in totipotent mouse F9 teratocarcinoma cells (Bikkavilli RK et al, 2008). Conversely, it seems that the p38 pathway feeds into the canonical Wnt pathway at least at the level of GSK3β, a key regulatory enzyme in the cytoplasmic destruction of β-catenin. Indeed, Thornton and colleagues demonstrated that p38 can phosphorylate GSK3β at Threonine 390, inactivating GSK3β kinase activity (Thornton TM et al, 2008).

Understanding these molecular mechanisms might be crucial knowledge when it comes to designing new therapeutic strategies to fight chemoresistance and improve treatment response in cancer patients.

1.5.1 p38α MAPK and chemoresistance in CRC

Cancer cells can develop chemoresistance in the course of chemotherapy due to the alteration of signaling pathways during tumorigenesis. Following drug exposure, some clones within the cancer tissue can reprogram the expression of a specific set of genes leading to overactive and/or suppressed signaling networks. These adaptive changes may ultimately favor survival by desensitizing cells to drug-induced death signals. This mechanism, can result in patients suffering from recurrent tumors originating from resistant clones (Benson VS et al, 2008; Katano K et al, 2002; Ferry KV et al, 2000; Roux PP et al, 2004).

The occurrence of chemoresistance is responsible for the limited success of various drugs in many cancers. For example, cisplatin, a chemotherapeutic agent frequently used against CRC, has been shown to induce cell death rates of up to 70% in the first phase of therapy. However, over time this rate gradually decreases to 15% due to the existence of unresponsive (chemoresistant) cells during chronic chemotherapy exposure (Rabik CA et al, 2007; Ozols RF et al, 1991; Marin JJ et al, 2012).

Thus, studies focusing on specific resistance mechanisms with the aim of finding new therapeutic strategies directed against specific targets have become increasingly desirable to improve patient's survival. p38α might well be one of these targets, since it has been shown to be involved in several chemoresistance mechanisms. Indeed, response to cisplatin treatment is potentiated upon p38α inhibition, resulting in ROS-dependent upregulation of the JNK pathway in cancer cells, including CRC. *In vivo,* p38α inhibition cooperates with cisplatin treatment to reduce the size and malignancy of xenografted breast tumors in mice (Pereira L et al, 2013). Moreover, it has been shown that p38α signaling is activated in cisplatin-treated CRC cells, and p38α genetic ablation or pharmacological blockade sensitizes chemoresistant cells to cisplatin. Furthermore, p38α inhibition showed an additive effect with cisplatin in chemosensitive cells and co-treatment induced Bax-dependent apoptosis in both sensitive and resistant cells in vitro and xenograft CRC mouse models (Germani et al, 2014). Using p38α inhibitors together with common chemotherapeutics has also given promising results in different experimental setups. Co-treatment with SB202190 and the chemotherapy drug irinotecan appears to sensitize chemoresistant CRC cells to chemotherapy thus

supporting the important role for p38α in controlling chemoresistance (Paillas S et al, 2011).

CRC cells treated with p38α inhibitors together with 5-fluorouracil which is the backbone of chemotherapy in CRC, showed increased caspase activity and sensitivity to chemotherapy due to increased *BAX* expression (Yang SY et al, 2011).

Finally, chemoresistant cells may either show specific resistance to a particular drug or display multidrug resistance. P-glycoprotein (P-gp) functions as a drug efflux pump and it is involved in the efflux of some chemotherapeutic agents like cisplatin, vincristine, and doxorubicin outside of cancer cells. When high p38α activity is observed in chemoresistant cells, P-gp expression is often upregulated and chemoresistance can be reversed by SB203580 treatment (Veneroni S et al, 1994; Barancik M et al, 2001) **(Figure 14)**.

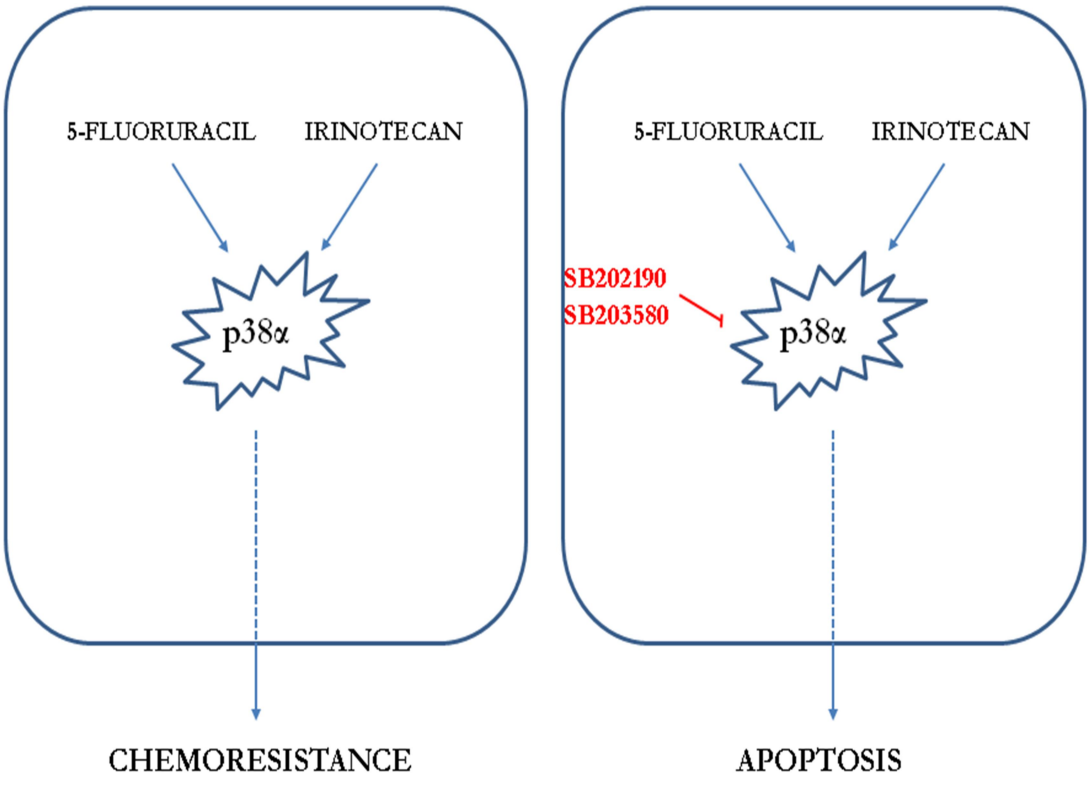

Figure 14. p38α and chemoresistance in CRC. (**a**) p38α is a mediator of resistance to irinotecan and 5-FU and its activation correlates with impaired response to therapy in CRC patients. (**b**) Pharmacological inhibition combined with chemotherapeutic agents decreases viability of cancer cells and increases apoptotic cell death. (Adapted from Grossi et al, 2014).

As a result of the correlation with metastatic potential, cell migration in advanced tumors is another important issue to overcome in cancer therapy. Inhibition of p38α by SB203580 has also been reported to be an effective sensitizer reducing cell migration/invasion and enhancing sensitivity to etoposide treatment through Cox-2 downregulation in neuroblastomas (Limami Y et al, 2011).

These studies show that chemoresistant CRC cells may induce a p38α-mediated resistance mechanism to support survival or to delay the ongoing cell death processes.

1.6 Aim of the study

Tumor development and progression is a multistep process characterized by the progressive alteration of multiple molecular pathways that control the fine balance between proliferation, differentiation and cell death. These anomalies selectively favor the loss of anti-proliferative and pro-apoptotic checkpoints, the acquisition of a metabolic profile capable of sustaining a high proliferation rate and the ability to invade surrounding tissues and migrate. In this scenario, some of the signaling pathways involved in preventing tumor development in healthy cells can acquire a tumor-supporting function in cancer cells, thus contributing to the maintenance of the malignant phenotype. Despite its tumor-suppressive role in healthy cells of various tissues, p38α is required to maintain CRC metabolism, as its inhibition leads to activation of autophagy, cell death, and tumor growth reduction both *in vitro* and *in vivo* (Comes F et al, 2007; Chiacchiera F et al, 2009). Moreover, recent studies identified p38α as a mediator of resistance to irinotecan and impaired response to FOLFIRI therapy, while its inhibition sensitized resistant CRC cells to irinotecan and 5-fluorouracil. Recently, it has been shown that tumor relapse and chemoresistance are dependent on a small cell population called cancer stem cells (CSCs). The gene expression programs that determine CSC features are controlled by c-Myc, which function as a link connecting malignancy and stemness. Unfortunately, finding small-molecule or biologic inhibitors of c-Myc has proved difficult because c-Myc is localized within the nucleus and does not have a deep surface binding pocket. Therefore, considering the role of ERK exercises on c-Myc, the proposed study model involves investigating the crosstalk between p38α and ERK and their function on c-Myc stabilization (**Chapter 1**). Also, the study plans to investigate the possible role of p38α as chromatin-associated kinase with β-catenin, the well known c-Myc transcription factor (**Chapter 2**). Finally, in order to find new potential therapeutic strategies for the purpose of targeting CSCs and bulk tumor population we finally investigated the role of p38α in CRC-SCs model (**Chapter 3**).

Since p38α is a promising therapeutical target directly placed on chromatin, the idea is to use Ralimetinib, p38α inhibitor, in current clinical trials for inflammatory disease and cancer, to inhibit the uncontrolled cellular proliferation of both stem and differentiated

cells prompted by c-Myc and other Wnt target genes, preventing metastatic dissemination and overcoming chemoresistance **(Figure 15)**.

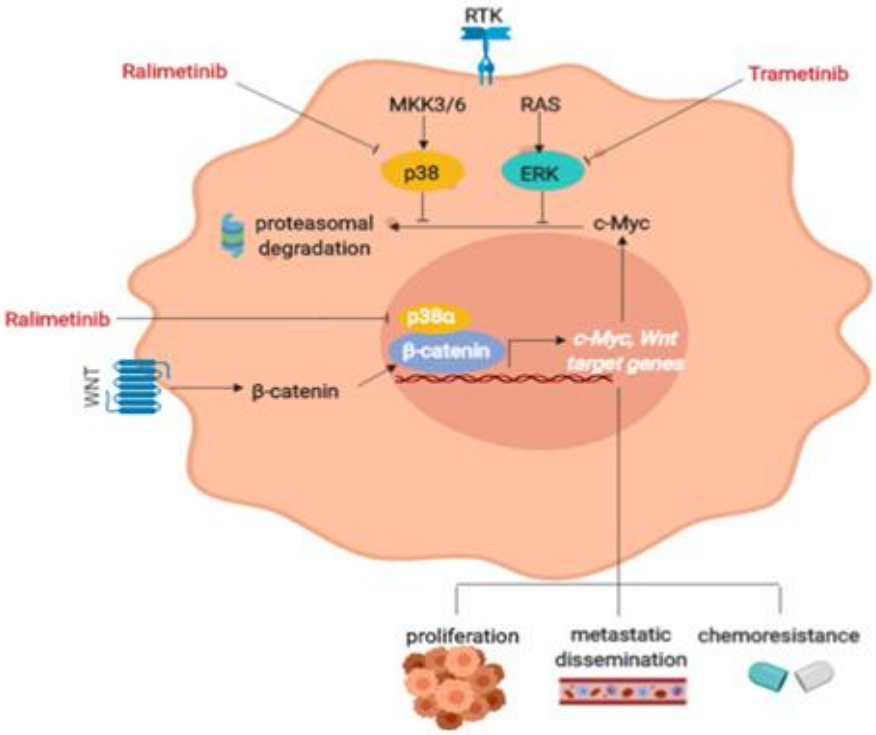

Figure 15. c-Myc is one of the most important factor in CRC. Considering the role of ERK exercises on c-Myc, the proposed study model involves investigating the crosstalk between p38α and ERK and their function on c-Myc stabilization (Chapter 1). Also, the study want to investigate the possible role of p38α as chromatin associated kinase with β-catenin, the well known c-Myc transcription factor (Chapter 2) and in the interest to find new potential therapeutic strategies aimed at selectively target CSCs and bulk tumor population we finally investigate the role of p38α in CRC-SC model (Chapter 3). The study advice the use of Ralimetinib (p38α inhibitor) in order to impair cellular proliferation of CSCs and differentiated cells, reduce metastatic dissemination and overcome chemoresistance.

Material and Methods

2.1 Cell culture and reagents

HCEC-1CT, HCT116, HT29 and Caco2 were purchased from ATCC. HCEC-1CT cells were maintained in Colo-UP medium supplemented with 1% of antibiotic. HCT116 and HT29 were maintained in DMEM supplemented with 10% fetal bovine serum (FBS) and 1% antibiotic. Caco-2 cells were maintained in DMEM supplemented with 20% FBS and 1% antibiotic. CRC-SC cells (511, G605, DA13 and ME59) were kindly provided by Prof. Giorgio Stassi from consenting patients. CSC cells were maintained in DMEM/F12 ADVANCED (cod. #12634-028) supplemented with 1% L-Glutamine (cod.25030081), 1% antibiotic, 0.6% glucose solution at 45% (cod. SIGMA G8769), B27 (cod. thermo 12587010), N2 (cod. Gibco 17502-048), 10 ng/ml bFGF (cod. Sigma F0291), 20ng/ml EGF (cod. Sigma E9644). The cells were routinely propagated under standard conditions.

SB202190 (5-10μM), PD988059 (5-20 μM), 3-Methyladenin (10 μM), trypan, Bafylomicin (B1793) and Wnt3a (H17001) were from Sigma Aldrich. Ralimetinib (LY22228820) (1-10 μM) was kindly provided by Eli Lilly and Company. Trametinib (GSK1120212) (25nm) and PRI-724 (S8262) were from Selleckchem, cycloheximide (239763), MG132 (474790) and TWS119 (361554) were all from Calbiochem.

2.2 Quantitative real-time PCR

Total RNA was isolated by TRIzol reagent (Sigma) following manufacturer's instructions. To avoid possible DNA contamination, RNA was treated with DNase-1 (Ambion). RNA purity was checked by spectrophotometer and RNA integrity by examination on agarose gel electrophoresis. cDNA was synthesized retro-transcribing 1μg of RNA total in 100μl using iScript cDNA synthesis kit Biorad and following the manufacturer's instructions. Real-time PCR primers were designed using Primer Express software. PCR assays were performed in 96 well optical reaction plates using the QuantStudio 3 machine (Thermo Fisher Scientific). PCR assay were conducted in

triplicate wells for each sample. Baseline values of amplification plots were set automatically and threshold values were kept constant to obtain normalized cycle times and linear regression data. The following reaction mixture per well was used: 5µl SYBR Green PCR Master Mix (Biorad), 1,2µl primer at the final concentration of 100nM, 2,3µl RNAse free water, 1,5µl cDNA.
For all experiments the following PCR conditions were used: denaturation at 95°C for 30seconds, followed by 40 cycles at 95°C for 15 seconds then at 60°C for 30 seconds. Quantitative normalization of cDNA in each sample was performed using β-actin as an internal control. Relative quantification was done using the ddCT method. Primer sequences are available on request.

2.3 RNA interference

For RNA interference, cells were transfected with 100nM Select Silencer siRNA against p38α and MEK (all from Ambion by life technologies) using Hiperfect Transfection reagent from Qiagen. On target plus control siRNA (Thermo Scientific) was used as control sequences.

2.4 Proliferation assays

Proliferation assays were conducted using the WST-1 reagent (Roche) as the manufacturer's instructions. Briefly, cells were seeded into 96-well plates one day before treatment. After 12h, 24h, 36h drugs (or DMSO) exposure, 10µl of the Cell Proliferation Reagent WST-1 was added to each well and incubated at 37°C in a humidified incubator for 30min-1h-2h. The absorbance was measured on a microplate reader (SPECTROstar OMEGA) at 450-655nm. Each assay was performed in 6 replicates and the experiment was repeated three times. The proliferation index was calculated as the ratio of WST-1 absorbance of treated cells at the indicated time point (12h-24h-36h) to the WST-1 absorbance of the same experimental group at 0h.

2.5 Nuclear/cytoplasmic fractionation and Immunoblot analysis

Nuclear/cytoplasmic fractionation was carried out using the Nuclear extraction kit from Abcam (ab113474). Immunoblot cells were collected and homogenized in lysis buffer (50mM Tris-HCl ph 7.4, 5mM EDTA, 250mM NaCl and 0.1% Triton x-100) supplemented with protease and phosphatase inhibitors. 20-40 μg of protein extracts from each sample were denatured in 5x Laemmli sample buffer and used for immunoblot analysis. Immunoblot were performed using Anti-βactin (#3700S), anti-c-Myc (#9402s), anti-p44/42 MAPK (Erk1/2) (#9102), anti-phospho p44/42 MAPK (Erk1/2) (Thr202/tyr204) (#9106S), anti-LC3 A/B (NK12741S), anti-p38 MAPK (#9212), anti-p38α MAPK (#9228S), anti-phospho-p38 MAPK(Thr180/Tyr182) (#9211), anti-MEK (#9122S), anti-phospho-MEK (#9154S), Anti-lamin (#12586S), anti-Keratin20 (BK13063S), Anti-phospho-MAPKAPK-2 (Thr334) (BK3316S), anti-PDI (#2446S), anti-βcatenin (#9562S), anti-Ubiquitin (#3936), anti-APC (#2504) all from cell signaling technologies-CST and anti-HSP90α/β sc-13119 from Santa cruz. HRPO-conjugated secondary antibodies were used (GE Healthcare) and the signal was revealed using the ECL-plus chemiluminescence reagent (GE Healthcare) as per manufacturer's instructions. The densitometric evaluations were carried out both by ImageJ software and ImageLab software.

2.6 Immunofluorescence staining

Cells were seeded on glass coverslips and after 12h were treated as indicated. At the end of the treatment, cells were fixed in 4% paraformaldehyde and permeabilized using 0,01–0,1% Triton X-100. Coverslips were incubated with the indicated primary antibodies (LC3 A/B). Secondary antibodies were Alexa Fluor 488 from Invitrogen; nuclei were counterstained using DAPI (Sigma). Slides were sealed using Vectashield mounting medium (Vector Laboratories). Images were acquired using a Zeiss fluorescence microscopy.

2.7 Immunoprecipitation

Cells were collected and homogenized in lysis buffer (50 mM Tris-HCl pH 7,4; 5 mM EDTA; 250 mM NaCl and 1% Triton X-100) supplemented with protease and phosphatase inhibitors. The coupling was performed between magnetic beads and antibody (p38α #8690 and βcatenin #9562S) in T-PBS for 30 min. Cell lysates were immunoprecipitated with antibody-beads or (IgG control) on the wheel for 45 min. Immunoprecipitated proteins were extensively washed with lysis buffer, resuspended in Laemmli buffer, separated on polyacrylamide gel and transferred to nitrocellulose membranes, after which precipitated proteins were subjected to immunoblot analysis.

2.8 Serum and LiCl stimulation

Cells were synchronized in the cell cycle by culturing theme for 48 hours without serum. Then, the medium was replaced with ones containing serum and/or 10mM LiCl for 4h.

2.9 Chromatin immunoprecipitation (ChIP)

ChIP assays were performed using the MAGnify Chromatin Immunoprecipitation System (Life Technologies) according to the manufacturer's instructions. IgG antibodies were included in the kit and 1 µg of anti-β-catenin, anti-p38α antibodies (CST) was used for each assay. PCR was performed on "input" DNA of different samples and equivalent amounts of immunoprecipitated DNA were amplified by real-time PCR as described in the "Quantitative Real-time PCR" method section. Quantification was done using the Input % method. The set of primers used for ChIP allows the amplification of target promoter regions including β-catenin binding sites (sequences are available upon request).

2.10 Microscopic quantification of viability and cell death

Cell viability and cell death of the reported cell lines were scored by counting. The supernatants (containing dead/floating cells) were collected, and the remaining adherent cells were detached by Trypsin/EDTA (Sigma). Cell pellets were resuspended in 1X PBS and 10µl were mixed with an equal volume of 0.01% trypan blue solution. Viable cells (unstained, trypan blue negative cells) and dead cells (stained, trypan blue positive cells) were counted with a phase-contrast microscope. The percentages of viable and dead cells were calculated. The data shown in the results section are representative of 3 or more independent sets of experiments.

2.11 Morphological evaluation

Numerous slides with a monolayer cells were either rapidly fixed in 95% ethyl alcohol for a minimum of 15 min. Slides were examined by optic microscopy.

2.12 Karyotype protocol

Colorectal cancer stem cells were seeded the day prior to the experiment at a high density. After 24h was added 10ug/ml of colcemid, which can collapse mitotic spindles and prevent the completion of mitosis, to each dish and mix gently. Incubated at 37 °C, 5 % CO_2 for 90minutes. Transfer medium to centrifuge tubes from the cell culture dishes. Further, centrifuge at 2000rpm for 5 min at room temperature. Discard the supernatant and leave 0.5 ml medium to mix the pellet gently. Resuspend the pellet in 5-7 ml 37 °C hypotonic solution (KCl 56%) and mix thoroughly. Incubate in a water bath at 37 °C for 10 min. Neutralize the hypotonic solution with 1 ml of methanol: glacial acetic acid (3:1) fixative. Centrifuge at 2000rpm for 5 min at room temperature. Discard the supernatant and leave 0.5 ml solution to mix the pellet gently. Resuspend the pellet in 5 ml cold fixative (drop by drop and flick the tube between drops to prevent cell clumping) to wash the pellet. Centrifuge at 2000rpm for 5 min at room temperature.

Discard the supernatant and leave 0.5 ml solution to mix the pellet gently. Resuspend the pellet in 5 ml cold fixative. Put the centrifuge tube on ice at least 60 min. Centrifuge at 2000rpm for 5 min at room temperature. Discard the supernatant and leave 0.5 ml solution to mix the pellet gently. Resuspend the pellet in 5 ml cold fixative. Repeat the washing steps other two times until the supernatant is clear and the pellet become white. After the final centrifugation, suspend the cells in a few drops of cold fixative to give a slightly opaque suspension. Drop 1-2 drops onto wet and clean slides (before that, the slides have to be rinsed by 1-2 drops of cold fixative). Dry the slides at room temperature. Observe the chromosomes with the microscope (Olympus DP71 with 200x magnification). Count the number of chromosomes about 50 cells.

2.13 Mutation analysis

Genomic DNA was purified from colorectal cancer stem cells according to manufacturer's instructions (Genomic DNA purification kit, ThermoFisher Scientific, K0512). The gene coding region were screened for mutations. promoter sequences were analyzed for mutations using a PCR-direct sequencing method. Sequencing and capillary electrophoresis were performed on the Applied Biosystems® 3130 Genetic Analyzer (ThermoFisher Scientific, Waltham). Mutations and polymorphisms were confirmed in independently amplified PCR products.

MSI analysis was performed with a reference panel of five fluorescent dye-labeled microsatellite primers (NR-21, BAT-25, MONO-27, NR-24, BAT-26) using the MSI Analysis System kit, Version_1.2 (Promega). Amplified fragments were detected by loading the PCR products for capillary electrophoresis using the ABI Prism 3500 Genetic Analyser and the POP-4 polymer (both from Applied Biosystems, Foster City, California, USA) according to manufacturer's instructions (Promega). MSI status was determined upon analysis with GeneMapper software, Version_4.1 (Applied-Biosystems).

2.14 In vivo studies

The $APC^{Min/+}$ experiments in Chapter 1 were performed with $APC^{Min/+}$ male mice (n=7) treated with vehicle (DMSO plus methylcellulose) and $APC^{Min/+}$ male mice (n=12) treated with 1mg/kg SB202190 by intraperitoneal injections in combination with 3mg/kg PD0325901 by oral gavage. $APC^{Min/+}$ mice (4-month-old) were treated daily for 15 days (combined inhibition or vehicle), followed by 15 days of recovery, after which another 15 days-cycle of treatment was performed. After this second cycle of treatment mice were monitored until they died.

For in vivo studies in Chapter 3 normal, adenoma and adenocarcinoma colon mucosa tissues were obtained from C57BL/6 male mice (n=4), $APC^{Min/+}$ male mice (n=4) and $APC^{Min/+}$ male mice treated with 12 mg/kg of azoxymethane (AOM) (Sigma) (n=4). The $APC^{Min/+}$ mice (4-month-old) were first administered with AOM 14mg/kg body weight once a week for 4 weeks, then, 1 month later, they were sacrificed. Bodyweight was recorded daily. Procedures involving animals and their care were conducted in conformity with the institutional guidelines that comply with national and international laws and policies.

1.15 Statistical Analysis

The statistical significance of the results was analyzed using Student's t-tail test, and $*P<0.05$ was considered statistically significant.

Results

3.1 Results 1

In the search for new strategies to efficiently fight CRC, efforts are being increasingly focused on targeting regulatory signaling pathways involved in cancer-specific features. As a result, several studies have recently addressed the therapeutic potential of molecularly-targeted drugs capable of inhibiting the activity of protein kinases involved in relevant signaling cascades.

As described in the introduction, by using pharmacologic approaches, our group showed that PD988059-dependent MEK/ERK inhibition triggers p38α phospho-activation in various colon cancer cell lines (HT29, HCT116, and Caco2 cells) with different genetic backgrounds. We also found that in CRC cells, SB202190-dependent p38α pharmacologic inhibition potentiates the MEK/ERK pathway, irrespectively of the mutational status of the ERK upstream activators RAS and RAF. Indeed, increased phospho-activation of both MEK1 and ERK1/2 was observed in BRAF mutant HT29 cells, in KRAS mutant HCT116 cells, and in Caco2 cells, which are wild-type for these two genes **(Figure 16a–e)**. This effect was confirmed by using a structurally and functionally different p38 inhibitor, BIRB796 **(Figure 16b)**, and was also observed *in vivo* in HT29-xenografted nude mice **(Figure 16c)** and colon sections from azoxymethane-treated $APC^{Min/+}$ mice injected with SB202190 **(Figure 16d)**. Importantly, this showed the existence of a p38α/ERK crosstalk in CRC cells (Chiacchiera F et al, 2012).

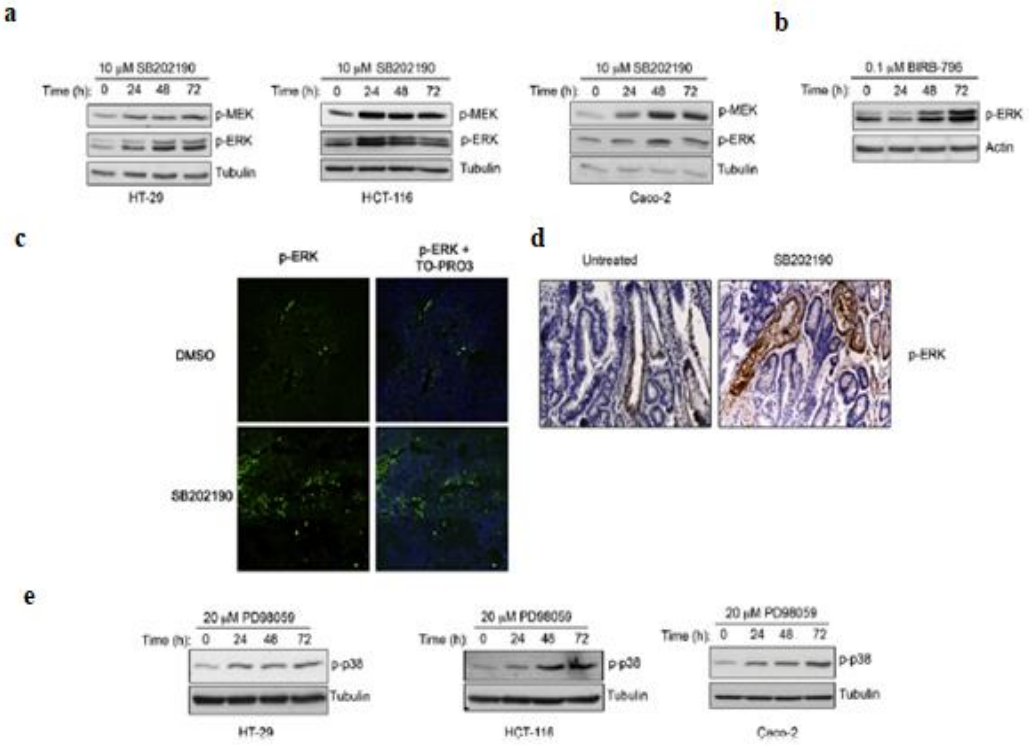

Figure 16. A crosstalk exists between p38α and ERK in CRC cells and tissues. (**a**) Inhibition of p38α using SB202190 for up to 72 hours triggered MEK-ERK1/2 signaling in HT-29, HCT-116, and Caco-2 CRC cells. (**b**) Use of a structurally and functionally different p38α inhibitor (BIRB-796) confirmed ERK1/2 phospho-activation. (**c,d**) Phosphorylated ERK1/2 was also observed after SB202190 treatment both in tumors derived from HT-29-xenografted nude mice (immunofluorescence analyses, green) (**c**) and in colon tissues explanted from AOM-treated $APC^{Min/+}$ mice (immunohistochemistry, dark precipitates) (**d**). (**e**) MEK1 inhibition using PD988059 induced p38 phospho-activation in HT-29, HCT-116, and Caco-2 CRC cell lines. (From Chiacchiera F et al, 2012).

3.1.1 p38α and ERK in c-Myc regulation

c-Myc plays a key role during intestinal carcinogenesis; in CRC, it is maintained upregulated by different mechanisms, including ERK-mediated post-translational stabilization.

Using CRC cell lines (HT29, HCT116, and Caco2 cells), we analyzed c-Myc protein levels following treatment with classical p38α and ERK chemical inhibitors (SB202190 and PD988059, respectively) and found that both induce a decrease in c-Myc amount regardless of the genetic background **(Figure 17a-b)**. Besides, combined inhibition of p38α and MEK/ERK significantly reduced c-Myc protein levels compared with the single treatments; this effect was already detectable after 24 hours **(Figure 17c)**.

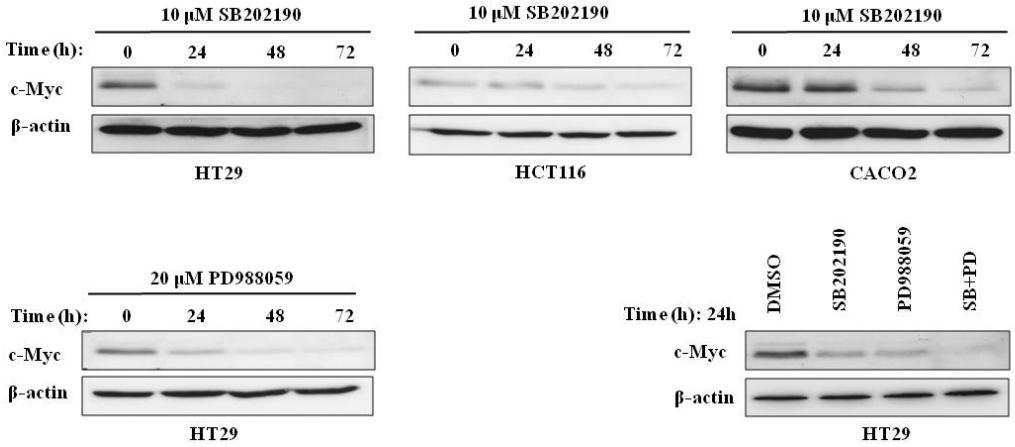

Figure 17. Effects of p38α/ERK crosstalk on c-Myc expression in CRC cells. (**a**) Inhibition of p38α using SB202190 for up to 72 hours induced a decrease in c-Myc protein levels in HT29, HCT116, and Caco2 cells. (**b**) Inhibition of MEK/ERK using PD988059 for up to 72 hours induced a decrease in c-Myc protein levels in HT29 cells. (**c**) Combined inhibition of p38α and MEK/ERK using SB202190 and PD988059 for 24 hours in HT29 cells induced a higher decrease in c-Myc protein levels compared to either single treatment. β-actin was used as a loading control. SB+PD: SB202190 + PD988059, DMSO: Dimethyl sulfoxide. The presented results are representative of at least three independent experiments.

Since protein half-life is an important feature of protein homeostasis, and both c-Myc mRNA and protein are inherently unstable, with a half-life of about 30 minutes (Herrickand D and Ross J, 1994; Gregory M A and Hann S R, 2014), we investigated c-Myc regulation in a short-term experiment. We performed p38α and ERK inhibition in HCT116 cells and found that these two kinases do not regulate *c-Myc* transcription but affect its protein levels. Indeed, we couldn't detect any change in c-Myc mRNA amount after any type of treatment (single or combined inhibition) **(Figure 18a)**; instead, we observed a significant decrease in c-Myc protein levels after the inhibition of a single pathway and an even greater effect after the combined inhibition of both the p38α and the MEK/ERK cascades **(Figure 18b)**.

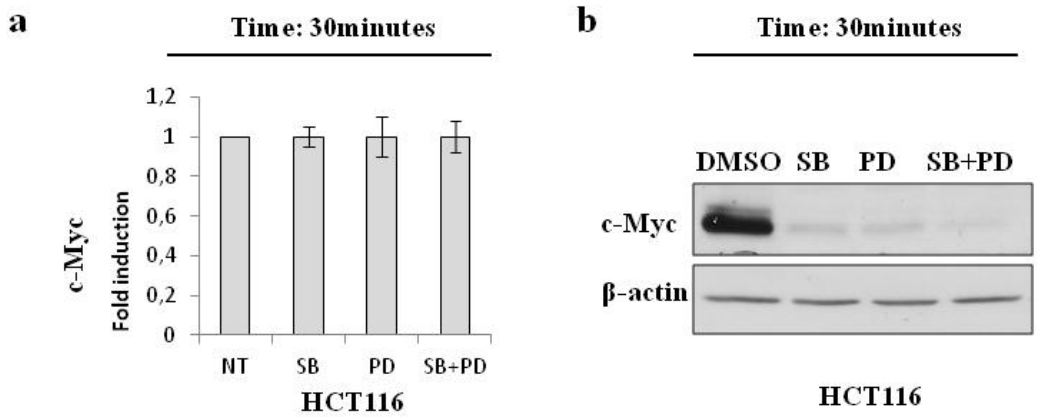

Figure 18. In a short-term inhibition study, p38α and ERK affect c-Myc protein expression. HCT116 CRC cells were treated with p38α and/or ERK inhibitors; after 30 minutes, mRNA (**a**) and total proteins (**b**) were extracted for RT-PCR and immunoblotting analyses, respectively. Short-term p38α and/or ERK inhibition, using SB202190 and/or PD988059 respectively, did not affect c-Myc mRNA expression, while it induced a decrease in c-Myc protein levels. β-actin was used as a loading control. SB: SB202190, PD: PD988059, DMSO: Dimethyl sulfoxide. The presented results are representative of at least three independent experiments.

Control of protein abundance involves regulation of both macromolecular synthesis (transcription and translation) and degradation (RNA decay and proteolysis). Analysis of proteins at a single time point provides a snapshot of steady-state protein abundance without revealing the relative contributions of synthesis and degradation. It is possible to infer the contribution of any step from synthesis to degradation by comparing abundance before and after inhibiting specific components of the mechanism (Bunchanan B W et al, 2016). For example, cycloheximide (CHX) is an inhibitor of protein biosynthesis that acts by blocking translational elongation. It is widely used in cell biology to determine the half-life of a specific protein and has gained much interest in cancer research (Kao S-H et al, 2015). Hence, to investigate whether p38α and ERK affect c-Myc translation, we used CHX at a final concentration of 30 ug/mL and collected cells after 0 to 1 hour. Cell lysates were then subjected to immunoblotting with a c-Myc antibody and normalized to β-actin, a commonly used control in CHX chase assays. This experiment showed that p38α and ERK do not affect c-Myc protein translational process, because CHX does not cause any change in the effect of these two inhibitors **(Figure 19)**.

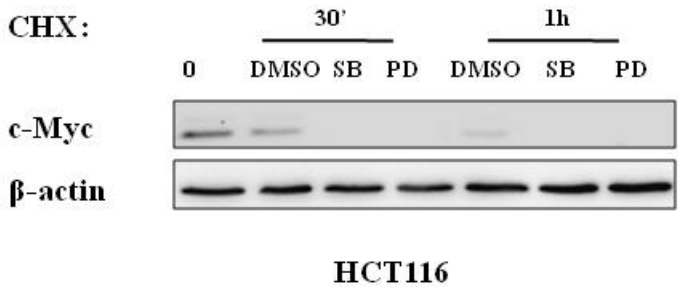

Figure 19. p38α or ERK inhibition does not affect c-Myc translational process. HCT116 CRC cells were treated with cycloheximide (CHX, inhibitor of protein biosynthesis) and p38α or ERK inhibitors (SB202190 or PD988059, respectively). Cells were collected after 0 to 1 hour. Total proteins were extracted and subjected to immunoblot analysis. The administration of CHX together with SB202190 or PD988059 did not change the effect of p38α or ERK inhibitors alone. β-actin was used as a loading control. SB: SB202190, PD: PD988059, DMSO: Dimethyl sulfoxide. The presented results are representative of at least three independent experiments.

As mentioned in the introduction, at the post-translational level, c-Myc stability is regulated by phosphorylation at two conserved residues, serine 62 (S62) and threonine 58 (T58). The ratio of T58 and S62 phosphorylation controls c-Myc ubiquitination and turnover in cells. In response to growth signals, ERK phosphorylates c-Myc on S62, increasing its stability and its oncogenic activity. When growth signals cease, S62-phosphorylated c-Myc can interact with GSK3β, which phosphorylates c-Myc at T58. Doubly phosphorylated c-Myc is then recognized by the Pin1 isomerase, which catalyzes the isomerization of the serine 62-proline 63 bond from a cis conformation to a trans conformation. This isomerization allows PP2A to de-phosphorylate c-Myc at S62. Phosphorylation at T58 but not at S62 makes c-Myc prone to subsequent recruitment of ubiquitin ligase E3 and promotes initiation of its proteasome-dependent degradation (Sears R, 2004) **(Figure 20)**.

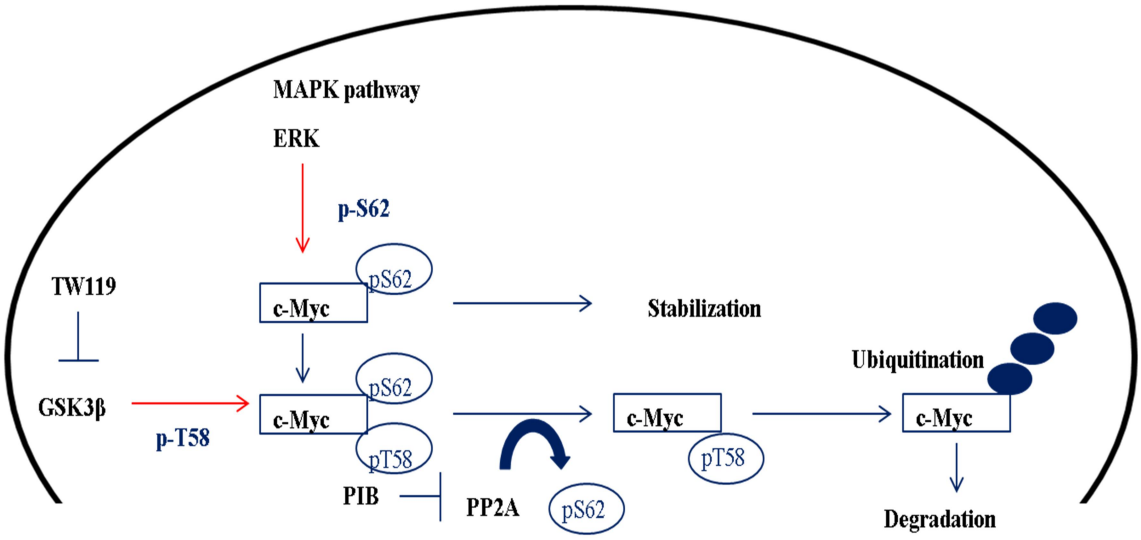

Figure 20. Schematic representation of c-Myc post-translational stabilization. In response to growth signals, ERK phosphorylates c-Myc on Serine 62 (S62), increasing its stability. When growth signals cease, GSK3β phosphorylates c-Myc on Threonin 58 (T58). Doubly phosphorylated c-Myc is recognized by the Pin1 isomerase, which catalyzes the isomerization of the serine 62-proline 63 bond. The resulting trans conformation allows the recruitment of PP2A, which can now dephosphorylate S62. Phosphorylation at T58 but not at S62 induces c-Myc proteasomal degradation. TW119: GSK3β inhibitor, PIB: PIN inhibitor.

Considering the above-mentioned post-translational regulation mechanisms, we performed experiments by inhibiting GSK3β or PP2A in combination with p38α. The results obtained from this analysis showed that c-Myc degradation induced by p38α inhibition is independent of PP2A and GSK3β.

Previous work from our group showed that p38α genetic depletion, or pharmacological blockade of its kinase activity, induces autophagy, a process that can be involved in protein degradation (Chiacchiera F et al, 2009). To investigate whether c-Myc degradation after p38α inhibition is regulated by autophagy-associated mechanisms, we evaluated c-Myc levels following inhibition of the cytoplasmic degradation process by adding 3-methyladenine and bafilomycin (two autophagy inhibitors), in addition to the p38α inhibitor SB202190. No significant changes were observed in c-Myc levels compared to the inhibition of p38α alone, suggesting that c-Myc degradation after p38α inhibition occurs through a different mechanism **(Figure 21a–b)**.

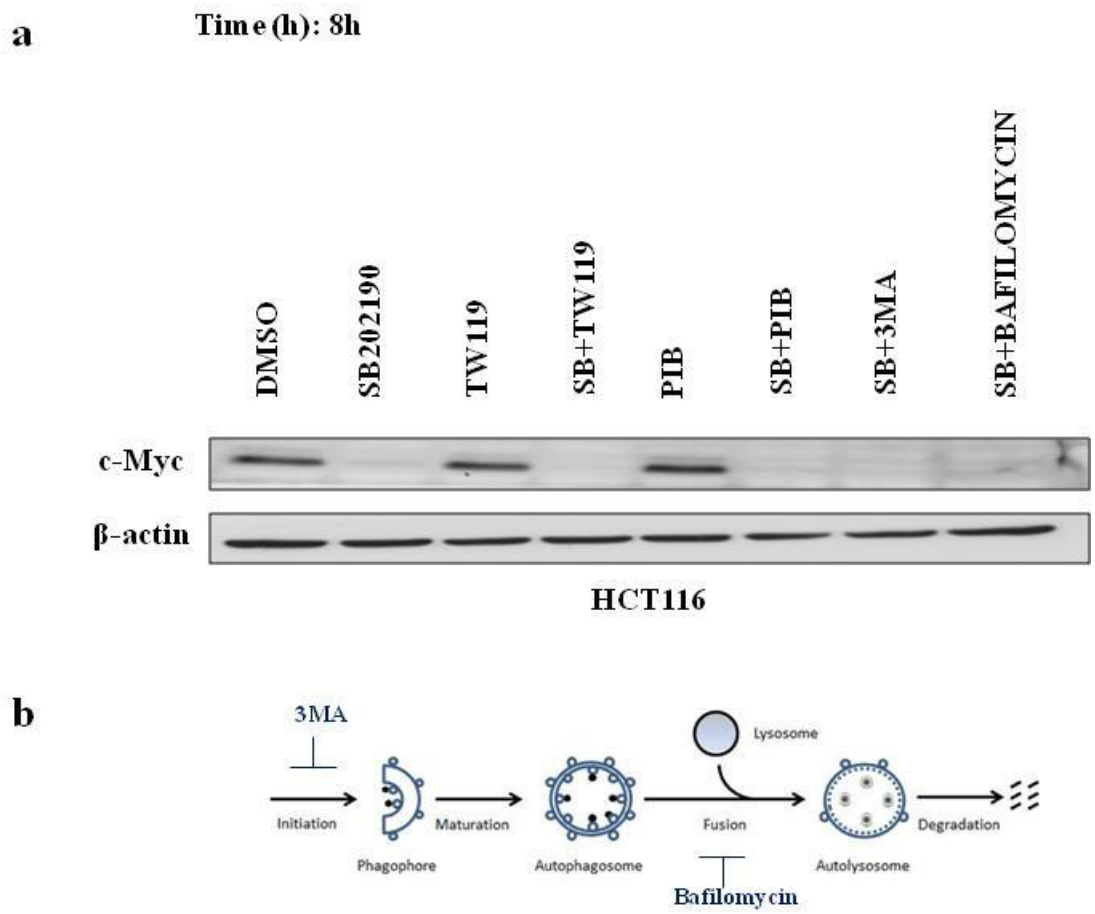

Figure 21. The effect of p38α inhibition on c-Myc is independent from PP2A, GS3Kβ, and autophagic response. (**a**) HCT116 CRC cells were treated for 8 hours with different inhibitors (TW119: GSK3β inhibitor, PIB: PIN inhibitor, 3-methyladenine and bafilomycin: autophagic inhibitors) in combination or not with SB202190 (p38α inhibitor). Total proteins were extracted and subjected to immunoblot analyses. The administration of inhibitors together with SB202190 did not induce significant changes in c-Myc levels compared with p38α inhibition alone. β-actin was used as loading control. The presented results are representative of at least three independent experiments. (**b**) Schematic representation of the autophagic flow showing the activity of the inhibitors used in this experiment. SB: SB202190, 3MA: 3-methyladenine.

It is well known that deregulated ubiquitin-proteasome pathway is critical to modulate c-Myc protein levels in cancers where no amplification is observed (Poole C J and Van Riggelen J, 2017). Hence, to elucidate the mechanism underlying c-Myc destabilization induced by p38α inhibition, we blocked the proteasome-dependent degradation. MG132 is a triterpene, peptide-aldehyde proteasome inhibitor derived from a Chinese medicinal plant. It inhibits 20S proteasome activity by covalently binding to the active site of the beta subunits and effectively blocks the proteolytic activity of the 26S proteasome complex. Through the formation of reactive oxygen species, MG132 inhibits tumor cell

growth by inducing cell cycle arrest and triggering apoptosis. Interestingly, MG132 could rescue SB202190-mediated c-Myc protein destabilization. Taken together, these data suggest that p38α may stabilize c-Myc protein by preventing its ubiquitination **(Figure 22)**.

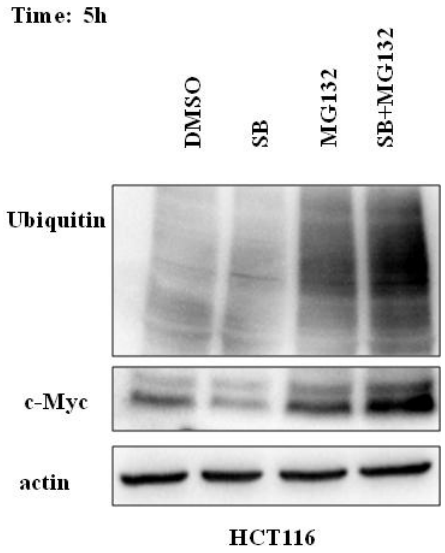

Figure 22. p38α stabilizes c-Myc protein by preventing its ubiquitination. HCT116 CRC cells were treated for 5 hours with SB202190 (p38α inhibitor) with or without 1 hour of MG132 (proteasome inhibitor). Cells were treated and then subjected to immunoblot analysis. SB: SB202190. The presented results are representative of at least three independent experiments.

3.1.2 Combined inhibition of p38α and MEK/ERK reduces CRC growth

In order to exclude potential off-target effects of p38α inhibition by SB202190, we ablated p38α expression with a specific siRNA. Our results were in agreement with the data obtained by using SB202190. Indeed, p38α genetic ablation not only significantly decreased phosphorylation of an endogenous target (P-MK2) but also resulted in a 50% reduction of c-Myc protein levels. As a further confirmation, we evaluated the amount of lipidated MAP1LC3 (LC3II) in order to confirm the well-known role of p38α in autophagic response **(Figure 23a)**. Densitometric analyses of immunoblot data were performed by Image Lab software **(Figure 23b)**.

Moreover, to characterize this autophagic response, we performed immunofluorescence experiments. Autophagic vacuoles and LC3II accumulation were visible in cells treated with SB202190 or a p38α-specific siRNA but not in control-treated cells **(Figure 23c)**. These results were also confirmed by genetic ablation experiments performed in HCT116 cells, where c-Myc completely disappeared upon co-silencing of p38α and MEK/ERK with specific siRNAs for 48 hours **(Figure 23d)**.

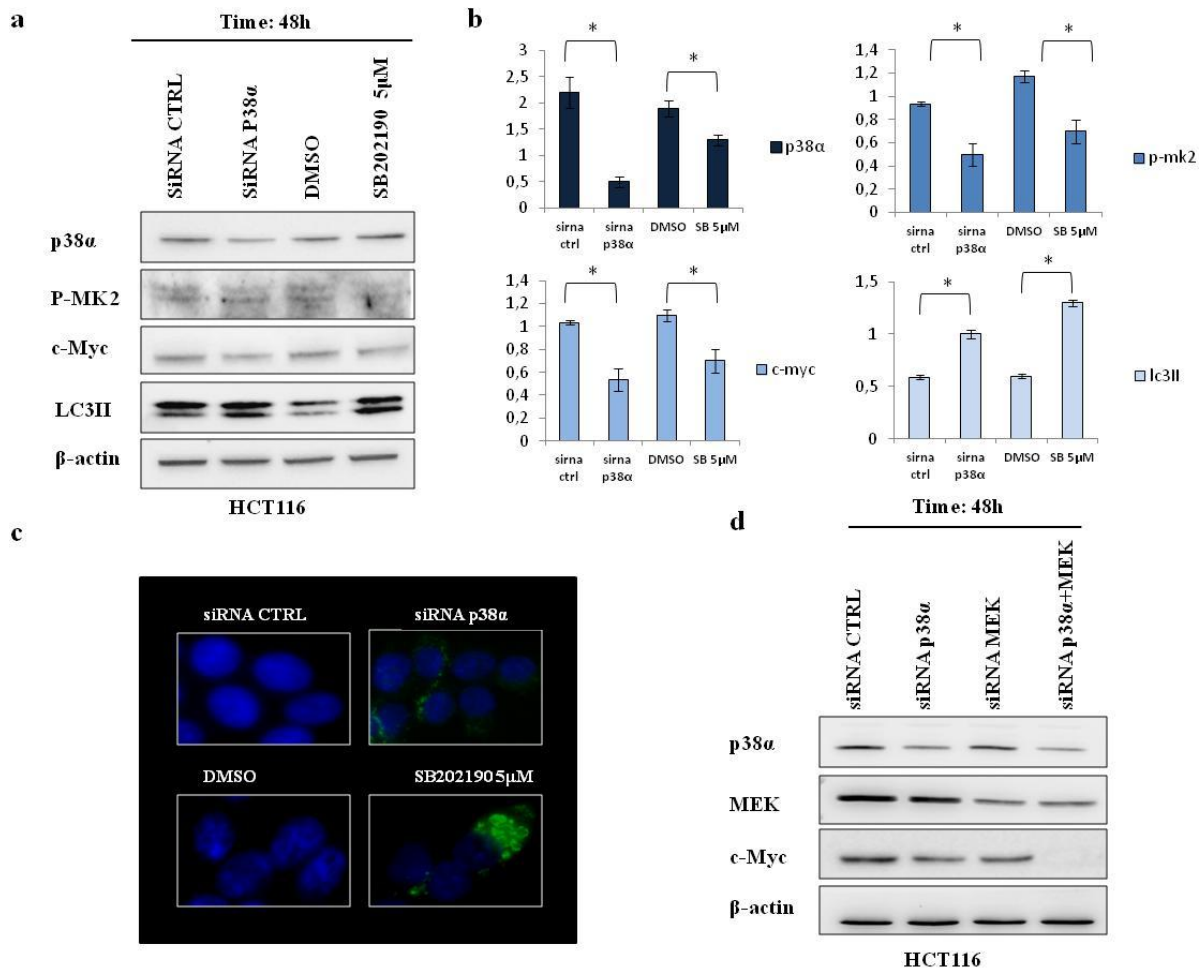

Figure 23. Genetic ablation confirms the role of p38α in c-Myc regulation. (**a**) HCT116 CRC cells were transfected with p38α-specific or control siRNAs, or treated with SB202190 (p38α inhibitor) or the vehicle. P-MK2, a direct downstream target of p38α, was used to confirm siRNA efficacy, LC3II was used to assess the activation of the autophagic response. p38α genetic ablation confirmed p38α active role in c-Myc stabilization. (**b**) Densitometric analyses of the immunoblot data shown in figure (a). c-Myc levels decreased by 50% in cells treated with p38α-specific siRNAs. (**c**) Immunofluorescence analysis showed autophagic vacuoles and the accumulation of LC3II (green) upon p38α inhibition. DAPI was used as nuclear staining. (**d**) Immunoblot analysis was performed with the indicated antibodies in cells treated with control or p38α-specific siRNAs and/or MEK-specific siRNAs. Co- treatment with specific siRNAs completely abolished c-Myc protein expression. Image Lab was used to perform densitometric analysis and β-actin was used as a loading control for immunoblot analyses. Ctrl: control. The presented results are representative of at least three independent experiments. Statistical analysis was performed using Student's t-tail test; *P< 0.05 was considered statistically significant.

To test whether the results described so far were confined to cell culture conditions, we performed *in vivo* studies. As described in the introduction, c-Myc is the critical mediator of the early stages of colorectal tumorigenesis; indeed, it has been found that

genetic removal of the *c-Myc* gene can rescue cancer phenotypes in $APC^{Min/+}$ mice (Sansom O et al, 2007). Interestingly, experiments performed using the same pre-clinical model showed that inhibition of the ERK pathway suppressed intestinal tumorigenesis and increased mice survival (Lee SH et al, 2010). In our study, 4-month-old $APC^{Min/+}$ male mice (n=12) were treated daily with both p38α and ERK inhibitors - SB202190 (1mg/kg) administered by intraperitoneal injections (I.P.) and PD0325901 (3mg/kg) given by oral gavage - while control $APC^{Min/+}$ male mice (n=7) were treated with vehicle (DMSO by I.P. plus methylcellulose by oral gavage). Mice were treated daily for 15 days (combined inhibition or vehicle), followed by 15 days of recovery, after which another 15-day treatment cycle was performed. After the second treatment cycle, mice were monitored until they died **(Figure 24a)** and their bodyweight was recorded daily. It is worth noting that concomitant inhibition of the p38α and the MEK/ERK pathways significantly increased the survival of $APC^{Min/+}$ mice. The Kaplan Mayer curve shown in figure 24 indicates that combined inhibition promoted a 64-day increase in median survival **(Figure 24b)**.

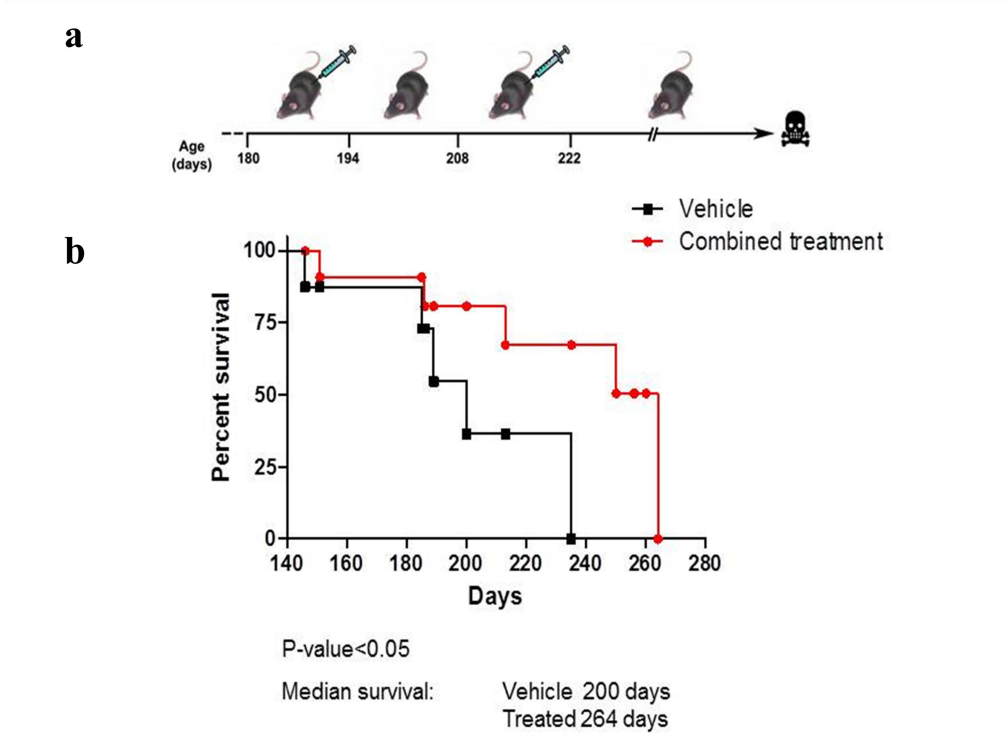

Figure 24. p38α and MEK/ERK combined inhibition increases the lifespan of $APC^{Min/+}$ mice. (**a**) Schematic representation of our treatment schedule. 4-month-old $APC^{Min/+}$ male mice were treated daily with p38α (1μmol/kg/day SB202190) and MEK/ERK inhibitors (3mg/kg/day

PD0325901) or the vehicle for 15 days, followed by 15 days of recovery, after which another 15 day-treatment cycle was performed. After this second treatment, mice were monitored until they died. (**b**) Percent survival of $APC^{Min/+}$ mice treated with p38α and MEK/ERK inhibitors (n = 12) or with the vehicle alone (n = 7) as indicated in (a). Combined inhibition of p38α and MEK/ERK promoted a 64-day increase in median survival compared with vehicle-treated animals.

In order to assess the practical implications of our findings, we confirmed whether our data could be replicated with Ralimetinib and Trametinib - a p38α and an ERK pharmacological inhibitor, respectively - which are being currently investigated in several clinical trials for inflammatory diseases and cancer. It is important to emphasize that various of these clinical trials are being conducted on CRC patients.

For this purpose, we performed a dose/time experiment to analyze the response of CRC cells (HT29 and HCT116) to Ralimetinib compared to the control treatment (SB202190). HT29 and HCT116 cells were treated with increasing doses of Ralimetinib (from 1μM to 10μM) for the indicated time points (12, 24, or 36 hours). Immunoblot analysis showed that 24-hour treatment with 10 μM Ralimetinib effectively inhibits p38α activity in both cell lines, as estimated by impairment of MK2 phosphorylation at threonine 334 **(Figure 25a)**. To evaluate cell death response in single treatment conditions, trypan blue staining scores were analyzed in HT29 and HCT116 cells at various time points. HT29 and HCT116 cells were exposed to different concentrations of Ralimetinib or SB202190. Then, trypan blue positive and negative cells were counted at various time points to analyze relative cell death. Treatment with Ralimetinib induced a significant increase in cell death in both HT29 and HCT116 cells. Besides, in HT29 cells, the cell death rate also showed a nearly 20% increase after 36-hour treatment with Ralimetinib 10 μM compared to SB202190 **(Figure 25b)**. Finally, we performed WST-1 assays in order to assess cytotoxicity and proliferation. Our results confirmed that Ralimetinib modulates cancer cell proliferation in both cell lines **(Figure 25c)**.

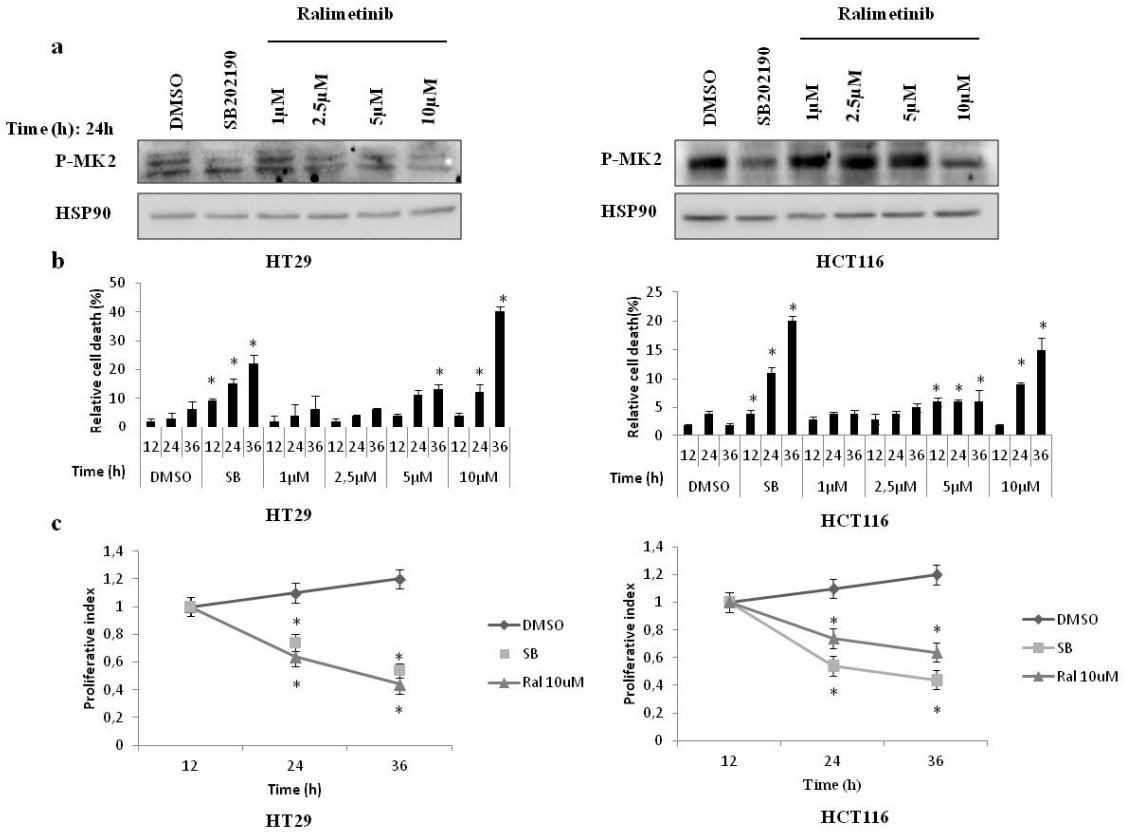

Figure 25. Treatment of CRC cells with Ralimetinib or SB202190 decreases relative viability while increasing relative cell death. (**a**) Immunoblot analyses showing the efficacy of Ralimetinib in targeting p38α activity, as indicated by inhibition of P-MK2 phosphorylation at threonine 334. β-actin was used as a loading control. (**b**) HCT116 and HT29 cells were treated with Ralimetinib (1-10μM), the new pharmacological p38α inhibitor or SB202190 (10μM) and relative cell death was calculated at the indicated time points. Administration of Ralimetinib or SB202190 strongly increased the number of dead cells in both CRC cell lines. (**c**) Ralimetinib or SB202190 treatment decreased cell viability in a time-dependent manner. Cells were treated with Ralimetinib (1-10μM) or SB202190 (10μM), analyzed by WST-1 assay and scored for their proliferative index. SB: SB202190, Ral: Ralimetinib. Statistical analysis was performed using Student's t-tail test; **P*<0.05 was considered statistically significant. The presented results are representative of at least three independent experiments.

After testing Ralimetinib effectiveness in our cellular model, we evaluated whether it affects c-Myc stability in HCT116 and HT29 cells. Both cell lines showed a decrease in c-Myc protein levels after 24-hour treatment with Ralimetinib, similar to the reduction induced by SB202190 **(Figure 26)**.

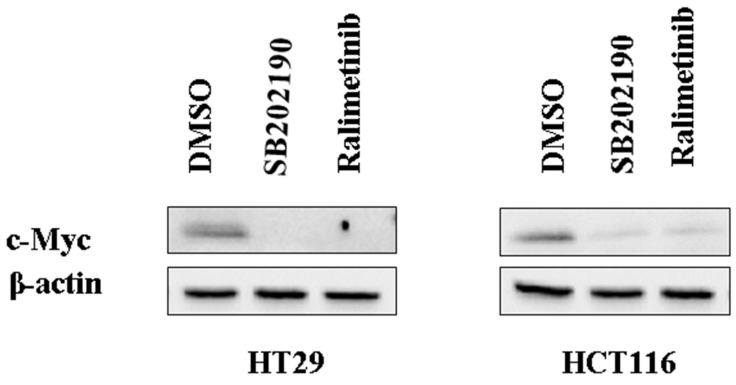

Figure 26. Ralimetinib induces c-Myc destabilization. HT29 and HCT116 CRC cells were treated with the indicated inhibitors for 24 hours and then c-Myc was detected by immunoblotting. β-actin was used as a loading control. The presented results are representative of at least three independent experiments.

Then, we used Ralimetinib in association with PD988059 (MEK/ERK inhibitor) in order to evaluate the decreasing of c-Myc protein levels under the combined inhibition in HT29 and HCT116 cell lines at different time points **(Figure 27a)**. These results were further confirmed by using Trametinib, a biological drug that inhibits the MEK/ERK pathway, which is currently used as targeted therapy **(Figure 27b)**.

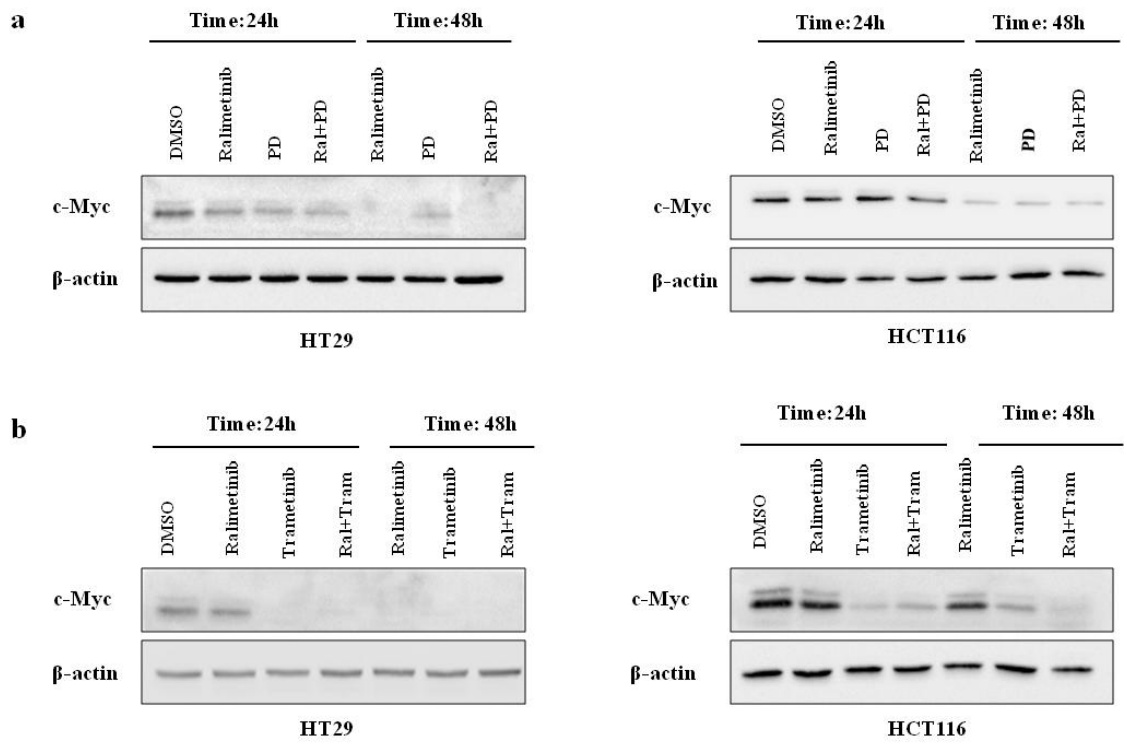

Figure 27. Pharmacological inhibitors that are currently in clinical trials effectively decrease c-Myc protein levels. (**a**) Single or combined inhibition with Ralimetinib (p38α inhibitor) and/or PD988059 (MEK/ERK inhibitor) induced a decrease in c-Myc protein levels in both HT29 and HCT116 CRC cell lines. (**b**) Combined treatment with Ralimetinib and Trametinib (MEK/ERK pharmacological inhibitor) was more efficient than either single treatment in promoting a decrease in c-Myc protein levels in HT29 and HCT116 CRC cell lines. β-actin was used as a loading control. SB: SB202190, PD: PD988059, Ral: Ralimetinib, Tram: Trametinib. The presented results are representative of at least three independent experiments.

Moreover, we determined the cell death response in single and combined treatments condition, trypan blue staining scores were analyzed to obtain the relative cell death in HT29 cells at 24 hours. The cell death rate showed a nearly 40% increase when Ralimetinib was administered alone, an 30% increase when Trametinib was administered alone, and finally an increase of about 70% when drugs were administered in combination **(Figure 28a)**. Finally, we performed WST-1 assay in order to assess cytotoxicity and proliferation. Our results confirmed that Ralimetinib and Trametinib induce the decrease of cancer cells proliferation **(Figure 28b)**.

Furthermore, considering the major role of c-Myc as a transcription factor in CRC initiation and progression, we evaluated the downregulation of c-Myc target genes following inhibition of p38α and ERK by using Ralimetinib and Trametinib.

HT29 cells treated for 24 hours with p38α and/or ERK inhibitors were analyzed by real-time PCR to test various c-Myc targets. In these cells, c-Myc inhibits the expression of p21 and activates the transcription of Cyclin E, which both play an important role in the transition from G1 to S phase of the cell cycle. The administration of Ralimetinib and/or Trametinib increased the expression of p21 and reduced the levels of Cyclin E, Cyclin A, and cdc25, which are all involved in cell cycle progression **(Figure 28c)**.

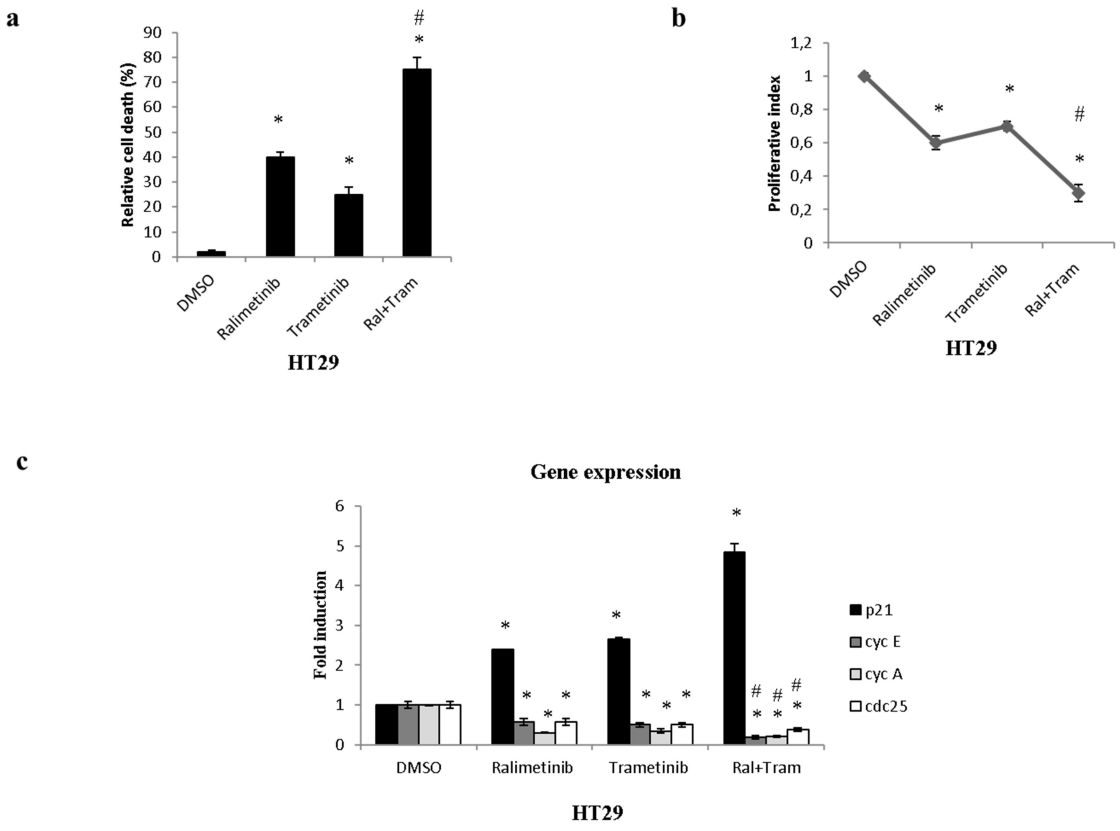

Figure 28. Combined inhibition of p38α and MEK/ERK modulates CRC cell proliferation and death, and c-Myc target genes. (**a**) HT29 cells were treated with Ralimetinib (10μM) (p38α inhibitor) and/or Trametinib (MEK/ERK inhibitor) (1μM), and relative cell death was calculated after 24 hours. Administration of Ralimetinib alone or in combination with Trametinib strongly increased the number of dead cells. (**b**) Ralimetinib and/or Trametinib treatment decreased CRC cell viability. HT29 cells were treated with Ralimetinib (10μM) or Trametinib (1μM), analyzed by WST-1 assay and scored for their proliferative index. Combined inhibition of p38α and MEK/ERK decreased relative viability while increasing relative cell death. (**c**) HT29 CRC cells were treated with Ralimetinib and/or Trametinib for 24 hours. mRNAs were isolated, reverse transcribed into cDNA, and gene expression was analyzed. Real-time PCR analyses of c-Myc

target genes involved in cell cycle showed increased expression of p21 and decreased expression of Cyclin E, Cyclin A, and cdc25. β-actin was used for normalization. Ral: Ralimetinib, Tram: Trametinib. Statistical analysis was performed using Student's t-tail test; *P<0.05: single treatment to untreated, # P<0.05: combined treatment (Ralimetinib+ Trametinib) to single treatment, were considered statistically significant. The presented results are representative of at least three independent experiments.

Moreover, we found that inhibition of ERK for 24 hours also affects c-Myc mRNA expression consistent with the data obtained by Kerkhoff and colleagues (Kerkhoff E et al, 1998). Surprisingly, our data showed that also p38α inhibition downregulates c-Myc transcription **(Figure 29a-b)**.

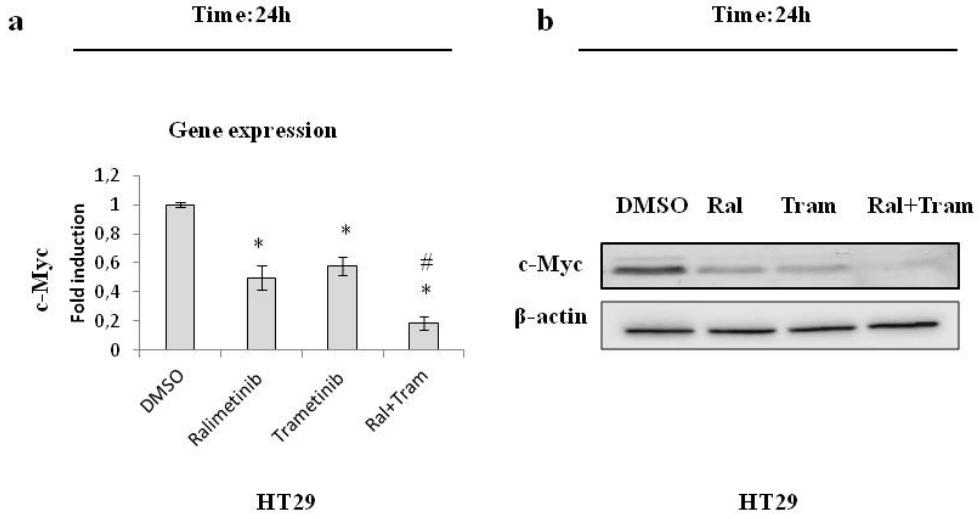

Figure 29. Single and combined inhibition of p38α and MEK/ERK efficiently abrogates c-Myc expression. Pharmacological inhibition with Ralimetinib (p38α inhibitor) and/or Trametinib (MEK/ERK inhibitor) for 24 hours efficiently reduced c-Myc levels both at the mRNA (**a**) and the protein (**b**) levels in HT29 cells, as measured by real time PCR and Immunoblotting, respectively. β-actin was used as a loading control. Ral: Ralimetinib, Tram: Trametinib. Statistical analysis was performed using Student's t-tail test; *P<0.05: single treatment to untreated, # P<0.05: combined treatment (Ralimetinib+ Trametinib) to single treatment, were considered statistically significant. The presented results are representative of at least three independent experiments.

These findings suggest a completely new scenario, where p38α exerts its transcriptional co-activator role in the regulation of c-Myc, the key player in the Wnt pathway.

3.2 Results 2

As described in the introduction, during intestinal tumorigenesis, c-Myc is maintained upregulated not only by post-translational stabilization induced by ERK-mediated phosphorylation at S62 but also by β-catenin-dependent transcriptional activation. Besides, the data reported above showed that inhibition of p38α, which is considered the prototype of chromatin-associated kinases, downregulates c-Myc mRNA and protein expression **(see Figure 29)**. This prompted us to ascertain whether p38α can physically interact and promote the activity of β-catenin, which is the best-known c-Myc transcription activator **(Figure30)**.

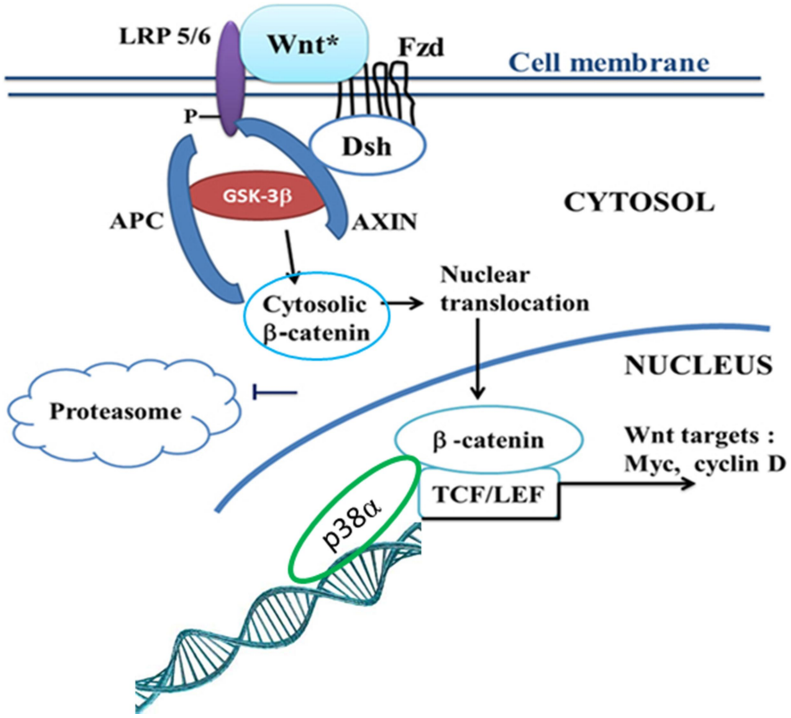

Figure 30. p38α is a chromatin-associated kinase (adapted from Lecarpentier Y and Vallee A, 2016). Part of our study was aimed at investigating whether p38 (green) could physically interact with β-catenin (blue) on chromatin and promote the activity of β-catenin, which is a well-recognized c-Myc transcriptional activator.

3.2.1 p38α and β-catenin localization in normal and CRC cells

As reported by Yochum and colleagues in previous studies, c-*Myc* gene expression has long been studied by analyzing the response of quiescent cells to growth factors. Indeed, c-*Myc* expression is undetectable in serum-starved quiescent cells but is dramatically induced upon serum addition (Yochum G, Cleland R and Goodman R, 2008).

First of all, we characterized c-Myc, p38α, and β-catenin protein localization by subcellular fractionation. HCT116 cells and the human colon normal epithelial cell line HCEC-1CT were first arrested in the G0/G1 phase of the cell cycle by culture in serum-depleted media for 48 hours, in order to inhibit β-catenin activity in the nucleus. We then replaced this medium with one containing serum with or without 10mM LiCl for 4 hours. LiCl is a well-established agonist of the Wnt/β-catenin pathway, as it inhibits GSK3β and stimulates nuclear β-catenin accumulation. This experiment confirmed that c-Myc and β-catenin expression is barely detectable under serum starvation and increases substantially after serum stimulation. Interestingly, p38α showed the same nuclear/cytoplasmic localization of β-catenin under all treatment conditions. Besides, β-catenin and p38α were predominantly found in the nucleus in the HCT116 cell line, while they were primarily located in the cytoplasm in HCEC-1CT cells. Similarly, c-Myc was located only in the nucleus in HCT116 cancer cells but was found both in the nucleus and in the cytoplasm in the HCEC-1CT normal cell line **(Figure31)**.

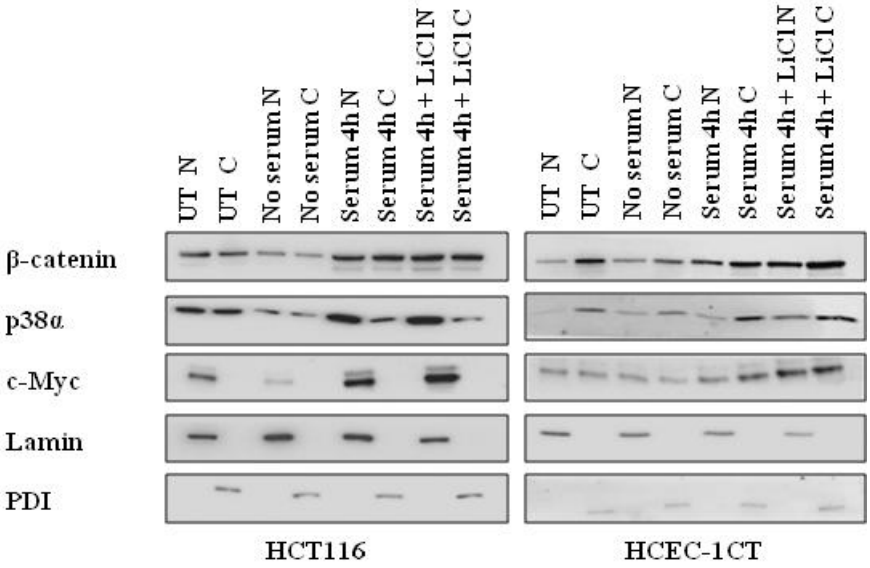

Figure 31. p38α and β-catenin show the same nuclear/cytoplasmic localization. CRC (HCT116) and normal colon epithelial (HCEC-1CT) cells were first arrested in the G0/G1 phase of the cell cycle by culture in a serum-depleted medium for 48 hours. Then, they were shifted to a serum-containing medium with or without the Wnt/β-catenin pathway agonist LiCl (10mM) for 4 hours. Immunoblot analyses were performed with the indicated antibodies. The purity of each fraction was controlled with specific markers (nucleus: lamin, cytoplasm: PDI). UT: untreated, N: nucleus, C: cytoplasm. The presented results are representative of at least three independent experiments.

Similar results were obtained in immunofluorescence experiments, where HCT116 and HCEC-1CT cells were stained for p38α and β-catenin, counterstained with DAPI and visualized to detect endogenous p38α-β-catenin complexes. These data showed that in cancer cells, p38α and β-catenin mainly co-localize in the nucleus, while in normal cells they are mostly found in the cytoplasm. The graph reflects the quantification of the co-localization analysis performed by confocal microscopy **(Figure32)**.

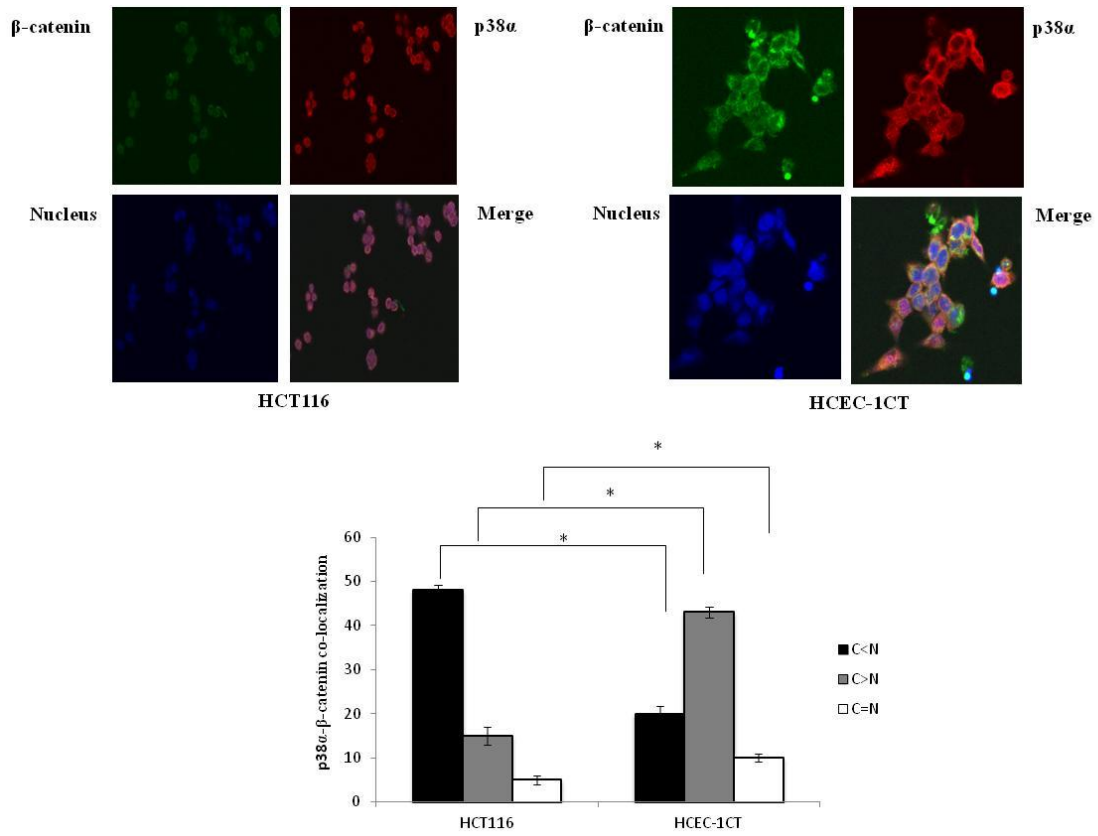

Figure 32. p38α co-localizes with β-catenin both in the nucleus and in the cytoplasm. Immunofluorescence analyses by confocal microscopy showing p38α and β-catenin co-localization in both CRC (HCT116) and normal colon (HCEC-1CT) cells. In HCT116 cells, p38α (red) and β-catenin (green) co-localized mainly in the nucleus, while in HCEC-1CT cells they co-localized mostly in the cytoplasm. DAPI (blue) was used as nuclear staining. N: nucleus, C: cytoplasm. Statistical analysis was performed using Student's t-tail test; **P*<0.05 was considered statistically significant. The presented results are representative of at least three independent experiments.

3.2.2 Functional interactions between p38 and the APC/β-catenin complex

Our previous results prompted us to evaluate the co-immunoprecipitation of p38α and β-catenin in normal and CRC cells.

Stabilization of β-catenin resulting from mutations in the APC protein or in β-catenin itself is found in most CRC cell lines. HCT116 cells are wild-type (wt) for APC and heterozygous for β-catenin, harboring one wt allele and one mutant allele with deletion of serine 45, which is required for the regulation mediated by GSK3β. Conversely, HCEC-1CT are wt for both APC and β-catenin.

HCT116 and HCEC-1CT cells were lysed, and the total lysates were subjected to immunoprecipitation with an antiserum against p38α or β-catenin, followed by

immunoblotting for APC, β-catenin, and p38α. The results obtained led us to speculate that p38α is a component of the APC/β-catenin complex in both normal and CRC cells **(Figure33)**.

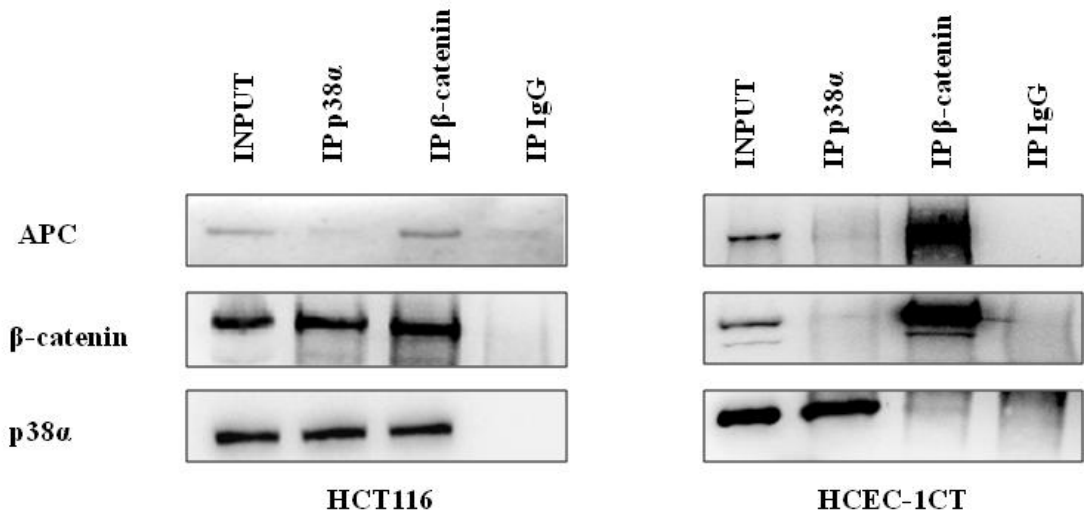

Figure 33. p38α co-immunoprecipitates with β-catenin in both CRC and normal colon cells. Immunoblotting analyses showing co-immunoprecipitation of p38α and β-catenin in both CRC (HCT116) and normal colon (HCEC-1CT) cells. Total lysates were immunoprecipitated for p38α or β-catenin and then immunoblotted for APC, p38α, and β-catenin. Immunoprecipitation with IgG was used as a negative control. The presented results are representative of at least three independent experiments.

Additionally, HCT116 and HCEC-1CT cells were subjected to a cellular fractionation protocol, and cytoplasmic and nuclear fractions were immunoprecipitated for p38α or β-catenin to detect the presence of the complex. Of note, we found that p38α co-immunoprecipitates with β-catenin in both normal and cancer cells; however, in normal colonocytes, they are confined to the cytoplasm, while in CRC cells they significantly occupy discrete nuclear regions. Based on these findings, it is reasonable to speculate that p38α may be involved in β-catenin transcriptional activity in cancer cells **(Figure34a-b)**.

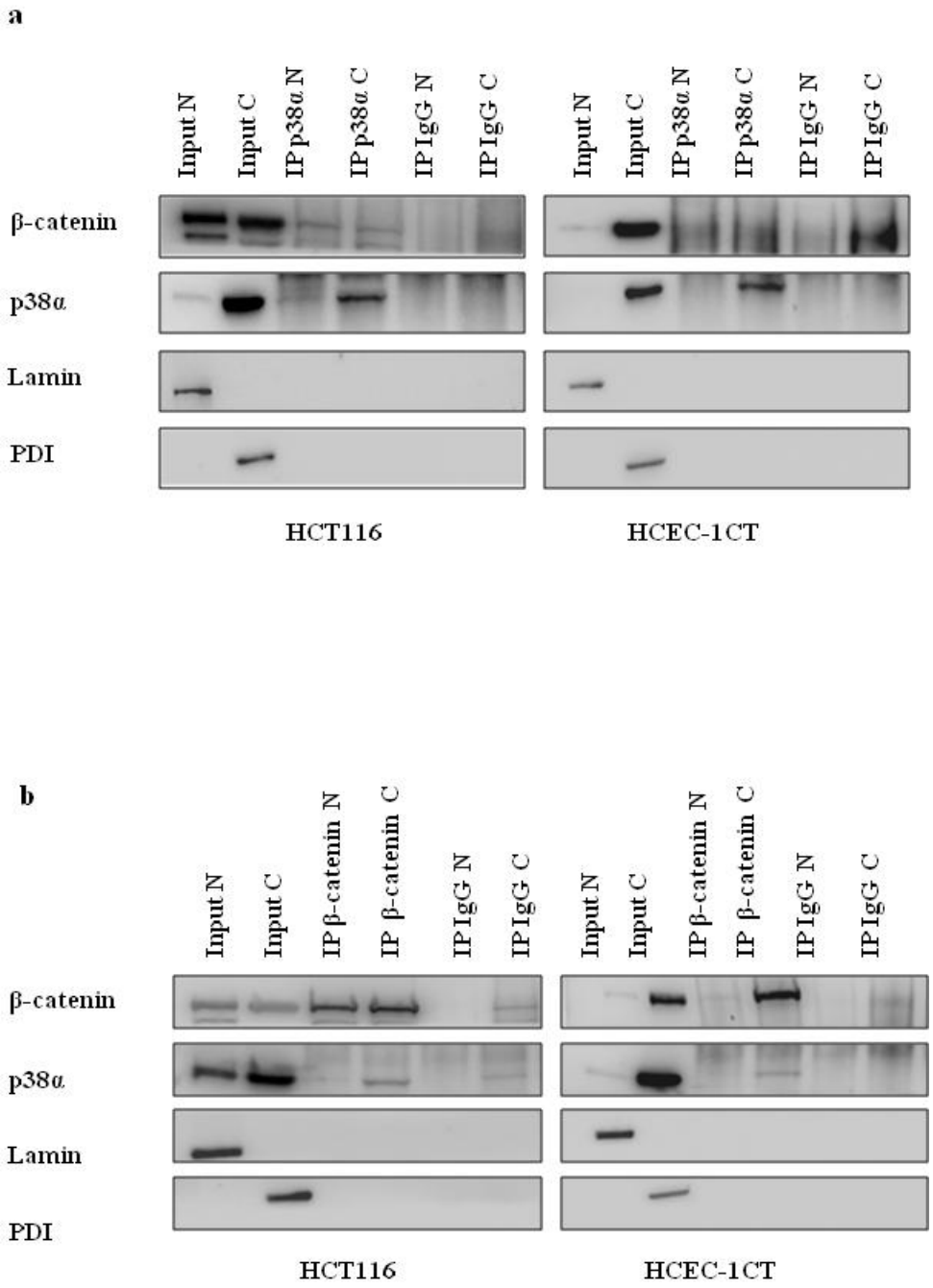

Figure 34. p38α co-immunoprecipitates with β-catenin both in the nucleus and in the cytoplasm. Immunoblotting analyses showing co-immunoprecipitation of p38α and β-catenin in both CRC (HCT116) and normal colon (HCEC-1CT) cells. In HCT116 cells, p38α and β-catenin co-precipitated mainly in the nucleus, while in HCEC-1CT cells they co-precipitated mostly in the cytoplasm. Cells were lysed and subjected to immunoprecipitation for p38α (**a**) or β-catenin (**b**). Immunoprecipitation with IgG was used as a negative control. The purity of each fraction was controlled with specific markers (nucleus: Lamin, cytoplasm: PDI). N: nucleus, C: cytoplasm. The presented results are representative of at least three independent experiments.

In the nucleus, β-catenin initiates transcription only as a member of bipartite or multimeric complexes wherein one partner provides association with specific response elements on target genes (e.g. Wnt response elements, WREs) and β-catenin acts as the central transcriptional activator. TCF/Lef transcription factors serve as the main nuclear partners of β-catenin, guiding it to specific DNA loci (Valenta T et al, 2012). After confirming the physical interaction between p38α and β-catenin, we investigated whether p38α affects β-catenin transcriptional activity.

In order to do so, HCT116 cells were treated with Ralimetinib (p38α inhibitor) or subjected to p38α genetic ablation. After mRNA extraction, real-time PCR experiments were performed in order to evaluate the expression of various β-catenin target genes, including CD44 and CyclinD1, which play a role in cell cycle, Survivin, which is involved in the inhibition of apoptosis, c-MET, which acts in different cellular signaling pathways such as migration and invasion, and Sox9 and Tcf7, which are implicated in cancer stem cell proliferation. Our results showed that p38α inhibition leads to β-catenin target gene downregulation **(Figure35)**.

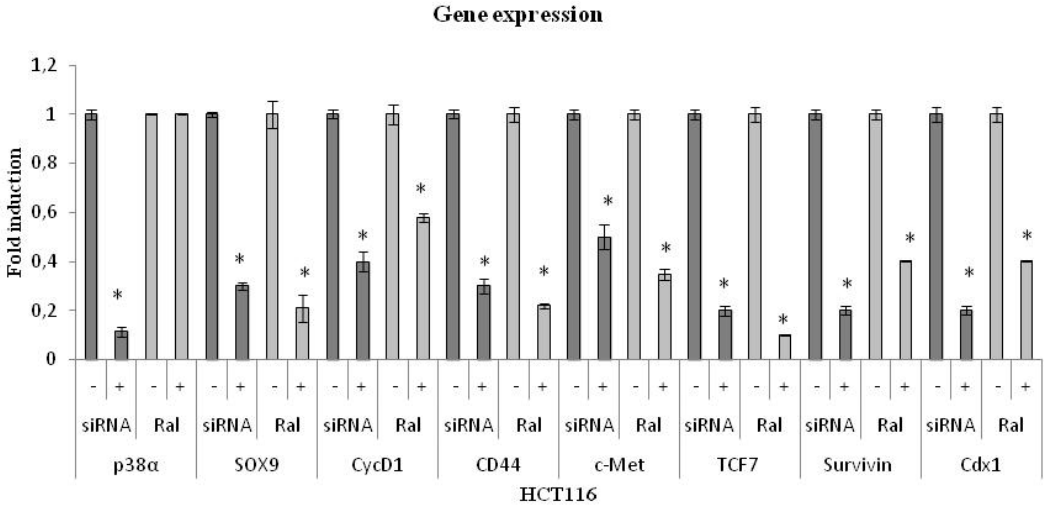

Figure 35. p38α inhibition induces the downregulation of β-catenin target genes. HCT116 CRC cells were treated with Ralimetinib (p38α inhibitor) or subjected to genetic ablation for p38α with a specific siRNA for 48 hours. mRNAs were isolated, reverse transcribed into cDNA, and gene expression was analyzed. Real-time PCR analyses were performed for SOX9, Cyclin D1, CD44, c-Met, TCF7, Survivin, and Cdx1, which are all β-catenin target genes. p38α amplification was used to confirm the efficacy of genetic ablation, β-actin was used for normalization. Statistical analysis was performed using Student's t-tail test; **P*<0.05 was considered statistically significant. The presented results are representative of at least three independent experiments.

These exciting results motivated us to further investigate the functional role of p38α and β-catenin complexes in transcriptional regulation. One of the commonly used assays to study transcriptional regulatory mechanisms is chromatin immunoprecipitation (ChIP), which enables the analysis of the association of regulatory molecules on specific promoters as well as histone modifications *in vivo*. By using this assay, we evaluated the actual co-recruitment of p38α and β-catenin on different binding motifs of β-catenin target genes. HCT116 cells were first arrested in the G0/G1 phase of the cell cycle by culture in serum-depleted medium for two days in order to inhibit β-catenin activity in the nucleus and then switched to a serum-containing medium. After mRNA extraction and reverse transcription, gene expression was analyzed. Serum mitogens dramatically stimulated β-catenin and p38α binding to WREs. Indeed, we confirmed p38α and β-catenin co-occupancy of the promoter sequence of all the analyzed β-catenin target genes, which exert different functions in cancer cells. For example, c-Myc, Sox9, c-Met, Survivin, CD44, and Cyclin D1, are all strongly involved in CRC progression. HDAC was used as a positive control of β-catenin transcriptional activity. These data suggest that p38α assists β-catenin in the activation of β-catenin target gene transcription **(Figure 36)**.

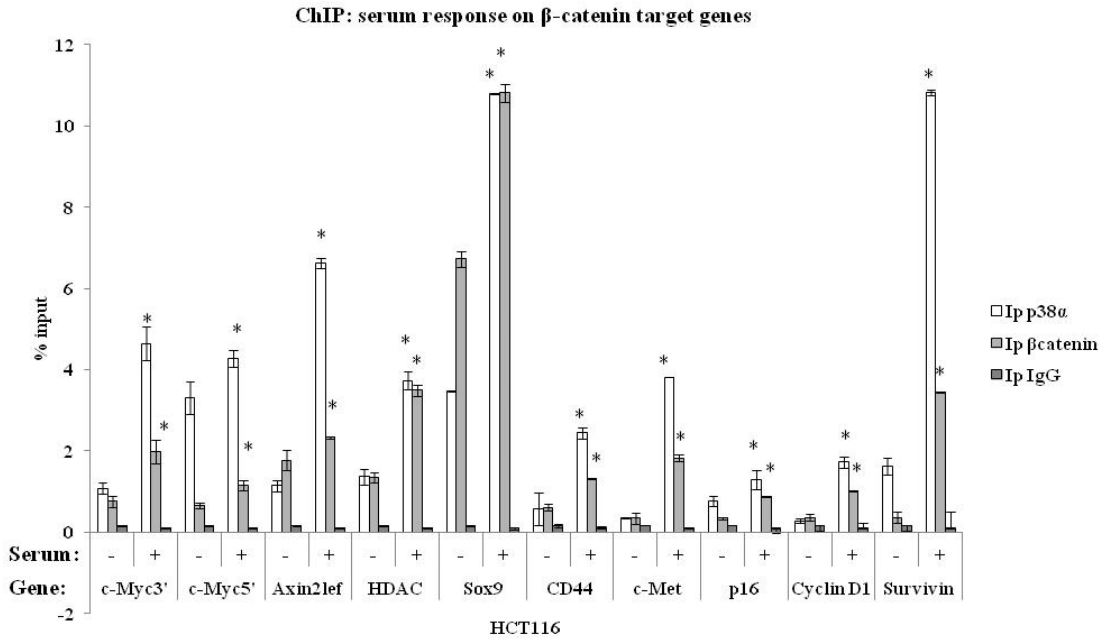

Figure 36. p38α co-operates with β-catenin in the activation of β-catenin target gene transcription. HCT116 CRC cells were starved in a serum-depleted media for 48 hours in order to arrest the cell cycle. Serum-deprived cells were then switched to a serum-containing medium for 4 hours prior to chromatin immunoprecipitation (ChIP) with specific antibodies (against p38α or β-catenin). Specific oligonucleotides were used to detect binding to Wnt responsive elements (WREs) on c-Myc (both WREs), Axin2lef, SOX9, Cyclin D1, CD44, c-Met, p16, Survivin. HDAC was used as a positive control of β-catenin transcriptional activity. Data are presented as induced expression relative to levels obtained in serum-deprived cells. Immunoprecipitation with IgG was used as a negative control. Statistical analysis was performed using Student's t-tail test; **P*<0.05 was considered statistically significant. The presented results are representative of at least three independent experiments.

Advances in CRC diagnosis and treatment do not always translate into a favorable clinical outcome, and disease-free survival of CRC patients remains poor. A critical challenge in the management of CRC is metastasis and relapse of the disease. Colorectal cancer stem cells (CRC-SCs) are closely related to tumor metastasis, drug resistance, and recurrence after primary treatment (Zhou Y et al, 2018); indeed, conventional anticancer therapies wipe out the bulk populations of a tumor, while CRC-SCs are resistant to chemo- and radiotherapy. Consequently, it is necessary to find new treatment approaches aimed at selectively targeting CRC-SCs and bulk populations in order to achieve complete tumor eradication (Szarynska M et al, 2017). Thus, studies focusing on chemoresistance mechanisms to identify novel therapeutic strategies directed against specific targets have become increasingly desirable to improve patients' survival. p38 might well be one of these targets. To test this hypothesis, we performed an extensive characterization of p38α in cancer stem cell models, with the purpose of countering uncontrolled proliferation, metastatic dissemination, and chemoresistance.

3.2.3 Characterization of p38α in CRC-SC models

We performed our p38α characterization studies in four different CRC-SC lines collected from consenting patients. The mutations identified so far are summarized in **Table 1**.

Cell line	Mutations												Ploidy	MSI
	KRAS	P53	PI3KCA	SMAD4	ERBB4	FGFR3	EGFR	MET	NOTCH1	FGFR2	APC	CTNNB1		
G605	X	X	X	X	X	X	X				X		Hyperdyploid	MSS
511			X	X		X					X		Hyperdyploid	MSS
ME59	X	X	X	X		X	X						Hyperdyploid	MSI
DA13		X			X	X	X	X	X	X			Hyperdyploid	MSI

Table 1. Colorectal cancer stem cells (CRC-SCs) obtained from consenting patients were investigated for mutations, ploidy status and microsatellite instability (MSI). X indicates a mutated gene, MSS indicates Microsatellite Stable, MSI indicates Microsatellite Instable.

Besides, to start characterizing these new cellular models, we performed a cytogenetic analysis for the detection of chromosome instability. As described by Howe et al., chromosome analysis is recommended as part of the quality control process, especially in stem cell research. Indeed, when followed by Q-banding techniques, this assay has the powerful ability to analyze individual cells for aberrations that involve gains or losses of portions of the genome and rearrangements involving one or more chromosomes (Howe B, Umrigar A and Tsien F, 2014).

Chromosomes were analyzed at the metaphase stage of mitosis, when they are most condensed and therefore more visible. All four investigated cell lines showed chromosomal instability, with the modal number ranging from 65 to 75 chromosomes. Thus, all four cell lines were hyperdiploid (3n +/- few). In particular, G605, DA13, and ME59 cells have a modal number of 65 chromosomes, while 511 cells have 75 chromosomes.

We analyzed more than 50 metaphases for each cell line and found structural chromosomal abnormalities in all of them, including inversions, deletions, duplications, translocations, isochromosomes, and ring chromosomes **(Figure37)**.

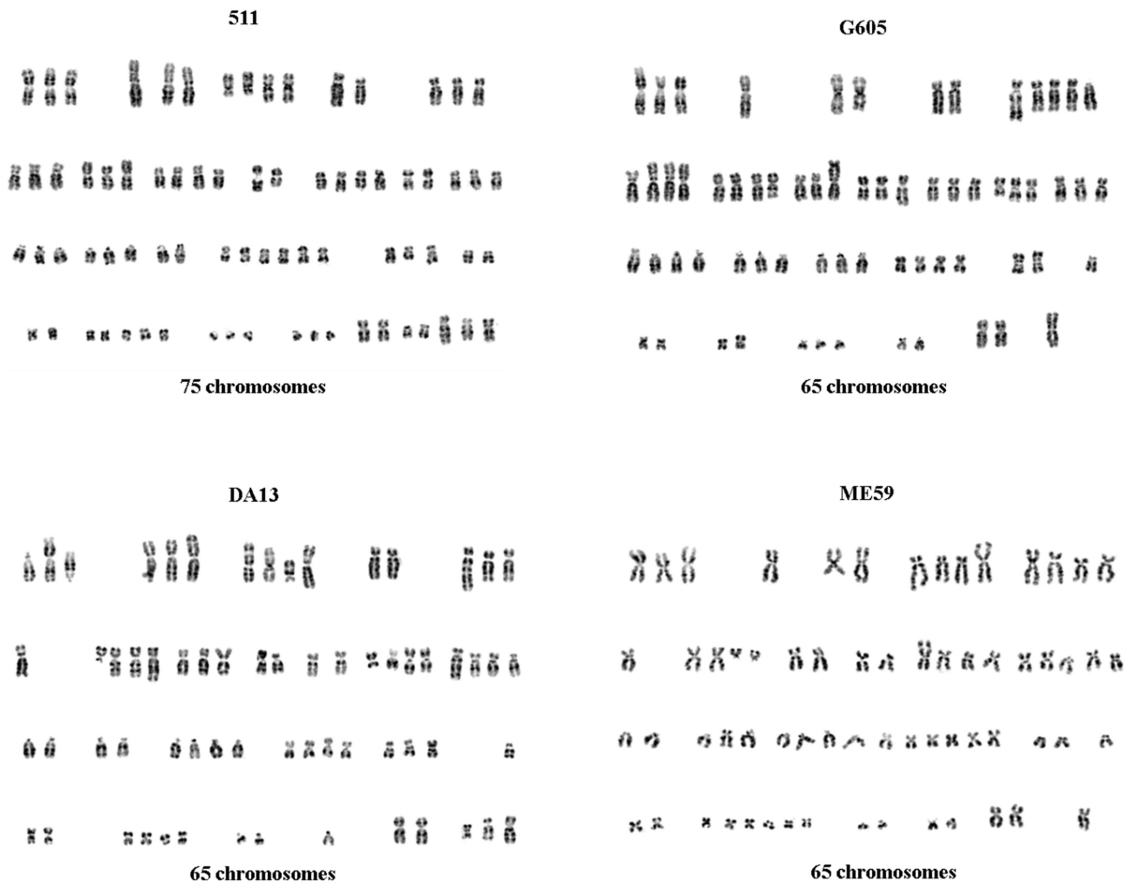

Figure 37. Image showing the karyotype Q-banding analyses obtained by fluorescence using Quinacrine (QFQ-banding). Q-banding involves use of the fluorescent dye quinacrine, which alkylates DNA and is subject to quenching over time. Quinacrine produces characteristic and reproducible banding patterns for individual chromosomes. All the analyzed CRC-SCs (511, G605, DA13, and ME59) were hyperdiploid (3n +/- few).

CRC-SC lines are identified via a group of surface markers. The main CRC-SC markers documented in the literature are CD44, CD133, and Lgr5. CD44 is a cell surface glycoprotein involved in malignant progression, cell adhesion, and migration, and is associated with lower sensitivity to apoptosis signals and greater resistance to therapies. CD133 is a cell transmembrane glycoprotein involved in stemness regulation. Lgr5 is a downstream target of the Wnt pathway and is related to tumorigenesis, 5-fluorouracil resistance, and cancer recurrence (Munro MJ et al, 2018). Thus, we performed immunoblot analyses to evaluate the expression patterns of these markers in 511(CRC-SC line), in the human colon normal epithelial cell line HCEC-1CT, and in the CRC cell lines used in previous experiments (HCT116 and HT29). Our data showed that CRC-SCs have larger amounts of c-Myc protein compared to the other cell lines. Moreover, CRC-SCs were rich in β-catenin, phospho-p38 (p38 active form), and stem cell markers, especially CD44 and CD133. Finally, we found that CRC-SCs have a low quantity of keratin 20, which is a major cellular protein of mature enterocytes and goblet cells. Consistent with the literature, HCEC-1CT cells expressed the stem cell marker Lgr5 and displayed low expression of keratin 20. Indeed, it has been shown that HCEC-1CT cells have increased amounts of keratin 20 under growth arrest conditions (Roig A et al, 2010). Lastly, consistent with the Catalogue of Somatic Mutations in Cancer (COSMIC) database, HT29 cells exhibit high expression of keratin 20 **(Figure38)**.

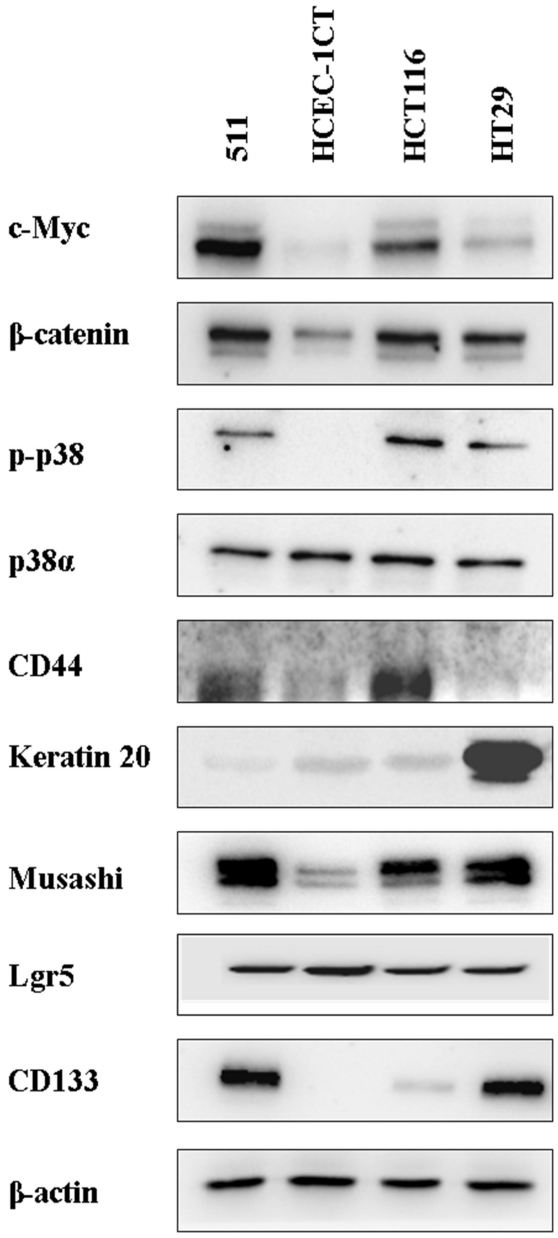

Figure 38. Analysis of CRC-SC molecular biomarkers. Total lysates from 511 (CRC-SC), HCEC-1CT, HCT116, and HT29 cells were subjected to immunoblotting analyses for the indicated antibodies. This experiment investigated the expression of different molecular biomarkers of CRC-SCs, such as CD44, CD133, and Lgr5, a differentiation marker (Keratin 20), the active form of p38α (p-p38), β-catenin, and c-Myc. β-actin was used as a loading control. The presented results are representative of at least three independent experiments.

Subsequently, we characterized c-Myc, p38α, and β-catenin protein localization by subcellular fractionation. CRC-SCs (511 and G605) were cultured with or without a Wnt pathway inhibitor (PRI-724) or activator (Wnt3a alone or in combination with LiCl). Again, our results confirmed the observation that c-Myc and β-catenin decrease

upon inhibition of the Wnt pathway and increase substantially after its activation. Interestingly, p38α showed the same nuclear/cytoplasmic localization of β-catenin under all treatment conditions in both cell lines analyzed **(Figure39)**.

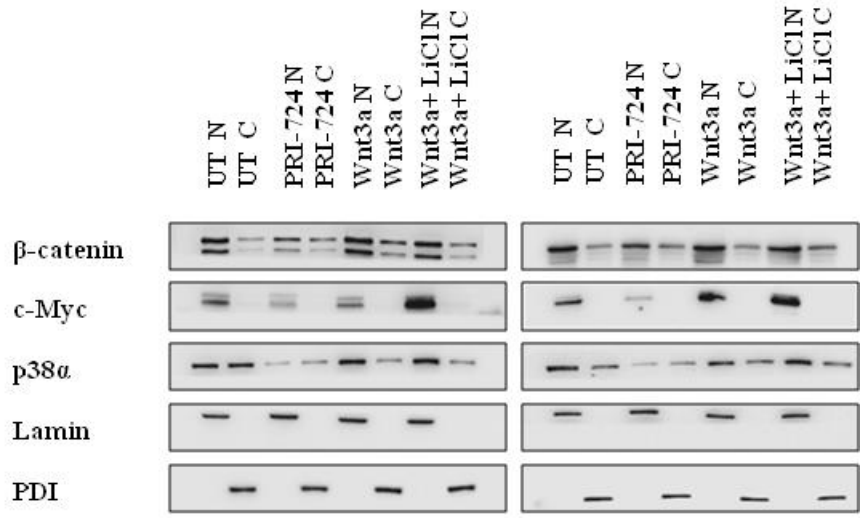

Figure 39. p38α and β-catenin show the same nuclear/cytoplasmic localization in CRC-SCs. Two different CRC-SC lines were treated with PRI-724 (Wnt pathway inhibitor) or with Wnt3a and/or LiCl (Wnt pathway activators). Immunoblot analyses were performed with the indicated antibodies. The purity of each fraction was controlled with specific markers (nucleus: Lamin, cytoplasm: PDI). UT: untreated, N: nucleus, C: cytoplasm. The presented results are representative of at least three independent experiments.

3.2.4 p38α: a new member of the β-catenin complex in CRC-SC models

In order to confirm the functional interaction between p38α and β-catenin, we performed a co-immunoprecipitation assay in 511, G605, and DA13 CRC-SCs. Cells were lysed and subjected to immunoprecipitation with an antiserum against p38α or β-catenin, followed by immunoblotting for APC, β-catenin, and p38α. We observed that p38α and β-catenin co-immunoprecipitate in all three CRC-SC lines used. Given the importance of CRC-SCs in colorectal tumorigenesis, these data emphasize the importance of inhibiting the activity of the p38α-β-catenin complex **(Figure 40a-b-c)**.

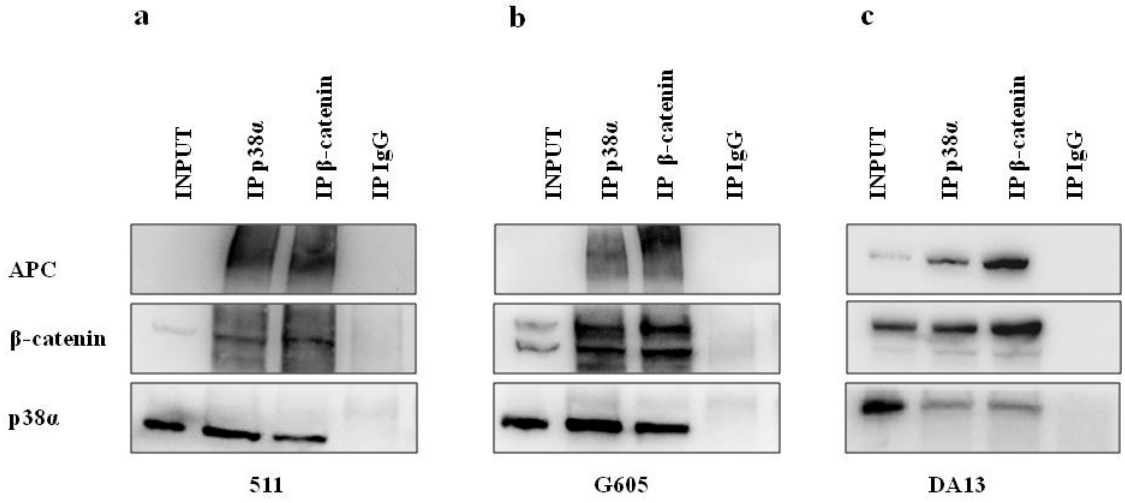

Figure 40. p38α is a component of the APC/β-catenin complex in the intestinal stem niche. Total lysates from 511 (**a**), G605 (**b**), and DA13 (**c**) CRC-SCs were immunoprecipitated for p38α or β-catenin and then immunoblotted for APC, p38α, and β-catenin. Immunoprecipitation with IgG was used as a negative control. The presented results are representative of at least three independent experiments.

Additionally, all three CRC-SC lines were subjected to a cellular fractionation protocol. Cytoplasmic and nuclear fractions were immunoprecipitated for p38α or β-catenin to detect the presence of the complex. Of note, p38α co-immunoprecipitated with β-catenin in both compartments. Importantly, these data reveal that p38α and β-catenin are components of the same complex in the stem niche, thus p38α may be involved in β-catenin transcriptional activity in CRC-SCs **(Figure 41a-b-c).**

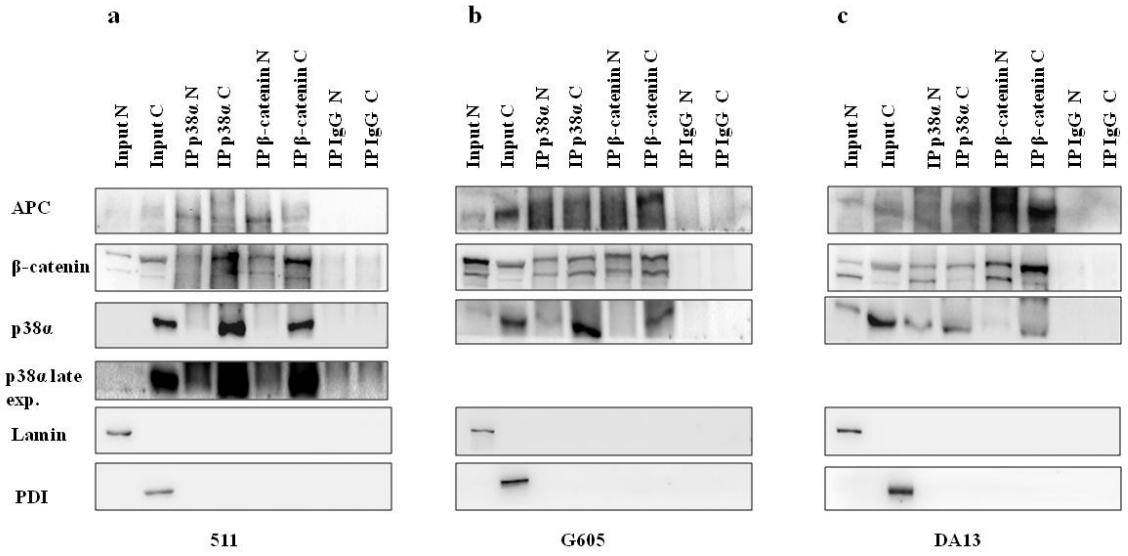

Figure 41. p38α is a component of the APC/β-catenin complex both in the nucleus and in the cytoplasm in all CRC-SCs analyzed. Cells were lysed and subjected to a fractionation protocol. Nuclear and cytoplasmic fractions were immunoprecipitated for p38α or β-catenin and subsequently subjected to immunoblotting analyses, which showed p38α and β-catenin co-immunoprecipitation in 511 (**a**), G605 (**b**), and DA13 (**c**) CRC-SCs. Immunoprecipitation with IgG was used as a negative control. The purity of each fraction was controlled with specific markers (nucleus: Lamin, cytoplasm: PDI). N: nucleus, C: cytoplasm. The presented results are representative of at least three independent experiments.

In order to verify the power of our new potential therapeutic strategy for the purpose of targeting CRC-SCs and differentiated cancer cells, we finally investigated the cell death response and the cell proliferation in CRC-SC model after the single or combined inhibition of the p38α and/or MEK/ERK pathways. Indeed, we determined the cell death response in single and combined treatments condition, trypan blue staining scores were analyzed in CRC-SCs (511, G605 and DA13) at 24 hours. The administration of Ralimetinib (10μM) alone and even more in combination with Trametinib (1μM), strongly increased the number of dead cells in CRC-SC lines **(Figure42a)**.

Finally, we performed WST-1 assay in order to assess cytotoxicity and proliferation. Our results confirmed that Ralimetinib and/or Trametinib induced the decrease of CRC-SCs proliferation. These results validate the idea to use the inhibition of p38α as therapeutic strategy to inhibit the uncontrolled cellular proliferation of both stem and differentiated cells **(Figure 42b)**.

a

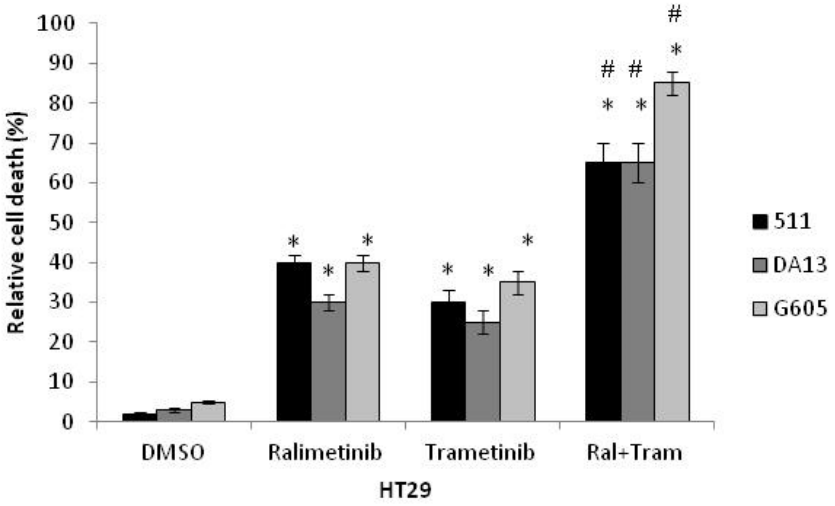

b

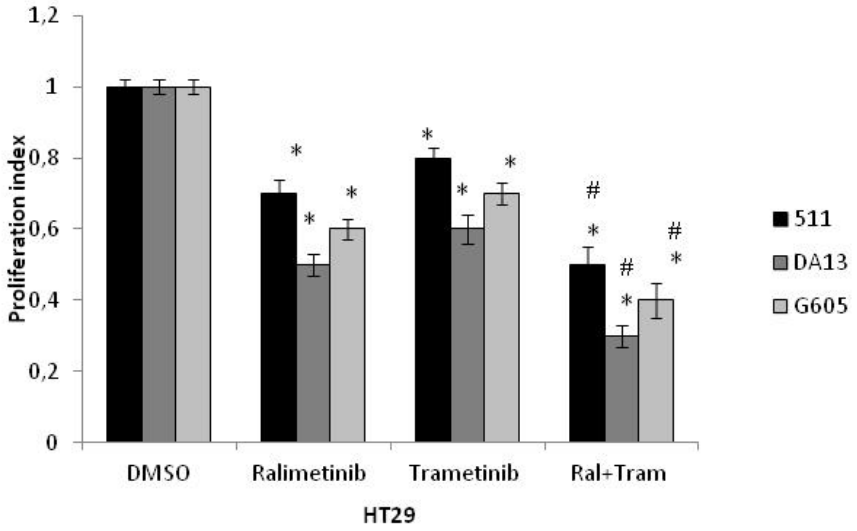

Figure 42. Combined inhibition of p38α and MEK/ERK decreases relative viability while increasing relative cell death in CRC-SCs. (**a**) 511, G605, and DA13 cells were treated with Ralimetinib (10 μM) (p38α inhibitor) and/or Trametinib (1μM) (ERK inhibitor), and relative cell death was calculated after 24 hours. Administration of Ralimetinib alone or in combination with Trametinib strongly increased the number of dead cells. (**b**) Ralimetinib and/or Trametinib treatment decreased cell viability in CRC-SCs. Cells were treated with Ralimetinib (10μM) or Trametinib (1μM), analyzed by WST-1 assay, and scored for their proliferative index. Statistical analysis was performed using Student's t-tail test; **P*<0.05: single treatment to untreated, # *P*<0.05: combined treatment (Ralimetinib+ Trametinib) to single treatment were considered statistically significant. The presented results are representative of at least three independent experiments.

To validate the results obtained *in cellulo*, we performed *in vivo* studies in three different mouse systems: $APC^{Min/+}$ mice, which are an important model for the study of FAP, as they are heterozygous for a missense mutation in the APC gene and develop multiple polyps; $APC^{Min/+}$ mice treated with the carcinogen azoxymethane (AOM), which are considered a highly reproducible model of CRC; and c57 mice, which are commonly used as a "genetic background", being the normal counterpart of $APC^{Min/+}$ mice. First of all, we assessed the expression of p-p38, p-ERK, β-catenin, and c-Myc in these three mouse systems and found increased levels of all these proteins in the two $APC^{Min/+}$ models compared to c57 wt mice **(Figure 43a)**.

Then, immunoprecipitation studies confirmed the results obtained *in cellulo*: p38α and β-catenin co-immunoprecipitated mainly in the cytoplasm in c57 wt mice, while they co-immunoprecipitated mostly in the nucleus in $APC^{Min/+}$ mice **(Figure 43b)**.

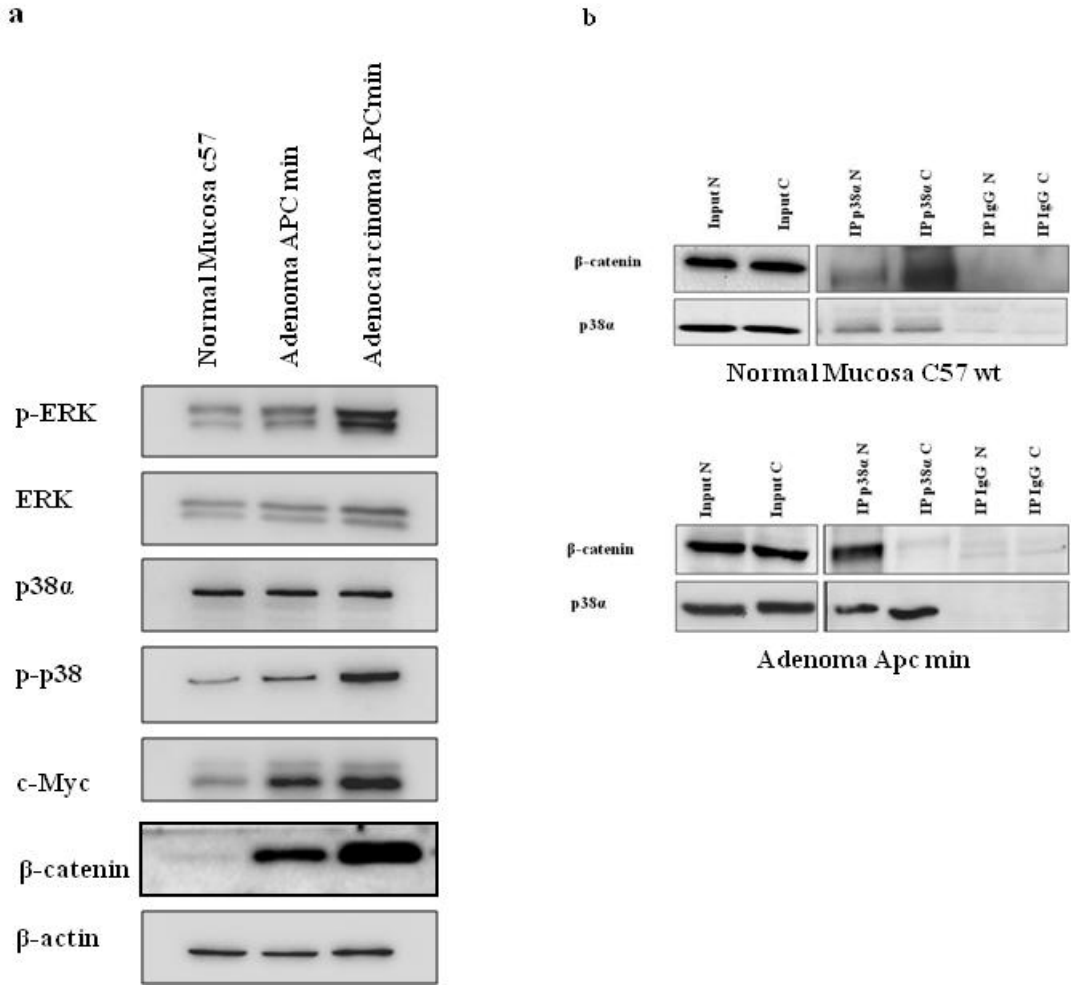

Figure 43. p38α and β-catenin belong to the same complex in *in vivo* experiments. (**a**) Analysis of p-p38, c-Myc, p-ERK, and β-catenin protein levels in three different mouse models (c57 wt mice, $APC^{Min/+}$ mice and $APC^{Min/+}$ mice treated with azoxymethane). (**b**) Colon tissues from C57 wt mice and $APC^{Min/+}$ mice were lysed and subjected to a fractionation protocol. Nuclear and cytoplasmic fractions were immunoprecipitated for p38α and subsequently subjected to immunoblotting analyses, which showed p38α and β-catenin co-immunoprecipitation in both mice models. In C57 wt mice, p38α and β-catenin co-precipitated mainly in the cytoplasm, while in $APC^{Min/+}$ mice they co-precipitated mostly in the nucleus. Immunoprecipitation with IgG was used as a negative control. AOM: azoxymethane, N: nucleus, C: cytoplasm. The presented results are representative of at least three independent experiments.

It should be remembered that scientific progress is almost always the result of the integration between the data obtained in man and the results of research carried out in other more or less advanced animal models. In fact, as often happens, man represents the final term and the confirmation of a cognitive process, often long, based on observations and working hypotheses generated in other experimental models.

The last phases of the drug development process or of any therapy pass through the so-called 'controlled clinical studies', which represent the certification of effectiveness.

Controlled clinical studies require previous experience in the experimental animal (preclinical studies), which form the basis for transferring a drug to humans. These experiences are of the utmost importance to guide the scientist regarding the doses to be used and the secondary effects to which treated patients are exposed. Indeed, p38α, our promising therapeutic target and MEK/ERK are actually targeted in several clinical trials on patients suffering of CRC. Few of them are summarized in **Table2**.

The results collected in this study confirmed the crucial role of the MAPK/c-Myc axis in the regulation of in intestinal tumorigenesis, suggesting that MAPK manipulation might be a potential therapeutic approach to counteract c-Myc-dependent carcinogenesis.

Target	Agent	Phase	Number	Tumor	Status
ALS, p38	Tamoxifen+ Ralimetinib	II	NCT02322853	Metastatic Breast Cancer	Terminated
CK1, p38	Prexasertib + Ralimetinib	I	NCT02860780	Metastatic Cancer, Colorectal and NSCL cancer	Completed
p38, NFKB	Ralimetinib + Temozolomide	II	NCT02364206	Glioblastoma	Active
BRAF, MEK, PD1	Dabrafenib + Trametinib + PDR 001	II	NCT03668431	Metastatic Colorectal Cancer	Recruiting
MEK, HDM2	Trametinib + HDM201	I	NCT03714958	Metastatic Colorectal Cancer	Recruiting
MEK, PDL-1	Trametinib + Durvalumab	II	NCT03428126	Colorectal Cancer	Recruiting
MEK	Lapatinib + Trametinib	II	NCT02230553	Colorectal Cancer	Recruiting
EGFR, MEK	Panitumumab +/- Trametinib	II	NCT03087071	Colorectal Cancer	Recruiting
PD-1, MEK, CTLA-4	Nivolumab + Trametinib + Ipilimumab	II	NCT03377361	Colorectal Cancer	Recruiting
MEK,EGFR	Trametinib + Panitumumab	II	NCT02399943	Colorectal Cancer	Recruiting
BRAF, MEK EGFR, TS	Dabrafenib + Trametinib + Panitumuab + 5FU	II	NCT01750918	Colorectal Cancer	Active
PDL-1, EGFR, IL1, MEK	PDR001 + EGF816 + Canakinumab + Trametinib	I	NCT02900664	Colorectal Cancer	Recruiting
MEK,TS	Trametinib + TAS-102	I	NCT03317119	Colorectal Cancer	Recruiting
CDK4/6, MEK	Ribociclib + Trametinib	II	NCT02703571	Colorectal Cancer	Recruiting
EGFR, MEK	MM-151/121/141 + Trametinib	II	NCT02538627	Colorectal Cancer	Terminated
BRAF, MEK AKT	Dabrafenib + Trametinib + GSK2141795	II	NCT01902173	Colorectal Cancer	Suspended
MEK, TS	Trametinib + Fluorouracil	I	NCT01740648	Colorectal Cancer	Active

Table2. Ongoing clinical trials with Ralimetinib (p38α inhibitor) and Trametinib (ERK inhibitor).

Discussion

CRC is the third most frequent malignancy but the second cause of death for tumor in the western population (Bhandari A, Woodhouse M, and Gupta S, 2017). Current treatment for CRC is based on combination therapies, which in most cases include surgery, local radiotherapy, and chemotherapy. The success of chemotherapy relies on the ability to kill or, better, to selectively induce apoptosis in cancer cells (Kauffman S and Earnshaw W, 2000). It has been demonstrated that chemoresistance depends on a small population of cells in the bulk tumor called cancer stem cells (CSCs). These cells are exposed to selective pressure (Merlo LM et al, 2006), thus it is not surprising that they evolve strategies to inhibit pro-apoptotic signaling pathways and favor pro-survival and proliferative cascades (Feitelson M A et al, 2016). Therefore, a promising approach consists in finding critical molecular targets that are positively selected and are essential for tumor growth. This concept is the base of current research, and several compounds that target crucial signaling pathways are now under clinical trials. Overall, over 2000 studies are ongoing on CSCs (https://clinicaltrials.gov/ct2/results?cond=cancer+stem+cell&term=&cntry=&state=&city=&dist=).

The gene expression program that determines CSC features is controlled by c-Myc, which acts as a link between stemness and malignancy. In CRC, c-Myc has been found overexpressed in up to 80% of sporadic cases, as a result of its transcriptional activation mediated by β-catenin following APC inactivation and its post-translational stabilization mediated by ERK. The MEK/ERK signaling pathway is involved in tumor initiation and progression by promoting cell proliferation and survival (Fang JY and Richardson BC, 2005), and is being widely studied as a promising pharmacological target (Thompson N and Lyons J, 2005). Intriguingly, MEK/ERK inhibition induces the phospho-activation of p38α, a kinase involved in CRC progression and cell migration. The existence of a p38α/ERK crosstalk has been previously established, since the inhibition of p38α also triggers ERK phospho-activation in different CRC cell lines.

Here we found that inhibition of p38α or ERK significantly reduces c-Myc protein levels in CRC cell lines regardless of the genetic background, and combined inhibition of both pathways has an even greater effect. Considering the crucial role of c-Myc in intestinal tumorigenesis and its high turnover, we investigated the role of p38α and ERK

in c-Myc regulation in a short-term experiment. Our results showed that 30-minute inhibition of p38α and ERK only affected c-Myc protein levels, while its mRNA expression remained unchanged. Given the significant effects of c-Myc on cell fate, it is not surprising that cancer cells have evolved sophisticated methods for ensuring proper c-Myc expression levels (Sears R, 2004). c-Myc protein expression is regulated both at the post-transcriptional (translation) and post-translational (protein stability) level. We thus performed experiments to assess p38α and ERK contribution to these processes. Since we found that p38α and ERK are not involved in c-Myc translation, we assessed whether they affect c-Myc stability. Indeed, increased c-Myc stability in malignant tissues may explain the high levels of c-Myc protein observed in human tumors in the absence of *c-Myc* gene amplification or deregulated mRNA expression (Junttila M and Wesrermarck J, 2008). Our results showed that p38α and ERK actually influence c-Myc protein stabilization, but they don't do so by affecting the GSK3β or PP2A pathways nor by regulating the autophagic response. Instead, we found that blocking proteasomal degradation rescues c-Myc protein levels after p38α inhibition or its genetic ablation, which was performed in order to exclude potential off-target drug effects. These data showed that p38α stabilizes c-Myc protein by preventing its ubiquitination.

The potential efficacy of p38α and MEK/ERK combined inhibition as a novel pharmacological strategy is also supported by results obtained in a preclinical mouse model. $APC^{Min/+}$ mice, which are heterozygous for a missense mutation in the *APC* gene, are widely used to study the effect of chemical compounds on the incidence and development of intestinal cancers. Notably, it has been shown that over half of the Wnt targets whose expression was increased after *APC* loss were no longer up-regulated in the absence of *c-Myc* (Samson O et al, 2007). In $APC^{Min/+}$ mice, combined inhibition of the p38α and MEK/ERK pathways promoted a 64-day increase in median survival compared with vehicle-treated animals. The results obtained with p38α and MEK/ERK combined inhibition highlight how important is the identification of protein kinases involved in tumorigenesis and tumor progression in order to shift the focus of cancer therapy on drugs rationally designed to target tumor-specific pathways. Several clinical studies are now underway to collect information on the polypharmacological profile of kinase inhibitors. In light of this approach, we decided to use compounds that are currently in clinical trials for CRC, i.e. the p38α inhibitor Ralimetinib and the ERK inhibitor Trametinib. After positively testing their inhibitory activity in our CRC cell

lines, we confirmed that these pharmacological inhibitors were effective in increasing cell death response, decreasing the proliferation rate, and reducing c-Myc protein levels. As a transcription factor, c-Myc regulates the expression of 15% of all genes by binding to an enhancer box sequence (E-box sequence). Indeed, c-Myc coordinates a complex cellular response by which cells are set to progress through the cell cycle and proliferate. Based on this assumption, we decided to ascertain the therapeutic potential of p38α and ERK inhibition in the regulation of c-Myc target genes. c-Myc regulates the expression of several genes, including Cyclin D1, which is activated, and p21, which is repressed. Consistently, the decrease in c-Myc levels promoted by p38α and/or ERK inhibition induced the downregulation of Cyclin D1 and the upregulation of p21, which are both implicated in cell cycle progression.

Intriguingly, we found that single and/or combined inhibition of p38α and ERK for 24 hours with Ralimetinib and/or Trametinib leads to the downregulation of both c-Myc mRNA and protein levels. These results are in accordance with data from Kerkhoff and colleagues, who demonstrated that the MEK/ERK signaling pathway activates c-Myc gene transcription (Kerkhoff E et al, 1998). To our knowledge, however, this is the first report showing a role for p38α in c-Myc transcription. This result is extremely important because it suggests a completely new scenario, in which p38α functions as a transcriptional co-activator in c-Myc regulation. Indeed, p38α is considered the prototype of chromatin-associated kinases and can associate with and phosphorylate several transcription factors. For instance, p38α phosphorylates BAF60c, thereby promoting chromatin remodeling and transcription initiation of MyoD target genes (Forcales S et al, 2012).

We thus investigated the potential mechanisms involved in the regulation of c-Myc transcription by p38α. The main transcription factor controlling c-Myc expression is β-catenin. As a first step in the study of this new role of p38α, we performed subcellular fractionation experiments to compare the nuclear and cytoplasmic localization of p38α and β-catenin in two different colorectal cellular models - normal and cancer cells - under different treatments that activate or inhibit the Wnt signaling pathway. In normal cells, p38α and β-catenin mainly co-localized in the cytoplasm, while in cancer cells they were predominantly found in the nucleus. These findings prompted us to speculate that in cancer cells p38α may be involved in some tumorigenic role associated with β-catenin in the nucleus. To further investigate this hypothesis, we performed p38α and β-

catenin co-immunoprecipitation studies in normal and cancer cells. p38α and β-catenin co-immunoprecipitated in total lysates from both cell types, suggesting that p38α is a component of the APC-β-catenin complex. Since immunolocalization studies have mapped endogenous APC-β-catenin complexes to various sites throughout the cell (Henderson B R and Fagotto F, 2002), we evaluated the subcellular localization of the APC-β-catenin-p38α complex in normal and cancer cells. Immunofluorescence experiments confirmed that p38α and β-catenin are mostly found in the cytoplasm in normal colonocytes, while they co-localize primarily in the nucleus in cancer cells. These data were further confirmed by co-immunoprecipitation assays. Indeed, p38α and β-catenin co-immunoprecipitated mostly in the cytoplasm in normal cells, while they co-immunoprecipitated mainly in the nucleus in cancer cells, where p38α could be involved in β-catenin transcriptional activity. Indeed, in the nucleus β-catenin acts as a transcription factor of several Wnt target genes involved in different cellular functions. We subsequently showed that 24-hour pharmacological inhibition or genetic ablation of p38α induces the downregulation of several β-catenin target genes, among which the most important is c-Myc.

Our findings identified p38α as a promising therapeutic target located on chromatin, as its inhibition induces the downregulation of Wnt target genes, the main pathway involved in CRC carcinogenesis. Indeed, gene expression is rarely controlled by the association of a single transcription factor with an enhancer element belonging to the proximal promoter. Rather, the association of multiple transcription factors and co-regulators within an enhancer allows for precise and specific regulation of gene expression in response to environmental stimuli (Bottomly D et al, 2010).

To uncover evidence on the functional interplay between p38α and β-catenin, we further investigated the co-recruitment of these two factors on different β-catenin target gene binding motifs. All of these loci showed the presence of the p38α-β-catenin complex. Indeed, our study demonstrates that p38α and β-catenin cooperation is involved in the transcriptional induction of several Wnt target genes in response to serum. This analysis suggests that mitogens and the Wnt signaling pathway likely converge on p38α and β-catenin to co-regulate target gene expression. Yochum and colleagues demonstrated that β-catenin and TCF4 act as bridging factors for the interaction between 5' and 3' *Myc* Wnt responsive elements (WREs). However, due to the fact that neither β-catenin nor TCF proteins are known to form homodimers, and based on structural analysis one β-

catenin molecule cannot simultaneously interact with 2 TCF proteins, the authors suggest that β-catenin and TCF4 might form a bridge through the recruitment of additional factors, such as APC (Yochum G S et al, 2009). Since we demonstrated that p38α co-immunoprecipitates in the nucleus of cancer cells with both β-catenin and APC, it can be speculated that p38α might be an additional factor involved in the β-catenin-APC-TCF4 chromatin loop bridge. This idea is further supported by the surprising observation that p38α and β-catenin were found on both 5' and 3' *c-Myc* enhancer sequences. Activation of p38α and nuclear β-catenin is characteristic of many tumors, and several genes targeted by these signaling pathways are crucial for cancer development and progression; hence, targeting p38α might prove an effective therapeutic strategy for CRC treatment.

Given the importance of Wnt signaling in adult stem cell biology, it is not surprising that Wnt pathway mutations are frequently observed in CSCs. Indeed, in CRC it has been shown that only cells with high levels of Wnt signaling display colorectal cancer stem cell (CRC-SC) features. Since CRC-SCs can survive traditional chemotherapy and result in tumor recurrence and drug resistance, therapies targeting this specific cell subpopulation may be a promising approach to eradicate CRC. To extend our findings to CSCs, we established four different CRC-SC lines from consenting patients and characterized them for specific surface markers, ploidy, and microsatellite stability. It was previously demonstrated that c-Myc is consistently overexpressed in CRC-SCs and its downregulation suppresses CRC-SCs self-renewal and xenograft growth (Sanchita R and Adhip P N M, 2012). Consistent with the literature, our 511 (CRC-SCs) showed higher c-Myc protein levels compared with CRC cell lines and normal cells. Moreover, also in these CSC models, p38α co-localized with β-catenin upon Wnt signaling activation or repression mediated by the administration of Wnt3a or PRI-724, respectively. In order to investigate the role of p38α and β-catenin in CRC-SCs, we performed co-immunoprecipitation studies, which suggested that p38α and β-catenin are components of the same complex also in the intestinal stem niche. Interestingly, once again p38α co-immunoprecipitated with β-catenin in both the nuclear and cytoplasmic subcellular compartments, but predominantly in the nucleus.

Furthermore, we proceed to evaluate the increase of cell death response and the reduction of the proliferation rate following the single and/or combined inhibition of

p38α and/or MEK/ERK pathways. Indeed, in all CRC-SC lines the combined inhibition of p38α and MEK/ERK decreases relative viability while increasing relative cell death.

The development of *in vivo* animal models that recapitulate the natural history of human cancers and their clinical response to therapy represents a major prerequisite for rapid bench-to-bedside translation of investigational anticancer therapies that have shown promise in *in vitro* models (Cekanova M and Rathore K, 2014). Thus, to further validate our findings we performed *in vivo* studies using three different mouse models, i.e. $APC^{Min/+}$ mice, which recapitulate human FAP, $APC^{Min/+}$ mice treated with azoxymethane, which are considered a model for sporadic CRC, and c57 mice, which represent the wild-type (wt) counterpart of the previous two. In these systems, we found higher levels of activated kinases (p-p38, p-ERK) and transcription factors (c-Myc and β-catenin) in colon tumor samples compared to pre-cancerous lesions and normal tissues. Besides, we performed a co-immunoprecipitation analysis of p38α and β-catenin in colon tissue from c57 wt and $APC^{Min/+}$ mice. Our results showed once again that in the normal model p38α and β-catenin co-immunoprecipitate mostly in the cytoplasm, while in $APC^{Min/+}$ mice they co-immunoprecipitate mainly in the nucleus. Since $APC^{Min/+}$ mice are characterized by the development of thousands of intestinal polyps, we speculate that a functional relationship between p38α and β-catenin in the nucleus could already exists before the transition from adenoma to carcinoma. This might be important in the perspective of using p38α pharmacological inhibition not only as a potential cancer therapy but also as a preventive treatment for tumor development.

Conclusion and perspectives

Although the association of p38α activation with pro-apoptotic functions has been studied for years, there is a significant number of reports highlighting its involvement in cancer cell survival, proliferation, and chemoresistance. Indeed, p38α is over-active in CRC cells and tissues and is required to maintain cancer-specific metabolism (Madia F et al, 2012). Combined use of p38α inhibitors (SB202190, SB203580, BIRB796) and autophagy inhibitors (3MA, bafilomycin), MEK inhibitors (PD98059, UO126, CI-1040), HER2 inhibitors (lapatinib), multikinase inhibitors (sorafenib), or chemotherapeutic agents (5-FU, irinotecan, cisplatin) significantly reduces CRC growth *in vitro* and in preclinical models by inducing a higher degree of apoptosis compared to each single treatment (Comes F et al, 2007; Chiacchiera F and Simone C, 2009; Chiacchiera F et al, 2012; Grossi V et al, 2012; Germani A et al, 2014). Thus, targeting p38α in CRC offers oncologists various options for combined therapies and personalized medicine approaches: p38α inhibitors may be used in association with autophagy inhibitors, with molecularly-targeted drugs directed against the EGF pathway, and with conventional chemotherapy.

Besides, the phosphorylation status of p38 MAPK might be used as a marker of resistance and a predictor of therapy response in CRC. Indeed, we showed that colorectal cancer stem cells (CRC-SCs), which are thought to be responsible for cancer relapse and tumor chemoresistance, have higher levels of activated p38 then their normal counterparts. Consistently, recent reports identified the p38-Hsp27 axis as a survival pathway in hypoxic and serum-starved CRC-SCs (Lin SP et al, 2012). Moreover, the p38-Hsp27 pathway has been shown to mediate CRC-SCs drug resistance to cisplatin (Chen SF et al, 2012) and anti-angiogenic agents (Lin SP et al, 2013). Besides, breast cancer stem cells are resistant to pulsed proton beams by upregulation of the p38 and ERK pathways, with MAPK inhibitors being able to reduce this type of radio-resistance (Myung-Hwan J and Jeong Chan P, 2015). Several p38α inhibitors passed phase I clinical trials and are currently in phase II or III for inflammatory diseases and cancer (Schreiber S et al, 2006; Lee MR and Dominguez C, 2005; Scott LJ et al, 2013; Alten R et al, 2013; Buhler S and Laufer SA, 2014; Patnaik A et al, 2016; Cicenas J et al, 2018). Of note, LY2228820 dimesylate (Ralimetinib dimesylate), a selective inhibitor of p38 MAPK, passed a human phase I study in

patients with advanced cancer (Patnaik A et al, 2016). Thus, these agents could be available for future combined therapy with chemotherapeutic agents and molecularly targeted drugs.

Our study identifies p38α as a promising therapeutic target that acts directly on chromatin in CRC-SCs. This finding may pave the way to more effective therapies, since these cells are involved in CRC proliferation, metastatic invasion, and chemoresistance. To this purpose, further clinical trials will be required to investigate the incorporation of molecularly targeted drugs into the multimodality treatment of CRC.

Bibliography

Abetov D, Mustapova Z, Saliev T, Bulanin D, (2015). Biomarkers and signaling pathways of colorectal cancer stem cells. Tumour Biol. Mar;36(3):1339-53. doi: 10.1007/s13277-015-3198-4. Epub 2015 Feb 14.

Alepuz P.M., E de Nadal, M. Zapater, G Ammerer, F. Posas, (2003). Osmostress-induced transcription by Hot1 depends on a Hog1-mediated recruitment of the RNA Pol II. EMBO J. May 15;22(10):2433-42.

Alten R, (2013). Intracellular targets – current data on effectiveness and safety profile. Z Rheumatol 72:867-72

Arnold M, Sierra MS, Laversanne M, Soerjomataram I, Jemal A, Bray F, (2016). Global patterns and trends in colorectal cancer incidence and mortality, Gut. doi.org/10.1136/ gutjnl-2015-310912.

Barancik M, Bohacova V, Kvackajova J, Hudecova S, Krizanova O, Breier A, (2001). SB203580, a specific inhibitor of p38-MAPK pathway, is a new reversal agent of P-glycoprotein-mediated multidrug resistance. Eur J Pharm Sci 14, 29-36.

Batlle E and Clevers H, (2017). Cancer stem cells revisited. Nat Med., Oct 6;23(10):1124-1134. doi: 10.1038/nm.4409.

Bence A L, McNeely S C, and Beckmann R P, (2017). Achieving precision death with cell cycle inhibitors that target DNA replication and repair. Clinical cancer research, 2017 Jul 1;23(13):3232-3240.

Benson VS, Patnick J, Davies AK, Nadel MR, Smith RA, Atkin WS, (2008). International Colorectal Cancer Screening Network. Colorectal cancer screening: a comparison of 35 initiatives in 17 countries. Int J Cancer 122, 1357-1367.

Bhandari Abhishek, Woodhouse Melissa, and Gupta Samir,(2017). Colorectal cancer is a leading cause of cancer incidence and mortality among adults younger than 50 years in the USA: a SEER-based analysis with comparison to other young-onset cancers. J Investig Med. 2017 Feb; 65(2): 311–315.

Biggs J R, NG Ahn, A S Kraft, (1998). Activation of the MAPK pathway in U937 leukemic cells induces phosphorylation of the amino terminus of the TATA binding protein, Cell Growh Diff. 9 667-676.

Bikkavilli RK, Feigin ME, Malbon CC, (2008). p38 mitogen-activated protein kinase regulates canonical Wnt-beta-catenin signaling by inactivation of GSK3beta. J Cell Sci 121: 3598-607.

Bottomly D, Lyler S, McWeeney S and Yochum G S, (2010). Identification of β-catenin binding regions in colon cancer cells using ChIP-Seq. Nucleic Acids Research 38(17):5735-45.

Brancho D, Tanaka N, Jaeschke A, Ventura JJ, Kelkar N, Tanaka Y, Kyuuma M, Takeshita T, Flavell RA, Davis RJ, (2003). Mechanism of p38 MAP kinase activation in vivo. Genes and Development 17: 1969–1978.

Brunet A, Sweeney LB, Sturgill JF, Chua KF, Greer PL, Lin Y et al., (2002). Stress-dependent regulation of FOXO transcription factors by the SIRT1 deacetylase. Science 303: 2011-5.

Brunet A, Sweeney LB, Sturgill JF, Chua KF, Greer PL, Lin Y, Tran H, Ross SE, Mostoslavsky R, Cohen HY, Hu LS, Cheng HL, Jedrychowski MP, Gygi SP, Sinclair DA, Alt FW, Greenberg ME, (2004). Stress-dependent regulation of FOXO transcription factors by the SIRT1 deacetylase. Science; 303: 2011-2015.

Buchanan B W, Lloyd M E, Engle S M and Rubenstein E M, (2016). Cycloheximide chase analysis of protein degradation in Saccharomyces cerevisiae. Journal of Visualized experiments (110): 53975.

Bulavin DV, Demidov ON, Saito S, Kauraniemi P, Phillips C, Amundson SA, Ambrosino C, Sauter G, Nebreda AR, Anderson CW, Kallioniemi A, Fornace AJ Jr,Appella E, (2002). Amplification of PPM1D in human tumors abrogates p53 tumor-suppressor activity. Nature Genetics 31: 210-215.

Bulavin DV, Phillips C, Nannenga B, Timofeev O, Donehower LA, Anderson CW, Appella E, Fornace AJ Jr, (2004). Inactivation of the Wip1 phosphatase inhibits mammary tumorigenesis through p38 MAPK-mediated activation of the p16Ink4a–p19Arf pathway. Nature Genetics 36: 343–350.

Cekanova M and Rathore K, (2014). Animal models and therapeutic molecular targets of cancer: utility and limitations. Drug Design, Development and Therapy 8: 1911-1922.

Chang J, Sonoyama W, Wang Z, Jin Q, Zhang C, Krebsbach PH, Giannobile W, Shi S, Wang CY, (2007). Noncanonical Wnt-4 signaling enhances bone regeneration of mesenchymal stem cells in craniofacial defects through activation of p38 MAPK. J Biol Chem. Oct 19;282(42):30938-48. Epub 2007 Aug 24.

Chen SF, Nieh S, Jao SW, Liu CL, Wu CH, Chang YC, Yang CY, Lin YS, (2012). Quercetin suppresses drug-resistant spheres via the p38 MAPK-Hsp27 apoptotic pathway in oral cancer cells. PLoS One 7:e49275.

Chiacchiera F, Matrone A, Ferrari E, Ingravallo G, Lo Sasso G, Murzilli S, Petruzzelli M, Salvatore L, Moschetta A, Simone C, (2009). p38alpha blockade inhibits colorectal cancer growth in vivo by inducing a switch from HIF1alpha- to FoxO-dependent transcription. Cell Death Differ.;16(9):1203-14.

Chiacchiera F, Grossi V, Cappellari M, Peserico A, Simonatto M, Germani A, Russo S,Moyer M P, Resta N, Murzilli S, Simone C, (2012). Blocking p38/ERK crosstalk affects colorectal cancer growth by inducing apoptosis in vitro and in preclinical mouse models. Cancer Letter, Nov 1;324(1):98-108.

Chiacchiera F, Simone C, (2008). Signal-dependent regulation of gene expression as a target for cancer treatment: inhibiting p38alpha in colorectal tumors. Cancer Letters 265: 16–26.

Chunfeng X, Jianyun Z, Xueqi W, Jiaqi C, Shanshan G, Jieshu W, Caiyun Z, (2019). Tobacco smoke induced hepatic cancer stem cell-like properties through IL-33/p38 pathway. Journal of experimental clinical cancer research. doi.org/10.1186/s13046-019-1052-z

Cicenas J, Zlyte E, Rimkus A, Dapkus D, Noreika R and Urbonavicius S, (2018). JNK, p38, ERK and SGK1 inhibitors in cancer. Cancers 10(1): 1.

Comes F, Matrone A, Lastella P, Nico B, Susca FC, Bagnulo R, Ingravallo G, Modica S, Lo Sasso G, Moschetta A, Guanti G, Simone C, (2007). A novel cell type-specific role of p38alpha in the control of autophagy and cell death in colorectal cancer cells. Cell Death and Differentiation 14: 693-702.

Cuadrado A and Nebreda AR, (2010). Mechanism and functions of p38 MAPK signaling. Biochem J. 429: 403-17.

Cuenda A and Rousseau S, (2007). p38 MAP-kinases pathway regulation, function and role in human diseases. Biochim. Biophys. Acta 1773: 1358–1375.

Dallas NA, Xia L, Fan F, Gray MJ, Gaur P, van Buren G 2nd, Samuel S, Kim MP, Lim SJ, Ellis LM, (2009). Chemoresistant colorectal cancer cells, the cancer stem cell phenotype, and increased sensitivity to insulin-like growth factor-I receptor inhibition. Cancer Res. 69: 1951–1957.

Dang, C V, O'Donnell K A, Zelle KI, Nguyen T, Osthus, R C, Li F, (2006). The c-myc target gene network. Semin. Cancer Biol. 16, 253–264.
Dhillon AS, Hagan S, Rath O, Kolch W, (2007). MAP kinase signaling pathways in cancer. Oncogene 26: 3279-3290.

Dolado I, Nebreda A, (2008). Regulation of Tumorigenesis by p38α MAP Kinase. In: Posas F, Nebreda A, editors. Stress-Activated Protein Kinases: Springer Berlin Heidelberg 99:128.

Estecio MR, Yan PS, Ibrahim AE, Tellez CS, Shen L, Huang TH, Issa JP, (2007) .High-throughput methylation profiling by MCA coupled to CpG island microarray. Genome Res 17: 1529–1536.

Elbadawy M, Usui T, Yamawaki H and Sasaki K, (2019). Emerging Roles of C-Myc in Cancer Stem Cell-Related Signaling and Resistance to Cancer Chemotherapy: A Potential Therapeutic Target Against Colorectal Cancer. International journal of molecular science, doi.org/10.3390/ijms20092340.

Fang JY and Richardson BC, (2005). The MAPK signalling pathways and colorectal cancer. Lancet Oncol 6: 322-7.

Fearon ER and Vogelstein B, (1990). A genetic model for colorectal tumorigenesis. Cell. 1990 Jun 1;61(5):759-67.

Feitelson M A, Arzumanyan A, Kulathinal R, Blain S, Holcombe R, Mahajna J, Marino M, Martinez-Chantar M L, Nawroth R, Sanchez-Garcia I, Sharma D, Saxena N K, Singh N, Vlachostergios P J, Guo S, Honoki K, Fukii H, Georgakilas A G, Amedei A, Niccolai E, Amin A, Ashraf S S, Boosani C S, Guha G, Ciriolo M R, Aquilano K, Chen S, Mohammed S, azmi A S, Bhakta D, Haliska D and Nowsheen S, (2016). Sustained proliferation in cancer: mechanism and novel therapeutic targets. Siminal cancer biology, PMC4898971.

Ferry KV, Hamilton TC, Johnson SW, (2000). Increased nucleotide excision repair in cisplatin-resistant ovarian cancer cells: role of ERCC1-XPF. Biochem Pharmacol 60: 1305-1313.

Flaherty KT, Infante JR, Daud A, Gonzalez R, Kefford R F, Sosman J, Hamid O, Schuchter L, Cebon J, Ibrahim N, Kudchadkar R, Burris H, (2012). Combined BRAF and MEK Inhibition in Melanoma with BRAF V600 Mutations. The new England journal of Medicine.

Forcales S, Albini S, Giordani L, Malecova B, Cignolo L, Chernov A, Coutinho P, Saccone V, Consalvi S, Williams R, Wang K, Wu Z, Baranovskaya S, Miller A,

Dilworth F J, and Puri P L, (2012). Signal-dependent incorporation of MyoD–BAF60c into Brg1-based SWI/SNF chromatin-remodelling complex, the EMBO journal, Jan 18;31(2):301-16.

Germani A, Matrone A, Grossi V, Peserico A, Sanese P, Liuzzi M, Palermo R, Murzilli S, Campese A F, Ingravallo G, Canettieri G, Tezil T, Simone C, (2013). Targeted therapy against chemoresistant colorectal cancers: Inhibition of p38 modulates the effect of cisplatin in vitro and in vivo through the tumor suppressor FoxO3A, Cancer letters, Mar 1;344(1):110-118.

Gleizes A, Cavailles V and Lapierre M, (2018). Transcriptional regulation of the intestinal cancer stem cell. Intech open, 10.5772/intechopen.71859.

Goldberg R M, Montagut C, Wainberg R A, Ronga P, Audhuy F,Taieb J, Stintzing S, Siena S, Santini D, (2018). Optimising the use of cetuximab in the continuum of care for patients with metastatic colorectal cancer, BMJ journal, 2018 May 5;3(4):e000353.

Gregory M A and Hann S R, (2014). c-Myc Proteolysis by the Ubiquitin-Proteasome Pathway: Stabilization of c-Myc in Burkitt's Lymphoma Cell. Cell Growth and development 10.1128/MCB.20.7.2423-2435.2000

Grossi V, Liuzzi M, Murzilli S, Martelli N, Napoli A, Ingravallo G, Del Rio A, Simone C. (2012). Sorafenib inhibits p38α activity in colorectal cancer cells and synergizes with the DFGin inhibitor SB202190 to increase apoptotic response. Cancer Biol Ther 2012; 13: 1471-1481.

Grossi V and Simone C, (2012). Special Agents Hunting Down Women Silent Killer: The Emerging Role of the p38α Kinase. J Oncol 2012: 382159.

Grossi V, Peserico A, Tezil T, Simone C, (2014). p38α MAPK pathway: A key factor in colorectal cancer therapy and chemoresistance. World Journal of Gastroenterology. 10.3748/wjg.v20.i29.0000.

Haggar FA And Boushey RP, (2009). Colorectal Cancer Epidemiology: Incidence, Mortality, Survival, and Risk Factors. Clin Colon Rectal Surg. 22(4): 191–197

Haiquan L, Linh T, Youngrok P, Ivan C, Jie L, Yangyiran X, and Gregg L, (2018). Reciprocally Regulation of DUSP9 and DUSP16 Expression by HIF-1 Controls ERK and p38 MAP Kinase Activity and Mediates Chemotherapy-Induced Breast Cancer Stem Cell Enrichment, Cancer research 2018 Aug 1;78(15):4191-4202.

Hanahan D and Weinberg RA, (2011). Hallmarks of cancer: the next generation. Cell 144: 646-74.

Henderson B R and Fagotto F, 2002. The ins and outs of APC and β-catenin nuclear transport, EMBO reports. 3(9): 834-839.

Herrickand D and Ross J, (1994). The Half-Life of c-myc mRNA in Growing and Serum Stimulated Cells: Influence of the Coding and 3' Untranslated Regions and Role of Ribosome Translocation. Molecular and cellular biology: p. 2119-2128.

Howe B, Umrigar A and Tsien F, (2014). Chromosome preparation from cultured cells. Journal of visualized experiment. doi: 10.3791/50203

Howe JR, Roth S, Ringold JC, Summers RW, Järvinen HJ, Sistonen P, Tomlinson IP, Houlston RS, Bevan S, Mitros FA, Stone EM, Aaltonen LA, (1998). Mutations in the SMAD4/DPC4 gene in juvenile polyposis. Science 280: 1086-8.

Hsieh YH, Wu TT, Huang CY, Hsieh YS, Hwang JM, Liu JY, (2007). p38 mitogenactivated protein kinase pathway is involved in protein kinase Calpha-regulated invasion in human hepatocellular carcinoma cells. Cancer Research 67: 4320–4327.

Hui L, Bakiri L, Mairhorfer A, Schweifer N, Haslinger C, Kenner L Komnenovic V, Scheuch H, Beug H, Wagner EF, (2007). p38alpha suppresses normal and cancer cell proliferation by antagonizing the JNK-c-Jun pathway. Nat Genet 39: 741–749.

Jeong W-J, Ro E J and Choi K-Y, (2018). Interaction between wnt/beta catenin and RAS-ERK pathways and an anti cancer strategy via degradations of beta catenin and RAS by targeting the wnt/beta catenin pathway. Precision oncology: 5 (2018).

Junttila MR , Ala-aho R , Jokilehto T, Peltonen J, Kallajoki M, Grenman R, Jaakkola P, Westermarck J, Kähäri V-M, (2007). p38α and p38δ mitogen-activated protein kinase isoforms regulate invasion and growth of head and neck squamous carcinoma cells. Oncogene 26: 5267–5279.

Kauffman S and Earnshaw W, (2000). Induction of apoptosis by cancer chemotherapy. Experimental Cell Research256,42– 49.

Kao S-H et al., (2015). Analysis of protein stability by the cycloheximide chase assay. Bio Protoc. Jan 5; 5(1): e1374.

Katano K, Kondo A, Safaei R, Holzer A, Samimi G, Mishima M, Kuo YM, Rochdi M, Howell SB, (2002). Acquisition of resistance to cisplatin is accompanied by changes in the cellular pharmacology of copper. Cancer Reserach 62: 6559-6565.

Kazi M M, Trivedi T I, Kobawala T P, Ghosh N R, (2016). The potential of Wnt signaling pathway in cancer : a focus on breast cancer. Cancer translational medicine, 10.4103/2395-3977.181437.

Kerkhoff E, Houben R, Loffler S, Troppmair J, Lee J-E and Rapp U R, (1998). Regulation of *c-Myc* expression by Ras/Raf signaling. Oncogene 16, 211-216.

Kinzler KW and Vogelstein B, (1996). Lessons from hereditary colorectal cancer. Cell 87: 159-70.

Kim MS, Lee EJ, Kim HR, Moon A, (2003). p38 kinase is a key signaling molecule for H-Ras-induced cell motility and invasive phenotype in human breast epithelial cells. Cancer Research 63: 5454–5461.

Koul H, Pal M, and Koul S, (2013). Role of p38 MAP kinase signal transduction in solid tumors. Genes & Cancer 4: 342-359.

Kyriakis JM and Avruch J, (2001). Mammalian mitogen-activated protein kinase signal transduction pathways activated by stress and inflammation. Physiol Rev. 81: 807-69.

Kyriakis JM and Avruch J, (2012). Mammalian MAPK signal transduction pathways activated by stress and inflammation: a 10-year update. Physiol Rev. 92: 689-737.

Kumar D, Kumar S, Gorain M, Tomar D, Patil HS, Radharani NNV, Kumar TVS, Patil TV, Thulasiram HV, Kundu GC, (2016). Notch1-MAPK Signaling Axis Regulates CD133+ Cancer Stem Cell-Mediated Melanoma Growth and Angiogenesis. Journal of investigative dermatology. 136(12):2462-2474.

Larsson LG and Henriksson MA, (2010). Yin and Yang functions of the c-myc oncoprotein in cancer development and as targets for therapy. Exp. Cellular Research, 1;316(8):1429-37.

Lee SH, Hu LL, Gonzalez-Navajas J, Seo GS, Shen C, Brick J, Herdman S, Varki N, Corr M, Lee J, Raz E, (2010). ERK activation drives intestinal tumorigenesis in Apc(min/+) mice. Nat Med.;16(6):665-70.

Lee MR and Dominguez C, (2005). MAP kinase p38 inhibitors: clinical results and an intimate look at their interactions with p38alpha protein. Curr. Med. Chem. 12: 2979–2994.

Limami Y, Pinon A, Leger DY, Mousseau Y, Cook-Moreau J, Beneytout JL, Delage C, Liagre B, Simon A, (2011). HT-29 colorectal cancer cells undergoing apoptosis overexpress COX-2 to delay ursolic acid-induced cell death. Biochimie 93: 749-757.

Lin SP, Lee YT, Wang JY, Miller SA, Chiou SH, Hung MC, Hung SC, (2012). Survival of cancer stem cells under hypoxia and serum depletion via decrease in PP2A activity and activation of p38-MAPKAPK2-Hsp27. PLoS One. 2012;7(11):e49605. doi: 10.1371/journal.pone.0049605.

Madia F, Grossi V, Peserico A, Simone C, (2012). Updates from the Intestinal Front Line: Autophagic Weapons against Inflammation and Cancer. Cells 1: 535-557.

Marin JJ, Sanchez de Medina F, Castano B, Bujanda L, Romero MR, Martinez-Augustin O, Moral-Avila RD, Briz O, (2012). Chemoprevention, chemotherapy, and chemoresistance in colorectal cancer. Drug Metab Rev 44: 148-172.

Markowitz SD & Bertagnolli MM, (2009). Molecular origins of cancer: Molecular basis of colorectal cancer. N Engl J Med. 361: 2449-60.

Matrone A, Grossi V, Chiacchiera F, Fina E, Cappellari M, Caringella AM, Di Naro E, Loverro G, Simone C, (2010). p38alpha is required for ovarian cancer cell metabolism and survival. Int J Gynecol Cancer 20: 203-11.

Merlo LM, Pepper JW, Reid BJ, Maley CC, (2006). Cancer as an evolutionary and ecological process. Nat Rev Cancer 6: 924-35.

Moser AR, Pitot HC, Dove WF, (1990). A dominant mutation that predisposes to multiple intestinal neoplasia in the mouse. Science. 247(4940):322-4.

Muncan V, Sansom OJ, Tertoolen L, Phesse TJ, Begthel H, Sancho E, Cole AM, Gregorieff A, de Alboran IM, Clevers H, Clarke AR., (2006). Rapid loss of intestinal crypts upon conditional deletion of the Wnt/Tcf4 target gene c-Myc. Molecular and Cellular Biology, pp. 26:8418-8426.

Myung-Hwan J and Jeong Chan P, (2015). ERK/p38 MAPK inhibition reduces radio-resistance to pulsed proton beam in breast cancer stem cells.

Ozols RF, (1991). Ovarian cancer: new clinical approaches. Cancer Treat Rev 18: 77-83.

Oeztuerk-Winder F and Ventura J-J, (2012). The many faces of p38 mitogen-activated protein kinase in progenitor/stem cell differentiation. Biochemical, 445,1-10.

Paillas S, Boissiere F, Bibeau F, Denouel A, Mollevi C, Causse A, Denis V, Vezzio-Vie N, Marzi L, Cortijo C, Ait-Arsa I, Askari N, Pourquier P, Martineau P, Del Rio M,

Gongora C, (2011). Targeting the p38 MAPK pathway inhibits irinotecan resistance in colon adenocarcinoma. Cancer Research 71: 1041-1049.

Patnaik A, Haluska P, Tolcher A W, Erlichman C, Papadopoulos K P, Lensing J L, Arcos R R, Kelly C S, Wijayawardana S R, Zhang X, Stancato L F, Bell R, Shi P, Kulanthaivel P, Pitou C, Mulle L B, Farrington D L, Chan E M and Goetz M P, (2016). Cancer Therapy : Clinical. CCR-15-1718.

Pelengaris S. and Khan M., (2013).The molecular biology of cancer: a bridge from bench to bedside. Science, SBN: 978-1-118-00881-2.

Pereira L, Igea A, Canovas B, Dolado I, Nebreda AR, (2013). Inhibition of p38 MAPK sensitizes tumour cells to cisplatin-induced apoptosis mediated by reactive oxygen species and JNK. EMBO Mol Med 5: 1759-1774.

Possemiers S, Grootaert C, Vermeiren J, Gross G, Marzorati M, Verstraete W, Van de Wiele T, (2009). The intestinal environment in health and disease - recent insights on the potential of intestinal bacteria to influence human health. Curr Pharm Des. 15: 2051-65.

Poole C J and van Riggelen J, (2017). MYC —Master Regulator of the Cancer Epigenome and Transcriptome. Genes (Basel). 8(5), 142.

Rabik CA and Dolan ME, (2007). Molecular mechanisms of resistance and toxicity associated with platinating agents. Cancer treatment reviews 33: 9-23.

Roig A, Eskiocak U, High S, Kim S, Delgado O, Spechler S, Wright W and Shay J, (2010). Immortalized Epithelial Cells Derived from Human colon biopsies express stem cell markers and differentiate in vitro; Gastroenterology, Mar;138(3):1012-21.e1-5.

Roux PP and Blenis J, (2004). ERK and p38 MAPK-activated protein kinases: a family of protein kinases with diverse biological functions. Microbiol Mol Biol Rev 68: 320-344.

Sanchita Roy , Adhip P N Majumdar, (2012). Signaling in colon cancer stem cells. Journal of molecular signaling, 10.1186/1750-2187-7-11.

Saulnier N, Lattanzi W, Puglisi MA, Pani G, Barba M, Piscaglia AC, Giachelia M, Alfieri S, Neri G, Gasbarrini G, Gasbarrini A, (2009). Mesenchymal stromal cells multipotency and plasticity: induction toward the hepatic lineage. Eur Rev Med Pharmacol Sci. Mar;13 Suppl 1:71-8.

Schreiber S, Feagan B, D'Haens G, Colombel JF, Geboes K, Yurcov M, Isakov V, Golovenko O, Bernstein CN, Ludwig D, Winter T, Meier U, Yong C, Steffgen J, (2006). BIRB 796 Study Group. Oral p38 mitogen-activated protein kinase inhibition with BIRB 796 for active Crohn's disease: a randomized, double-blind, placebo-controlled trial. Clin Gastroenterol Hepatol 4: 325–334.

Scott LJ, (2013). Tofacitinib: a review of its use in adult patients with rheumatoid arthritis. Drugs 73: 857-7498.

Sears R, (2004). The life cycle of c-Myc from synthesis to degradation. Cell Cycle 3:9, 1133-1137.

Shomereeta R , Souvick R, Madhabananda K, Swatishree P, Arka S, Kumari A and Birendranath B, (2018). Role of p38 MAPK in disease relapse and therapeutic resistance by maintenance of Cancer Stem Cells (CSCs) in Head and Neck Squamous Cell Carcinoma. Journal of oral pathology and medicine, 2018 May;47(5):492-501.

Simone C, (2007). Signal-dependent control of autophagy and cell death in colorectal cancer cell: the role of the p38 pathway. Autophagy 3: 468-71.

Simone C, Forcales SV, Hill DA, Imbalzano AN, Latella L, Puri PL, (2004). p38 pathway targets SWI-SNF chromatin-remodeling complex to muscle-specific loci. Nat Genet 36: 738–743.

Shen L, Toyota M, Kondo Y, et al,(2007). Integrated genetic and epigenetic analysis identifies three different subclasses of colon cancer.Proc Natl Acad Sci U S A 104: 18654–18659.

Soloaga A, Thomson S, Wiggin G R, Rampersaud N, Dyson M H, Hazzalin C A, Mahadevan L C, Arthur J S, (2003). MSK2 and MSK1 mediate the mitogen- and stress-induced phosphorylation of histone H3 and HMG-14, EMBO J. 22 (2003) 2788–2797.

Szarynska M, Olejniczak A, Kobiela J, Spychalski P, Kmiec Z, (2017). Therapeutic strategies against cancer stem cells in human colorectal cancer. Oncology letters, 14(6): 7653–7668.

Thompson N and Lyons J, (2005). Recent progress in targeting the Raf/MEK/ERK pathway with inhibitors in cancer drug discovery. Curr Opin Pharmacol. 5: 350-6.
Thornton TM, Pedraza-Alva G, Deng B, Wood CD, Aronshtam A, Clements JL, Sabio G, Davis RJ, Matthews DE, Doble B, Rincon M, (2008). Phosphorylation by p38 MAPK as an alternative pathway for GSK3beta inactivation. Science 320: 667-70.

Toyota M, Ohe-Toyota M, Ahuja N, et al. ,(2000). Distinct genetic profiles in colorectal tumors with or without the CpG island methylator phenotype. Proc Natl Acad Sci U S A 97: 710–715.

Tront JS, Hoffman B, Liebermann DA, (2006). Gadd45a suppresses Ras-driven mammary tumorigenesis by activation of c-Jun NH2-terminal kinase and p38 stress signaling resulting in apoptosis and senescence. Cancer Research 66: 8448–8454.

Vachon PH, Harnois C, Grenier A, Dufour G, Bouchard V, Han J, Landry J, Beaulieu JF, Vézina A, Dydensborg AB, Gauthier R, Côté A, Drolet JF, Lareau F, (2002). Differentiation state-selective roles of p38 isoforms in human intestinal epithelial cell anoikis. Gastroenterology 123: 1980-91.

Valenta T, Hausmann G and Basler K, (2012). The many faces and functions of beta catenin. EMBO J Jun 13; 31(12): 2714–2736.

Valle A and Lecarpentier Y, (2016). Alzherimer disease: crosstalk between the canonical wnt/beta catenin pathway and PPARs alpha and gamma. Frontiers neuroscience, 19;10:459.

Veneroni S, Zaffaroni N, Daidone MG, Benini E, Villa R, Silvestrini R, (1994). Expression of P-glycoprotein and in vitro or in vivo resistance to doxorubicin and cisplatin in breast and ovarian cancers. Eur J Cancer 30: 1002-1007.

Ventura JJ, Tenbaum S, Perdiguero E, Huth M, Guerra C, Barbacid M, Pasparakis M, Nebreda AR, (2007). p38Alpha MAP kinase is essential in lung stem and progenitor cell proliferation and differentiation. Nature Genetics 39: 750–758.

Vila PM., Takahashi R., Wataru Usuba, Isaku Kohama, and Takahiro Ochiya, (2017). Drug Resistance Driven by Cancer Stem Cells and Their Niche. Int J Mol Sci. 2017 Dec; 18(12): 2574.

Vita M and Henriksson M, (2006). The Myc oncoprotein as a therapeutic target for human cancer. Simnal Cancer Biology , 16(4):318-30.

Walker T L, White J D, Esdale W J, Burton M A, DeCruz E E, (1993). Tumour cells surviving in vivo cisplatin chemotherapy display elevated c-myc expression. Br. J. Cancer 1996, 73, 610–61.

Wang Z, Yang H, Wang, X, Wang L, Cheng Y, Zhang Y, Tu Y, (2016). The molecular mechanism and regulatory pathways of cancer stem cells. Cancer translational medicine, 147-153.

Weisenberger DJ, Siegmund KD, Campan M, et al., (2006). CpG island methylator phenotype underlies sporadic microsatellite instability and is tightly associated with BRAF mutation in colorectal cancer. Nat Genet 38: 787–793.

Widmann C, Gibson S, Jarpe MB, Johnson GL, (1999). Mitogen-activated protein kinase: conservation of a three-kinase module from yeast to human. Physiol. Rev. 79:143.

Wilkins JA and Sansom OJ,(2008). C-Myc is a critical mediator of the phenotypes of Apc loss in the intestine. Cancer Res.68(13):4963-6.

Wilson KP, Fitzgibbon MJ, Caron PR, Griffith JP, Chen W, McCaffrey PG, Chambers SP, (1996). Crystal structure of p38 mitogen-activated protein kinase. J. Biol. Chem. 271: 27696–27700.

Wolfer A, Wittner BS, Irimia D, Flavin RJ, Lupien M, Gunawardane RN, Meyer CA, Lightcap ES, Tamayo P, Mesirov JP, Liu XS, Shioda T, Toner M, Loda M, Brown M, Brugge JS, Ramaswamy S, (2010) . MYC regulation of a “poor-prognosis metastatic cancer cell state. Proc Natl Acad Sci U S A. 2010 Feb 23;107(8):3698-703.

Yang SY, Miah A, Sales KM, Fuller B, Seifalian AM, Winslet M, (2011). Inhibition of the p38 MAPK pathway sensitises human colon cancer cells to 5-fluorouracil treatment, International journal of oncology, 38: 1695-1702.

Yochum G S, Sherrick C, Macpartlin M and Goodman R, (2009). A β-catenin/TCF coordinated chromatin loop MYC integrates 5’ and 3’ Wnt responsive enhancers, PNAS 5;107(1):145-50.

Yochum G, Cleland R and Goodman R, (2008). A genome wide screen for beta catenin binding sites identifies a downstream enhance element that controls c-Myc gene expression. Molecular and Cellular Biology p. 7368-7379.

Zhang Huan-Le, Wang Ping, Miao-Zhen Lu, San-Dian Zhang, and Lu Zheng, (2019). c-Myc maintains the self-renewal and chemoresistance properties of colon cancer stem cells. Oncol Lett. 2019 May; 17(5): 4487–4493.

Zhang F, Strand A, Robbins D, Cobb MH, Goldsmith EJ, (1994). Atomic structure of the MAP kinase ERK2 at 2.3A ° resolution. Nature 367: 704–711.

Zhang ZG, Harstrick A, Rustum YM, (1992). Modulation of fluoropyrimidines: role of dose and schedule of leucovorin administration. Semin. Oncol. 19: 10–15.

Zhou Y, Xia L, Wang H, Oyang L, Su M, Liu Q, Tian Y, Liao Q, and Cao D,(2018). Cancer stem cells in progression of colorectal cancer . Oncotarget Sep 7; 9(70): 33403–33415.